BONDING MATERIAL DEVELOPMENT AT WAFER LEVEL VACUUM PACKAGING FOR MEMS DEVICES BY TRANSIENT LIQUID PHASE (TLP) METHOD

A THESIS SUBMITTED TO
THE GRADUATE SCHOOL OF NATURAL AND APPLIED SCIENCES
OF
MIDDLE EAST TECHNICAL UNIVERSITY

BY

EYÜP CAN DEMİR

IN PARTIAL FULFILLMENT OF THE REQUIREMENTS
FOR
THE DEGREE OF MASTER OF SCIENCE
IN
METALLURGICAL AND MATERIALS ENGINEERING

SEPTEMBER 2016

Approval of the thesis:

BONDING MATERIAL DEVELOPMENT AT WAFER LEVEL VACUUM PACKAGING FOR MEMS DEVICES BY TRANSIENT LIQUID PHASE (TLP) METHOD

submitted by **EYÜP CAN DEMİR** in partial fulfillment of the requirements for the degree of **Master of Science in Metallurgical and Materials Engineering Department**, **Middle East Technical University** by,

Prof. Dr. Gülbin Dural
Dean, Graduate School of **Natural and Applied Sciences** _____

Prof. Dr. Cemil Hakan Gür
Head of Department, **Metallurgical and Materials Engineering** _____

Assoc. Prof. Dr. Yunus Eren Kalay
Supervisor, **Metallurgical and Materials Eng. Dept., METU** _____

Prof. Dr. Tayfun Akın
Co-Supervisor**, Electrical and Electronics Eng. Dept., METU** _____

Examining Committee Members

Prof. Dr. Cemil Hakan Gür _____
Metallurgical and Materials. Eng. Dept., METU

Assoc. Prof. Dr. Yunus Eren Kalay _____
Metallurgical and Materials. Eng. Dept., METU

Assist. Prof. Dr. Mert Efe
Metallurgical and Materials Eng. Dept., METU _____

Assist. Prof. Dr. Batur Ercan
Metallurgical and Materials Eng. Dept., METU _____

Assist. Prof. Dr. Mehmet Ünlü _____
Electrical and Electronics Eng. Dept., YBU

Date 09.09.2016

I hereby declare that all information in this document has been obtained and presented in accordance with academic rules and ethical conduct. I also declare that, as required by these rules and conduct, I have fully cited and referenced all referenced material and results that are not original to this work.

Name, Surname: Eyüp Can Demir

Signature:

ABSTRACT

BONDING MATERIAL DEVELOPMENT AT WAFER LEVEL VACUUM PACKAGING FOR MEMS DEVICES BY TRANSIENT LIQUID PHASE (TLP) METHOD

Demir, Eyüp Can
M.S., Department of Metallurgical and Materials Engineering
Supervisor: Assoc. Prof. Dr. Yunus Eren Kalay
Co-supervisor: Prof. Dr. Tayfun Akın

September 2016, 91 Pages

In this thesis, wafer level bonding material for hermetic encapsulation of MEMS devices was studied. Chip level packaging has been used for a quite long time. The main problems with this technique are the low efficiency and the high cost. Wafer level packaging has been attracted attention mainly due to an increase in compatibility of the packaging procedure at relatively low cost. Wafer level packaging is still problematic. During wafer level packaging, micro porosities or ineffective bonding may be occurred; so, obtaining hermetic encapsulation becomes difficult. These problems can be solved using basic principles of metallurgy. During bonding process, melting and solidification should be well controlled in metallic systems chosen for MEMS packaging. The two wafers were bonded together using Au-Sn and Au-In metallic systems. In order to decrease cost of the research, dummy packages were designed and fabricated without using real MEMS devices. Glass wafer was used as a substrate wafer and Si wafer was used as a cap wafer. Bonding of Au-Sn was performed at 300°C. The bonding mechanisms selected for Au-Sn system were eutectic and TLP bonding. TLP bonding was generated from eutectic composition and pure Sn metal. Metals were deposited using sputter and thermal

evaporator. Adhesion layers such as Cr, TiW, or Ti were deposited with various designs and their effect on bonding quality was investigated. It is the first time that the effects of adhesion layer on bonding metal was examined deeply by using scanning electron microscope / energy dispersive spectroscopy (SEM/EDS), transmission electron microcopy (TEM/EDS) and differential scanning calorimetry (DSC) tools. Au-Sn hermetic bonding with low yield was obtained using Cr as the adhesion layer. Shear strength of TLP and eutectic Au-Sn bonding was obtained higher than 15 MPa.

Au-In bonding was performed at 200°C. Ti as an adhesion layer and Ni as a barrier layer were used and their effects were studied. While the sputter system was used in order to deposit Ti, Ni and Au metals, e-beam evaporator was conducted for In deposition. In the reliability test, reasonable mechanical properties were observed for Au-In. With the help of Ni barrier layer, hermetic encapsulation was obtained. Hermeticity of the bonding was tested by the deflection method. Furthermore, the bonded and deflected wafer was heated to 400°C for 10 minutes to test hermeticity at high temperature. There was no degradation in either hermeticity or mechanical property.

In conclusion, Au-In and Au-Sn metallic bonding were succeeded with hermetic and high strength features at low temperature. This thesis contributed to the literature in terms of both the detailed examination of bonding material development and characterization of adhesion layer effect. In addition, this study was partially supported by the Turkish Scientific and Technical Research Council- TÜBITAK (Project Number E115E060).

Keywords: Packaging, Low Temperature Bonding, Wafer Level Packaging. Hermetic Bonding.

ÖZ

MİKRO ELEKTRONİK VE MEKANİK SİSTEMLER İÇİN GEÇİCİ SIVI FAZ YÖNTEMİ İLE VAKUM ALTINDA SİLİKON DİSK BOYUTUNDA BAGLAMA MALZEMESİ GELİŞTİRME

Demir, Eyüp Can

Yüksek Lisan, Metalurji ve Malzeme Mühendisliği Bölümü

Tez Yöneticisi: Doç. Prof. Dr. Yunus Eren Kalay

Ortak Tez Yöneticisi: Prof. Dr. Tayfun Akın

Eylül 2016, 91 sayfa

Bu tezde, MEMS cihazlarının sızdırmaz paketlenmesi için pul seviyesinde bağlama malzemesi çalışılmıştır. Çip boyutunda paketleme uzun bir zamandır kullanılıyordu. Çip boyutunda paketlemedeki temel problem düşük verimlilik ve yüksek maliyettir. Pul seviyesinde paketlenmesi, bağlama sürecine uygunluk ve düşük maliyet büyük sebebi ile büyük dikkat çekiyor. Ancak pul seviyesinde paketleme konusu hala problemlidir. Pul seviyesinde paketleme esnasında mikro boyuttaki boşluklar veya verimli olmayan bağlama işlemleri olmaktadır, bu da sızdırmaz paket elde etmeyi zorlaştırmaktadır. Bu problemler yalnızca metalürjinin temel prensipleri kullanılarak çözülebilir. MEMS'lerin paketlenmesi için seçilen metalik sistemlerin paketleme esnasındaki erime ve katılaşmaları iyi şekilde kontrol edilmelidir. Bu çalışmada, iki pul Au-Sn ve Au-In metalik sistemleri kullanılarak birbirine bağlanmıştır. Araştırma maliyetini düşürmek için, gerçek MEMS cihazları kullanılmadan, model-deneme paketleri tasarlanmış ve üretilmiştir. Altlık pul olarak cam, kapak pulu ise silisyum kullanılmıştır.

Au-Sn paketleme 300°C gerçekleştirilmiştir. Paketleme mekanizması olarak Au-Sn ötektik ve geçici sıvı faz yöntemi (GSF) seçilmiştir. Geçici sıvı faz bağlaması ötektik kompozisyondan ve saf Sn metalinden gerçekleştirilmiştir. Metaller sıçratma yöntemi ve termal buharlaştırma yöntemi ile kaplanmıştır. Yapıştırma katmanlarından Cr, TiW ve Ti farklı tasarımlarda kaplanmış ve onların paketleme üzerine etkisi incelenmiştir. Yapıştırma malzemesinin bağlama metaline olan etkisinin derin bir şekilde SEM/EDS, TEM/EDS ve DSC cihazları ile incelenmesi bir ilktir. Au-Sn sızdırmaz paketleme Cr yapıştırma katmanı ile düşük bir verimlilikte elde edilmiştir. GSF ve ötektik Au-Sn bağlamasıyla 15 MPa değerinden yüksek kesme mukavemeti elde edilmiştir.

Au-In bağlaması 200°C gerçekleştirilmiştir. Ti yapıştırma ve Ni bariyer katmanı kullanılmış ve etkileri incelenmiştir. Ti, Ni, ve Au kaplamaları için sıçratma yöntemi kullanılırken, In kaplamaları için elektron ışını ile buharlaştırma yöntemi kullanılmıştır. Güvenilirlik testinde Au-In için makul kesme dayanç değerleri elde edilmiştir. Ni bariyer katmanın yardımı ile sızdırmaz paketleme elde edilmiştir. Bağlamanın sızdırmazlığı için bükülme yöntemi ile test edildi. Üstelik yüksek sıcaklıkta sızdırmazlığı test etmek için bükülmüş olan pul 400°C'ye ısıtıldı ve 10 dakika bekletildi. Bükülmede veya mekanik özelliklerde herhangi bir bozulma gerçekleşmedi.

Sonuç olarak, yüksek kesme dayancı ve sızdırmaz paketleme Au-In ve Au-Sn metalik sistemlerle düşük sıcaklıkta başarılmıştır. Bu tez yapıştırma katmanın detaylı karakterizasyonu ile bağlama malzemesi geliştirilmesinde literatüre katkıda bulunmuştur. Ayrıca bu çalışma kısmi olarak Türkiye Bilim ve Teknolojik Araştırma Kurumu (TUBİTAK) E115E060 projesi kapsamında desteklenmiştir.

Anahtar Kelimeler: Paketleme, Düşük Sıcaklıkta Bağlama, Pul Seviyesinde Paketleme, Sızdırmaz Bağlama.

To People and Future

ACKNOWLEDGEMENTS

First of all, I would like thank to Assoc. Prof. Dr. Yunus Eren Kalay and Prof. Dr. Tayfun Akın for their support, guidance, and encouragement during my graduate studies. It is a great chance for me to work in MEMS Research Group and SDML Research Group. I would like to thank to Assoc. Prof. Dr. H. Emrah Ünalan to encourage me to be researcher.

I would like to express my gratitude to Dr. M. Mert Torunbalcı, the legend of the clean room, for his worthy helps while in the adaptation to clean room process and for transferring deeply knowledge on packaging to me. Special thanks to İnci Dönmez, my first friend and colleague in METU MEMS Center. She introduce me to MEMS people and clean room. The other special thanks goes to Oğuzhan Temel, my research, folk dance, astroturf and basketball partner for his valuable suggestions, discussion and help in process. All of three person helps me to get important decisions about fabrication and life.

I would like to express my thanks to Dr. Ebru Topallı, Gülşah Demirhan, Orhan Şevket Akar and İlker Comart for their helps in the fabrication process and for their friendship. Mikail Şahin, Ferdag Ercan, Tuncer Can, Aykut Bakırcı, Levent Abant, Kamil Sürer, Macit Araz, Ali Aytekin help us to sustain MEMS Center so special thanks for their labor. Thanks to Ayşegül Afal who motivated me to start M.S. in METU MEMS Center. Special thanks to Doğa Doğanay, Ozan Ertürk, Osman Aydın, Evren Erdil and Özgecan Dervişoğlu for their friendship. Moreover, I would like to thank all members of the METU-MEMS research group for providing a nice research environment.

I would express gratitude to my parent Nazlı and Zeki and my grandmother Güllü (Gülgez) who has incredible labor on me from my birth to today. Many thanks to my siblings Dilara and Deniz for their being at my elbow forever. Deeply gratitude to my wife, Yağmur for her endless support, love and encouragement.

TABLE OF CONTENTS

LIST OF FIGURES

FIGURES

LIST OF TABLES

TABLES

CHAPTER 1

INTRODUCTION

1.1 Introduction to MEMS

The famous talk "There is a Plenty of Room at Bottom" given by Prof. Richard Feynman in 1959 [1] can be considered as the beginning of the era of miniaturization technology. This fascinating technology has been rapidly grown up. Today, micro electro-mechanical systems (MEMS) can be given as an evidence how miniaturization affect human's life. MEMS are not only the electronic systems but also an integration of mechanics and electronics. These systems can sense the outer world and respond to it. The respondence technology mainly consists of data processing, communication and actuation [2]. The properties make the MEMS smart and utilizable. MEMS size may change from few micrometers to millimeters. In their fabrication, Integrated Circuits (IC) are used. These systems consist of mechanical structures, microsensors, microelectronics, and microactuators on the same silicon chip. The micron level components are fabricated from silicon or other substrate materials by micromachining processes such as wet etching, dry etching or deposition systems PVD (physical vapor deposition) and CVD (chemical vapor deposition). MEMS are reliable systems and also they provide low-cost and high-performance technology for the industrial market. There is a huge effort to develop these technology further. The inertial sensors, the flow and pressure sensors, RF MEMS, optical MEMS, Power MEMS and BioMEMS are major commercially available devices. They are used in automotive, transportation, telecommunication and human health care systems. The MEMS market forecast in the next five years can be seen in Figure 1.1.

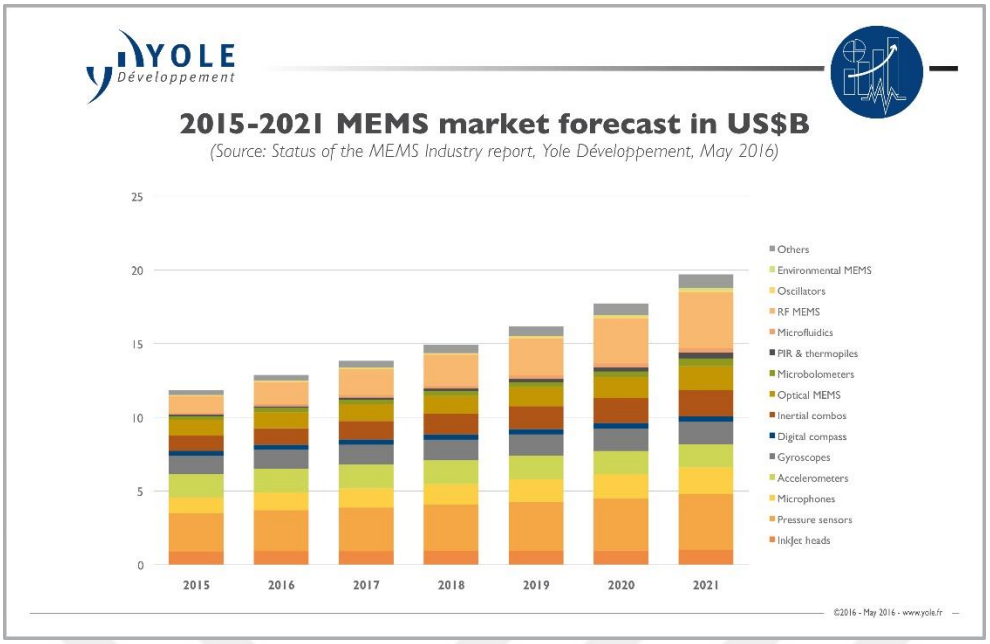

Figure 1.1: 2015 -2021 MEMS market forecast [3].

An electronic packaging is a critical process in MEMS fabrication. MEMS packaging stays as the major obstacle in decreasing production cost. In addition to production, reliability and durability of the MEMS rely on the packaging efficiency. Each MEMS devices works in a specific environment. Thus, packaging must satisfy the requirements of this special environment. It should be noted that packaging is a process that is integrated into the system during device fabrication. For this reason, packaging must be in good agreement with the device fabrication. Each packaging process should be designed based on the specific device fabrication. MEMS are produced in clean room, therefore; many parameters should be taken into account such as the selectivity of metal, deposition and patterning technique, cleaning process, or bonding temperature. Therefore, it is very important that packaging design should be considered from the beginning in order to maintain the process compatibility.

In this perspective, the aim of the study is to develop and examine the wafer level hermetic packaging for MEMS with Transient Liquid Phase (TLP) bonding and eutectic bonding technology.

1.2 MEMS Packaging

MEMS are the system that sense the outside world and respond to this environment. Package is the main part that provides an interaction between MEMS and the outside in the case of sensing, transducing and actuating. Package must supply specific properties such as mechanical support, protection from environment and electrical connection. There are many risks depending upon the undesirable physical interaction of MEMS device with the outside. These physical interactions can be mechanical shock, undesirable vibration and contaminations. They cause MEMS device damage physically. Package should protect the device from these physical damages. It should be noted that environmental effect is not only related with physical damage. There is always a risk of oxidation or of humidity that can easily affect the working routines of MEMS device. Therefore, MEMS packaging is significant to prevent optical, chemical and thermal effects. For instance; while pressure sensors have to access to the ambient atmosphere for sensing, MEMS gyroscope needs a vacuum environment to give higher performance [4]. The last important assignment of the package is an electrical connection. Electrical connection should be supplied by the package for the MEMS devices with lateral feedthrough or vertical feedthrough. This should be considered in the package design as well.

Historically, the improvement in the IC packaging, started at 1960s, contributed the MEMS packaging with the highest level. The main motivations behind the development of IC packaging were thermal managements, interconnection and the cost [5]. Lately, wafer level chip scale packaging has been developed. This technology allows packaging of many chips on the wafer at once. Wafer level chip scale packaging leads several advances in MEMS packaging. Chip level and wafer level packaging are two main methods used in MEMS. Figure 1.2 shows schematic illustration of MEMS packaging in chip level. As shown in this illustration, wafer is firstly diced into chips, then each chip is processed separately. After device is released, each chip is encapsulated using flip chip packaging. This is an expensive process totally. Device releasing and bonding at chip level are time consuming, as well. Besides time consumption, each chips' process conditions must be adjusted to the same condition. Thus, each device releasing and subsequent packaging create risk

based on changing condition. A performance of the chip is dependent on clean room processes deeply. Chip level packaging may be improved in a way that releasing of dies can be performed at wafer level followed by dicing process. In this case, only packaging becomes a time consuming and expensive part.

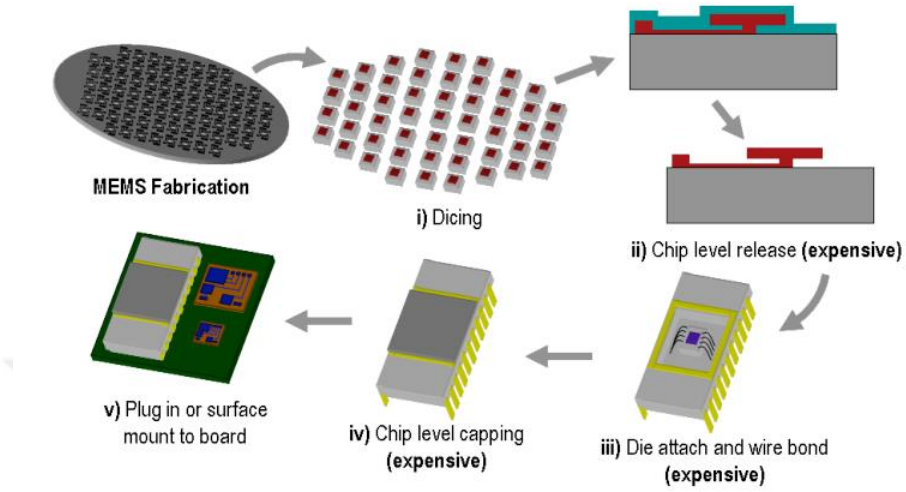

Figure 1.2: Schematic illustration of MEMS packaging at chip level [5].

Wafer level packaging provides a major reduction in production cost. Figure 1.3 shows schematic illustration of MEMS packaging in wafer level.

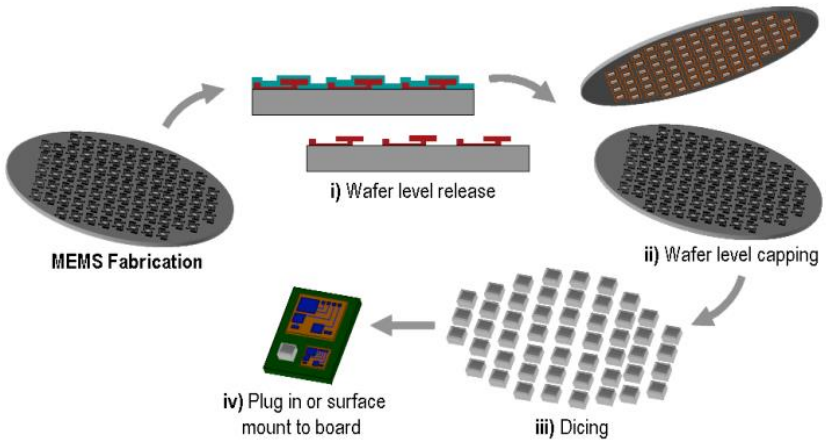

Figure 1.3: Schematic illustration of MEMS packaging at wafer level [5].

In wafer level packaging of MEMS, die releasing and packaging are performed at wafer level. These two steps save a lot of time compared with chip level packaging. Besides to this, each die releasing is performed together which means that clean room

process conditions are preserved, thus performance of the devices are identical, which are produced by wafer level packaging. In this regard, wafer level packaging has become promising technique from the cost and performance point of view.

1.3 Vacuum Encapsulation Requirements

As explained previously, MEMS devices can only work properly in special environment. This special environment can only be provided by good packaging. While some devices requires vacuum environment, some requires 1 atm pressure. Vacuum is a major requirement for two types of MEMS device. First group is resonating structures in which vacuum is used for obtaining higher oscillation amplitude with smaller voltages. MEMS inertial sensor can be example for the first group. Second group is the sensor which requires thermal isolation. Vacuum environment provides better thermal isolation. Microbolometer can be added in the second group [4]. Table 1.1 shows working pressure values of the some MEMS sensors.

Table 1.1: Working pressure values of the common MEMS sensors [6].

Sensor	Working Pressure
Accelerometer	300-700 mbar
Resonator	10^{-1}-10^{-4} mbar
Gyroscope	10^{-1}-10^{-4} mbar
RF switch	10^{-1}-10^{-4} mbar
Microbolometer	$<10^{-4}$ mbar

1.4 Issues Related to Vacuum Packaging

There are four major issues related with vacuum packaging that must be considered seriously. These are (i) leak, (ii) outgassing, (iii) getter activation and (iv) permeation. This section summaries these issues.

1.4.1 Leakage

Leakage can be thought as the flow of liquid or gas from outside to inside. There is a huge driving force of flow of gas from outside atmosphere to the inside, because; an inside of the package is under vacuum. Leakage is the main issue of hermeticity. Actually, the level of hermeticity is directly related with the amount of leak. If there is no leak inside, then hermeticity is ensured. Leak rate ($Pa.m^2/s$) from ultra-fine 10^{-15}-10^{-16} to gross $9x10^{-16}$ is defined in MIL-STD-883 for hermetic sealing. Helium leak test can be used for leakage measurement.

1.4.2 Outgassing

Outgassing is the other important phenomena related with vacuum packaging. Outgassing can be described as releasing of the gas from the materials' surface in the device [7]. The amount of outgassing is directly related to history of the bonding process. In many processes, different gases are used such as Ar, O_2 or N_2. These gasses can be pushed under the metal or other materials. They can be released whenever vacuum environment is ensured. Therefore, at the beginning of the process, the pressure value of the package is low, and it becomes higher when time passes. Outgassing can be reduced by changing process history or with adapting a getter.

1.4.3 Getter Activation

Getters can be thought as pump after bonding is completed. As mentioned previously, after the bonding some outgassing is commonly observed. Getter absorbs undesirable gasses inside the package, with chemically or physically. Getters have both porous and thin film structure which makes surface area high. Porosity of the getter helps trapping of the gasses physically and high surface area of the getter makes the chemical reaction easy. However, getter should be activated at relatively high temperatures to act as the pump. Depending on the getter material, activation temperature and time may vary; for example, Ti, activation can be completed at 400°C for a minute. Ti, Zr, Ta are the most common getter materials.

1.4.4 Permeation

Permeation can be described as the movement of the gas or vapor through solid material. The difference between the leak and permeation should be considered

carefully. While permeation is a material property depending on nature of the material, leak is directly related to bonding process. Therefore, bonding material selection depends firstly on permeation of the material. Figure 1.4 shows permeability of common materials. In hermetic bonding, metals are frequently used instead of polymer [8–13]. Metals are the most promising materials for hermetic encapsulation while epoxies or polymers are mentioned as non-hermetic materials.

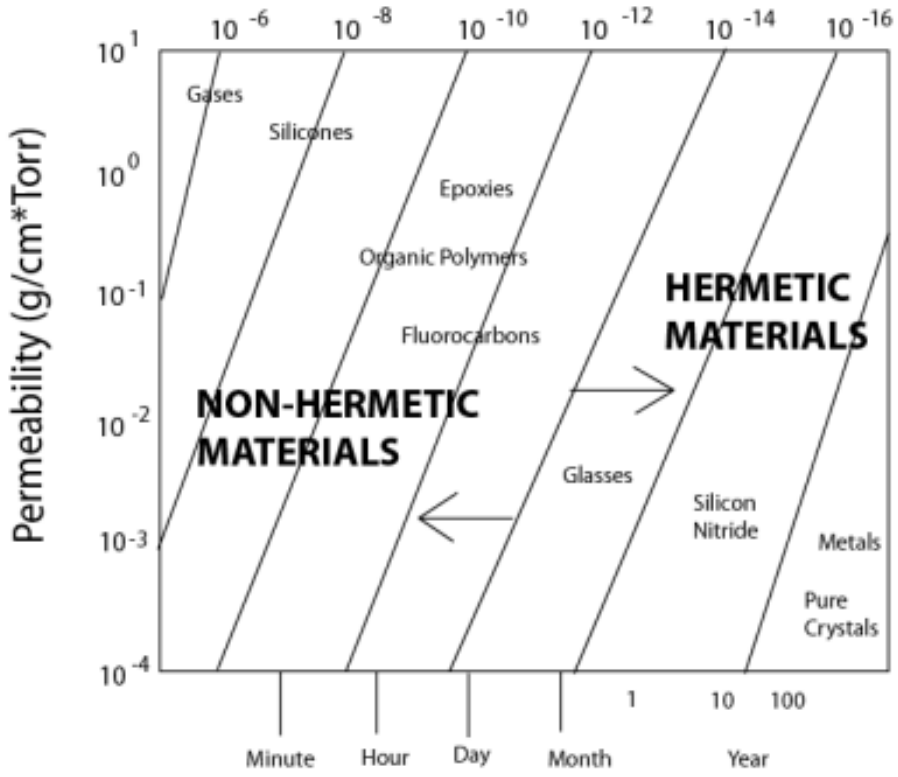

Figure 1.4: Permeability of materials [7].

1.5 Wafer Level MEMS Packaging

There are two important wafer level packaging techniques which are (i) the thin film deposition bonding and (ii) the wafer bonding.

1.5.1 Thin Film Deposition Bonding

The logic behind the thin film bonding is to encapsulate the MEMS device with thin film deposition technique. At the beginning of the device and bonding process, device can be fabricated with or without sacrificial layer. Then, thin film is deposited on this

layer. Etch holes are formed on the thin film in order to remove the sacrificial layer. From the etch holes, sacrificial layer is removed. Then, new thin film is deposited to close the etch holes. Figure 1.5 shows schematic illustration of thin film deposition bonding. This technique has several benefits such as low cost, smaller package size, and unnecessary of bonding equipment. However, process complexity increases with this method since sacrificial layer removing process requires new masks. Polysilicon, amorphous silicon, metals, semiconductors and polymers are commonly used in thin film deposition technique [14–17].

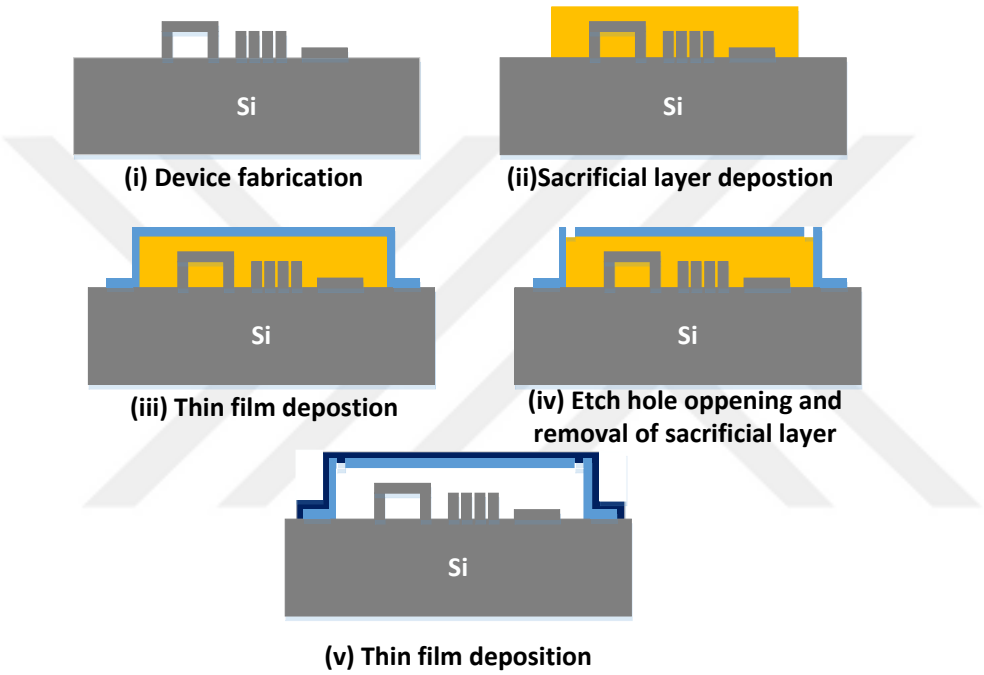

Figure 1.5: Schematic illustration of thin film deposition bonding [18].

1.5.2 Wafer Bonding

In wafer bonding technique, packaging is performed with cap wafer as a second wafer in addition to substrate wafer. Two wafer are processed separately based on the bonding and device designs. After the fabrication of two wafers are completed, bonding alignment is performed and these two wafers bring into bonder. In the bonder, pressure is applied and these wafers are bonded together. There are several wafer bonding methods such as anodic, fusion, glass frit, polymer and solder bonding. Solder bonding technology covers the eutectic and TLP bonding. Each bonding

technique is discussed at the following subsection. Figure 1.6 shows schematic illustration of general wafer bonding technic. The main steps can be summarized as: (i) Initiation of the process, (ii) release of device at wafer level, bonding material deposition and patterning on both wafers, (iii) cap cavity opening, (iv) wafer level bonding, and (v) dicing of the wafer to chips.

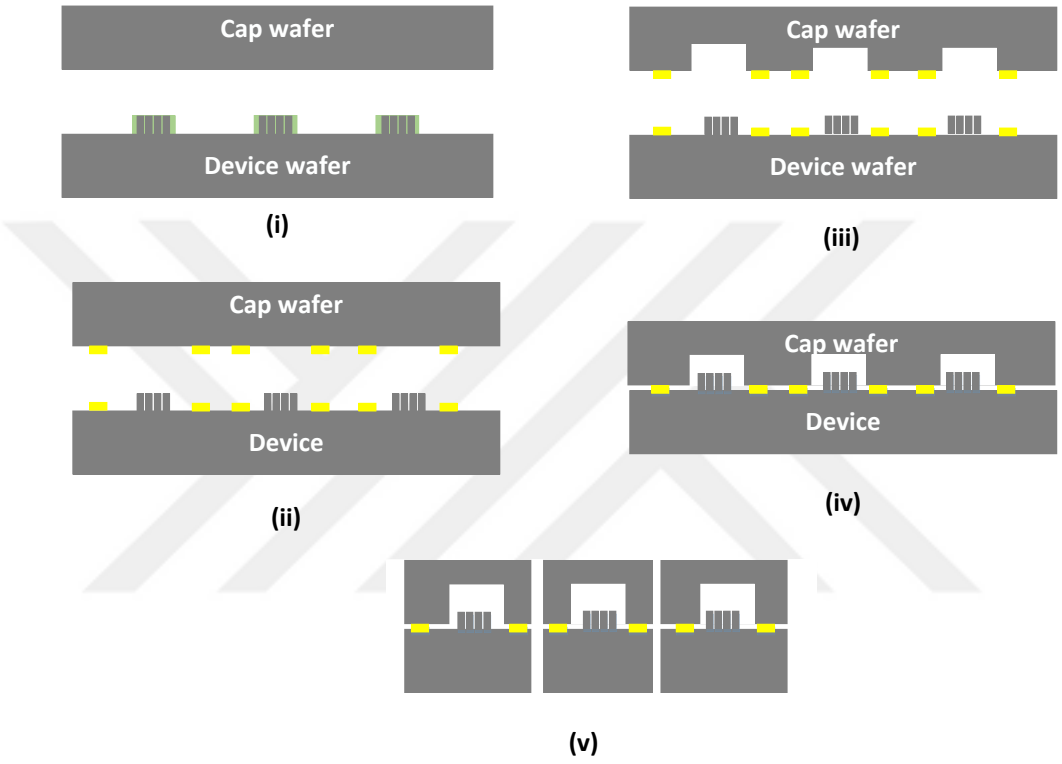

Figure 1.6: Schematic illustration of general wafer bonding technique [18].

1.5.2.1 Anodic Bonding

Anodic bonding is performed between the metal and insulator or semiconductor and insulator as described in [19]. Bonding between the Si and the Pyrex glass, which is sodium rich, is the most common materials for anodic bonding. During bonding, electric field is applied while the wafer are heated [20,21]. It is believed that sodium ions moves away from glass and oxygen ions goes through the Si with the help of temperature and applied electric field. As a result, at the interface, where the wafers are in contact, the chemical bonds are formed between oxygen and silicon. Voltage to create an electric field changes between 400V and 1500V depending on the

substrate materials, bonding temperature and composition. Temperature range is between 300°C and 500°C for anodic bonding. Anodic bonding provides hermetic packaging, but; unfortunately it requires smooth surfaces, because; bonding exists only at the contact surfaces. It can be applied for lower than 300Å surface roughness [5]. Even if chemical bonds are very strong, it is not applicable for rough surfaces.

1.5.2.2 Fusion Bonding

Fusion bonding is performed with covalent bonding. It is similar to anodic bonding process from the chemical point of view. In fusion bonding, surfaces of the wafers are activated before the bonding in order to have ability to create covalent bonding. Activation can be performed as follows: surfaces are etched and impurities at the surface is oxidized or desorbed away at elevated temperature before the bonding. As a result of activation, OH groups are obtained at the surface and during the bonding, the contact surfaces creates covalent bond. It is applied to very range of materials such as silicon-silicon, silicon-silicon dioxide, silicon-silicon nitride, silicon-gallium arsenide and silicon sapphire [22]. Bonding temperatures is relatively high, for example; for Si-Si bonding, temperature is 600°C and bonding temperature of Si-SiO_2 is 1200°C. In addition to fusion bonding, plasma enhance fusion bonding has been improved. This plasma enhanced bonding provides decrease in bonding temperature up to 300°C for Si_3N_4 - Si_3N_4 bonding [23]. This bonding has some disadvantages. Firstly, surface of the bonding must be extremely smooth. Roughness of the surface should be lower than 50Å. Secondly, it requires special equipment like activation tools so its cost is high. Thirdly, particle lower than 1μm may create unbonded region of 100μm in length [5].

1.5.2.3 Glass Frit Bonding

In glass frit bonding, glass paste mixture which has low melting point is used to bond two wafers [24]. In glass frit bonding method, main idea is to soften the glass frit by heating and to contact wafer by pressure. Glass frit is generally put on one wafer with printing method while the other wafer does not require any special process. Glass frit technology provides hermetic bonding and it can be applied almost any kind of material. In addition, it can tolerate the topologies on the wafer due to softening

property of glass frit. It fills up the holes or other things on the surface. Actually, it seems very promising bonding technology; however, it should be noted that lead is used to decrease the melting point of the glass. Lead is dangerous for environment and it is forbidden in many countries. Second disadvantage is that even if hermetic bonding is achieved, bonding temperature changes between 450°C and 600°C. These temperature are relatively high and they may be hazardous for MEMS devices.

1.5.2.4 Thermocompression Bonding

As its name implies, temperature and force are the main parameters in thermocompression bonding. On the contrary to glass frit bonding, materials are deposited in both wafers as a ring. Then, pressure is applied at elevated temperature which provides softening of the metals. Some metallic bonding is established with the pressure. This method is quite attractive, because; there is no need extra tool like in fusion bonding or there is no electric field like in anodic bonding. However, it again requires smooth surfaces, because; when metals do not touch each other, bonding cannot be performed effectively. Therefore, hermeticity for the topographic surfaces stays as question. In addition to topography problem, oxide layer on the metal may become an issue. It prevents contact between two metals. Therefore, Au-Au thermocompression bonding is commonly used among the others and bonding temperature is around 400°C.

1.5.2.5 Polymer Bonding

In this method polymer is used as a bonding material. It is spinned on the wafer in liquid form. Then, liquid polymer is cured at different temperature range from room temperature to 300°C with varying curing times. There are two main advantages of using polymer bonding. Firstly, it provides the low temperature bonding. It is known that polymers are melted or softened at low temperature and this enables bonding of two wafers at low temperatures. Secondly, polymers are able to fill up the topography on the surface, due to melting and visco-fluid property. SU-8 [25], BCB (benzoctclobutene) [26] , Paralyne (poly-paraxyleyne) [27] and PMMA (polymethylmethacrylat) [28] are some example of the polymer bonding materials. There are many different types of epoxies used as bonding material. However, due to high permeability property of the polymer, it is not preferred for hermetic

encapsulation. Furthermore, it would show high amount of outgassing probably due to gas entrapment during liquid deposition spin-on process.

1.5.2.6 Eutectic and TLP Bonding

Eutectic bonding and TLP bonding are explained together, because; in both cases there is liquid metal formation. Eutectic is the name of reaction that explains liquid transformation to two different solid phases. The eutectic reaction, eutectic temperature and eutectic composition are commonly used terms in metallurgy. MEMS terminology also uses the same term as eutectic bonding. Actually, this term first come up with Au-Si bonding. Generally, in eutectic bonding, there are two materials which have high melting temperature. As known from the nature of the materials like Au-Si, at special composition (which is the eutectic composition) melting is occurred at lower temperature than both of the materials' melting temperature. Au-Si phase diagram may be the best diagram to understand eutectic concept. Figure 1.7 shows Au-Si binary phase diagram. Eutectic point corresponds to around 18% (at) Si in Au at 363°C. Different material systems may have their own eutectic points like Al-Ge, Al-Si, and Au-Sn. During bonding, eutectic composition is arranged and melting is observed above the eutectic temperature. While the wafer is at above the eutectic temperature, pressure is applied. With this applied pressure, the wafers let cool down to room temperature. Below the eutectic temperature, the bonding materials become a solid. By this way, the wafers are bonded together. If the wafers are heated to above the eutectic temperature again, the bonding materials show melting at that temperature. Therefore, it does not have high re-melt temperature. It is a good candidate for hermetic sealing for highly topographic surfaces, since liquid formation is observed during bonding. Au-Si eutectic bonding is widely used in MEMS technology packaging [27–30].

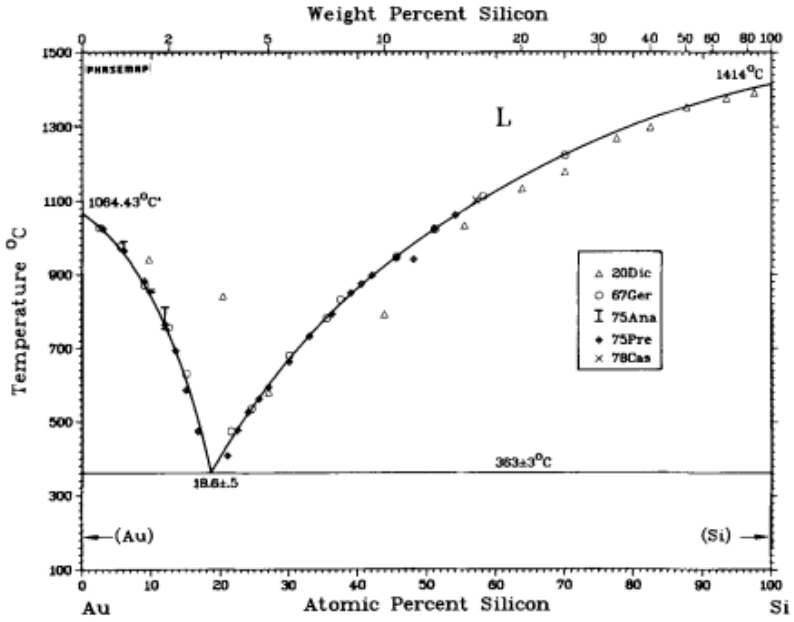

Figure 1.7: Au-Si binary phase diagram [33].

TLP is the acronym of transient liquid phase. As it can be understood from the name, during bonding, liquid is formed only for a short time. There are one high melting temperature metal and one low melting temperature metal deposited on the wafers in the shape of bond ring. When the wafers are heated above the melting point of low melting point metal, liquefaction starts. Once this liquid formation starts, pressure should be applied to initiate the bonding. In TLP bonding, high melting temperature metal is deposited relatively thicker than low melting temperature metal. The aim of creating thickness difference is to finalize alloy composition closer the high melting temperature metal. Alloy composition closer to high melting metal results in high re-melt property. This alloy is formed with liquid diffusion into solid. Some liquefaction would be observed from the high melting temperature metal; however, final phase of the metal become a solid with a higher melting temperature, when time and temperature is appropriate. Figure 1.8 shows schematic illustration of TLP bonding mechanism. TLP bonding can be applied to many systems such as Cu-Sn [21–25], Au-In [35–40], Au-Sn [12, 44, 45], Ag-In and Ni-Sn [46, 47].

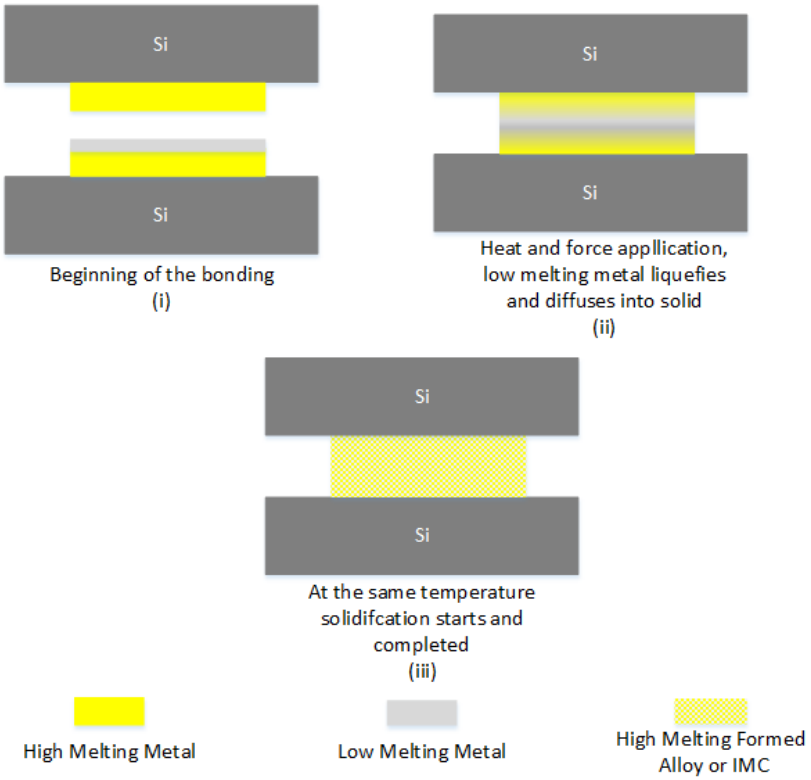

Figure 1.8: Schematic illustration of TLP bonding mechanism.

1.6 Objective and Organization of Thesis

The main objective of the thesis is to develop low temperature hermetic packaging at wafer level for MEMS devices. Wafer level packaging is performed by metal based wafer bonding technology. Within the scope of thesis, Au-Sn and Au-In material systems were studied in a detailed manner. In this study, the advanced characterization of the bonding material with observing adhesion and barrier layer effects on Au-In and Au-Sn bonding are the main contributions to the existing literature.

The organization of the thesis with chapter content are listed as follows.

Chapter 1 describes the basic literature review regarding to electronic packaging of MEMS.

Chapter 2 describes the main experimental procedure emphasizing the fabrication and characterization methods. Bonding metal selection is also explained in this chapter in

a detailed manner. The infrastructure at Metallurgical and Materials Engineering Department and METU MEMS Research and Application Center are presented.

Chapter 3 presents Au-Sn eutectic and TLP bonding studies. Previous works related with Au-Sn system was reviewed and bonding plan was explained in detail. In this section, the effects of Cr, Ti, and TiW as an adhesion layer were also examined. Results regarding to Au-Sn bonding were discussed.

Chapter 4 provides information on Au-In TLP bonding. Effect of Ni barrier layer was observed and discussed. The shear test results and hermeticity behavior of Au-In bonding was given. The hermetic encapsulation behavior was tested at high re-melt temperature conditions.

Chapter 5 concludes the overall work performed for Au-Sn and Au-In. Future work was discussed in this section.

CHAPTER 2

EXPERIMENTAL PROCEDURE

2.1 The selection of Bonding Metal

Au-Sn and Au-In were chosen as packaging metal. The first reason of choosing these metals is to perform bonding at relatively low temperatures. Sn and In provide low melting ability for the bonding. The ease of Au interaction with Sn and In is the other advantage for effective packaging. It can be seen from the phase diagrams given in the Chapter 3 and 4, high re-melt intermetallics and eutectics can be obtained in these systems. This is particularly important to access TLP and eutectic bonding. Furthermore, Au is well known clean room material which can be deposited and etched easily. Au does not have oxide layer on the surface which is a major advantage in bonding practices.

2.2 Fabrication and Equipment

In this section, fabrication for the bonding trials is explained. The equipment required for these fabrication steps are described, as well.

2.2.1 Metal Patterning

In dummy bonding, metals are mainly patterned as a bond ring shape. Metal patterning process was performed with photolithography, metallization and lift-off process respectively. Each process was explained exclusively in the following sections. Figure 2.1 shows schematic illustration of metal patterning with lithography, metal deposition and lift-off process: (i) photo resist coating, (ii) expose, (iii) development, (iv) metal deposition and (v) lift-off.

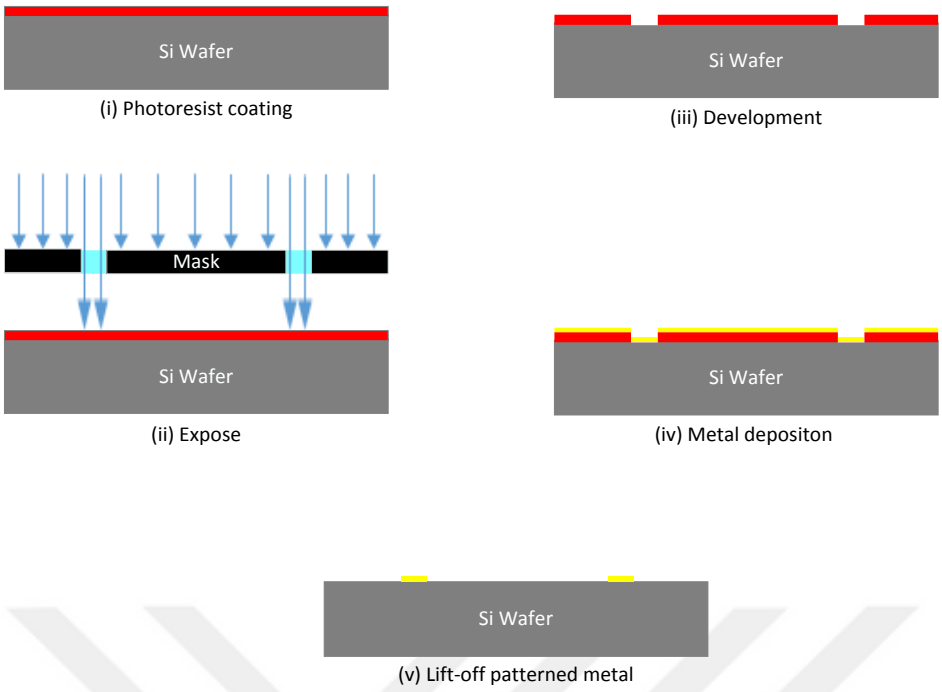

Figure 2.1: Schematic illustration of metal patterning by lift-off process.

2.2.2 Photolithography

Photolithography is the process that is used for microfabrication. It enables to pattern thin film to use light (photon), mask and fluid polymer (photoresist). The main logic is to form desired geometric pattern on a polymer (photoresist) that is spinned on a wafer. Desired geometric pattern is formed by help of light. Masks are produced which are previously designed according to geometric pattern that would be on the wafer. When UV light is applied, desired regions are protected by the mask. Chemical property of the polymer is varied when it is exposed to UV light. After changing chemistry of resisting with UV light, resist is etched with the help of developer which is kind of solution. Therefore, geometric pattern on the mask is transferred to resist. Patterning of the polymer with the help of UV light is called photolithography. Photolithography consist of dehydration of wafer, resist spinning, exposure, development and soft bake. In this work, metal patterning process was performed with lift-off method. Thus, schematic illustration shown in Figure 2.1 is given for lift-off process. For the exposure of light, mask aligner is used. Figure 2.2 shows EVG 501 mask aligner device.

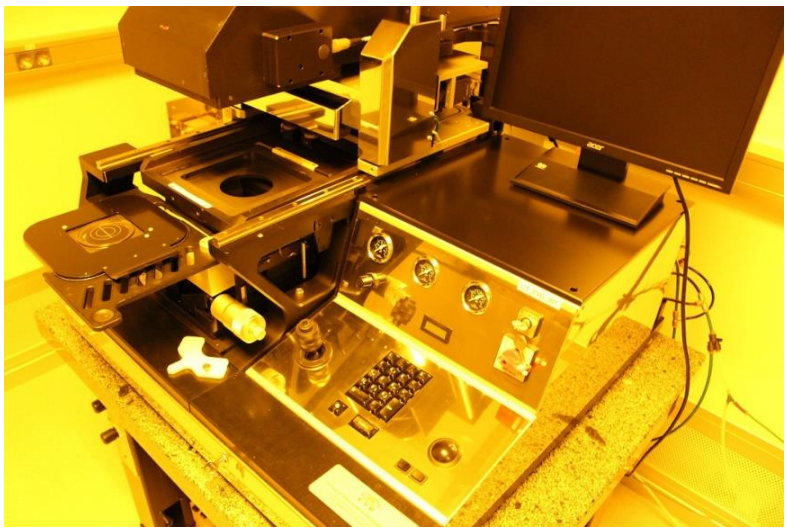

Figure 2.2: EVG 501 mask aligner device.

2.2.3 Metal Deposition

There are many different types of metal deposition technique such as e-beam evaporator, thermal evaporator, atomic layer deposition, sputter and electro plating. In this study, In was deposited using Varian e-beam evaporator, Au and adhesion layers Ti, TiW, Cr were deposited using AJA sputter systems. Sn and protective Au were deposited using Varian thermal evaporator. Figure 2.3 shows AJA sputter system for metal deposition.

Figure 2.3: AJA sputter system for metal deposition.

Figure 2.4 shows the photos metal deposition tools: (a) of the Varian 3119 e-beam evaporator and (b) Varian 3119 thermal evaporator.

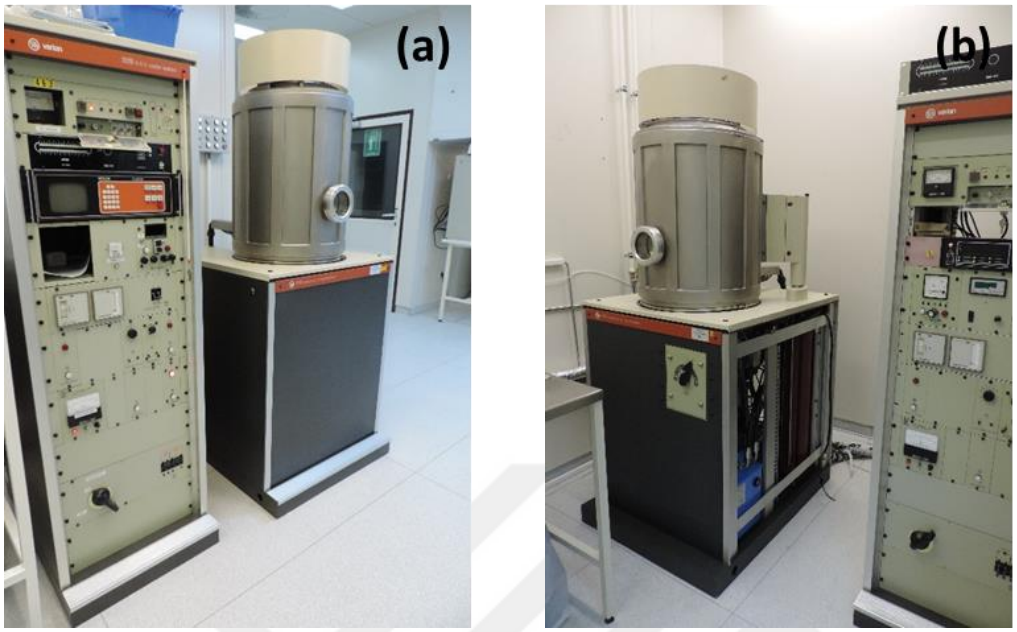

Figure 2.4: Photo of the metal deposition instruments: (a) Varian 3119 e-beam evaporators and (b) Varian 3119 thermal evaporator.

2.2.4 Lift-off

In this study, lift-off process was performed using acetone. The primary reason of using lift-off is to pattern Au, Sn, and other metals at once. Acetone was used to remove photoresist which stays under the metal layer. The patterned metal layer was obtained after photoresist was removed.

2.2.5 Cap Cavity Opening

Cap cavity opening is dry etching process, which was performed for the deflection test. The aim of the deflection test is to test hermeticity of the package. Test method was explained in the hermeticity section. First, cap cavity lithography was performed on Si cap wafer. Then, the cavity was formed with deep reactive ion etching (DRIE) technology at around 300µm. After etching of Si wafer, approximately 200µm thickness was remained for 4 inches wafer, because thickness of the Si wafer is 500µm with 25µm error. Figure 2.5 exhibits STS Pegasus DRIE system for dry etching of Si and cap cavity opening.

Figure 2.5: STS Pegasus DRIE system for dry etching of Si.

2.2.6 Bonding

Bonding was performed under the relevant heat and pressure, applied to the wafer. The wafers were aligned in EVG Aligner 620 and they were inserted in EVG Bonder 520. Heating rate was adjusted to 45°C/min and cooling rate was adjusted to be the maximum cooling rate provided by given N_2 within the chamber. Figure 2.6 shows EVG 520 wafer bonder device.

Figure 2.6: EVG 520 wafer bonder device.

2.3 Characterization

Characterization was performed both before and after the bonding. Thermal and microstructural characterizations were performed before the bonding. This gives critical information about as-deposited conditions of the bonding metals. Thermal analysis, microstructural investigation, fracture surface analyses, mechanical and hermetic characterization were performed after the bonding. They give critical feedback for future bonding trials.

2.3.1 Thermal Characterization

Thermal characterization was performed using SEIKO SII X-DSC 7000 Differential Scanning Calorimeter (DSC) in Metallurgical and Materials Engineering Department. It gives information about melting or solidification temperature of the deposited metals. Aluminum crucibles are used for DSC analyses. 3mmx3mm dimensions specimens, which were diced with the dicer in METU MEMS Center, were placed into aluminum crucibles. Thermal characterization was performed before and after the bonding. Before the bonding, characterization gave important information about the bonding temperature. After the bonding, characterization gave re-melt temperature of the bonded pair. Heating and cooling rate can be arranged so they were adjusted to 45°C/min for both heating and cooling rate to mimic the bonder. Figure 2.7 shows DSC instrument used in this study.

Figure 2.7: DSC instrument.

2.3.2 Microstructural Characterization

Optical microscope, scanning electron microscope (SEM) and transmission electron microscope (TEM) were used for microstructural characterization. In each step microstructural characterization was performed to measure metal thickness, to identify the crystal structure and to analyze the fractures surfaces. Elemental analysis was performed with using energy dispersive X-ray spectroscopy (EDS), attached to SEM and TEM. The electron microscope (JEOL F2100 FEG TEM and FEI Nova NanoSEM) in METE Department and (JEOL SEM) in METU MEMS Center were frequently used in this study. Figure 2.8 shows electron microscopes used in this study.

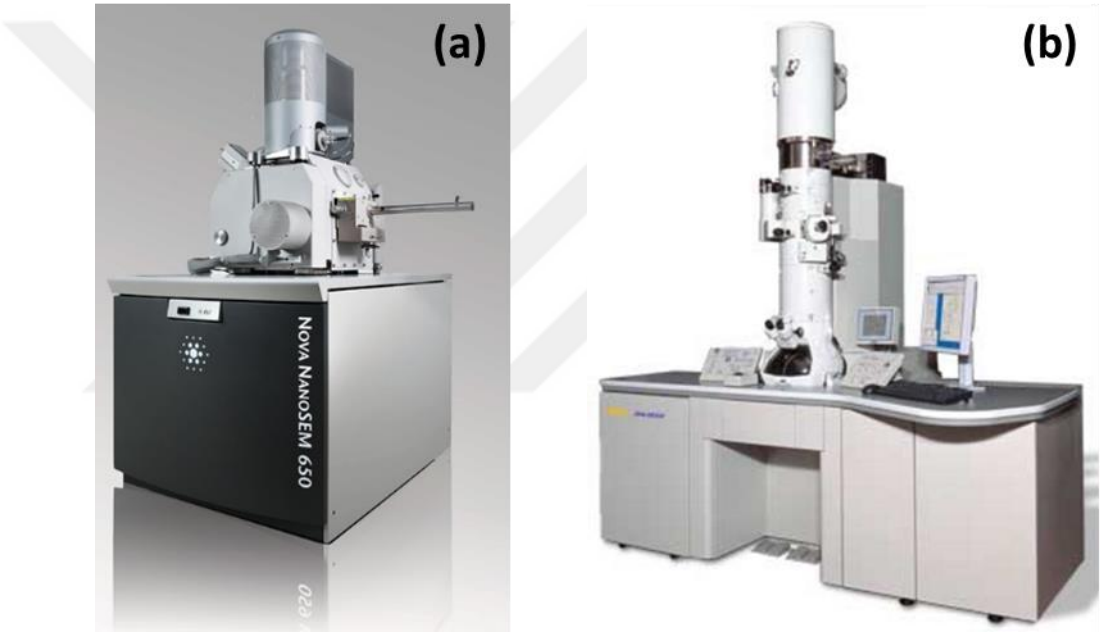

Figure 2.8: Images: (a) FEI Nova NanoSEM 650 Scanning Electron Microscope and (b) JEOL F2100 FEG Transmission Electron Microscope.

2.3.3 Mechanical Characterization

Mechanical characterization studies mainly comprise the shear test measurements. In this study, the die thicknesses are generally lower than 1mm, so it is almost impossible to hold the dies for tensile test. Thus, two methods were adapted for shear test. The first one was performed with universal tensile test machine, and second one was conducted using Dage 4000 Bondtester. The universal tensile test machine,

designed for larger specimens, is not appropriate for chip technology. In that sense Dage 4000 Bondtester is a better instrument to test the mechanical performances of small chips. However, this instrument was not available at the beginning of the current thesis study. Therefore, universal test machine was adapted to test chips with the help of copper plates. Figure 2.9 shows schematic illustration of shear test set up, adapted to universal tensile test machine to measure the shear strength of small size chips.

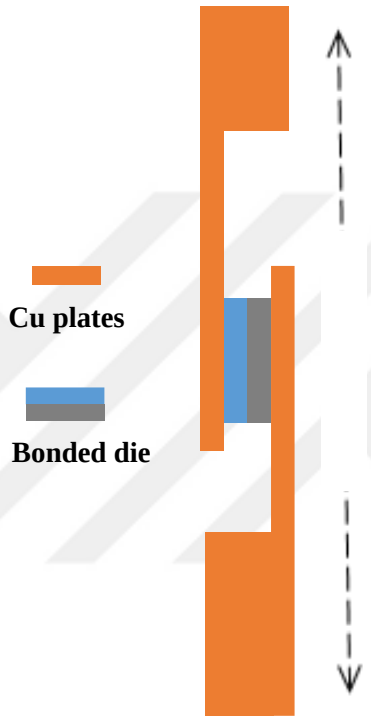

Figure 2.9: Schematic illustration of shear test set up, adapted to universal tensile test machine to measure the shear strength of small size chips.

The bonded dies were attached to Cu plates with the help of cement based adhesive material. There was no problem related with the adhesive material, because the shear strength of the adhesive material was tested and was found as much higher than bonding material of the chip due to large area of the adhesive material. Examinations also confirmed that there was no deterioration in the bonding regions. Figure 2.10 shows a representative photo of the shear test setup with (a) general view and (b) magnified view respectively. Besides universal test machine, new holders was designed and manufactured at METU MEMS Center for Dage 4000 Bondtester. In

this design, barrier was produced according to the chip thickness. For 4" wafers barrier thickness was 450µm and a vacuum hole was drilled to support the barrier layer and to hold the specimen.

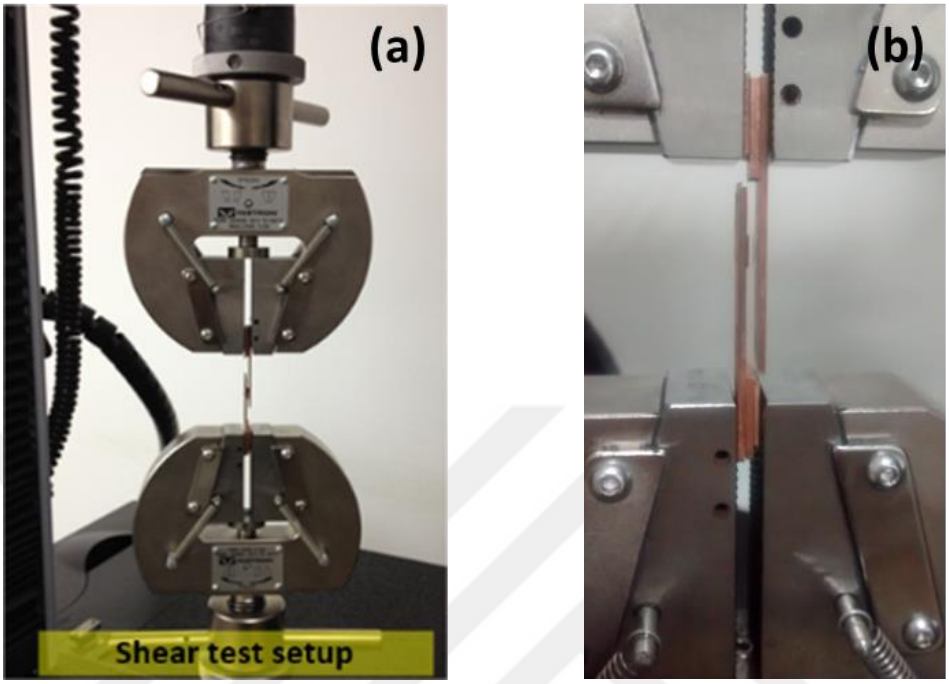

Figure 2.10: Photo of the shear test setup: (a) general view and (b) magnified view.

Figure 2.11 and Figure 2.12 show the Dage 400 Bondtester, used for shear test and the holder, specially designed and manufactured for the dies, respectively.

Figure 2.11: General view of the Dage 4000 Bondtester which is used for shear test of the dies.

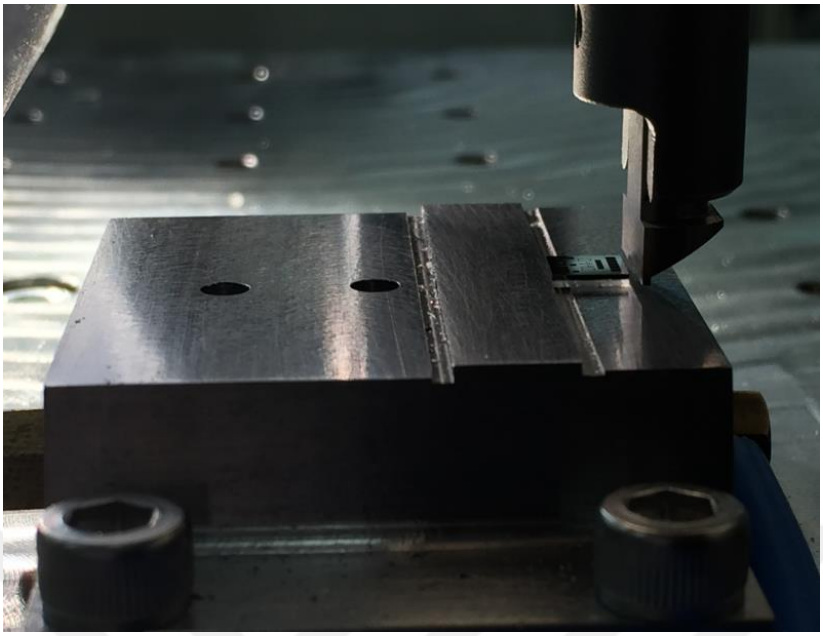

Figure 2.12: Photo of the holder specially designed and manufactured for dies, die and shear tip.

According to MIL-STD 883 shear test standard, the die has higher than 12.3 MPa shear strength passes the test for this type of bondings.

2.3.4 Hermeticity Testing

Hermeticity means the impermeability of liquid or gas flow from outside to inside or vice versa. Test for hermeticity is one of the most important step to determine whether or not bonded die stays under vacuum. There are several methods to characterize hermeticity of the bonding such as helium leak testing, or designing resonator to detect pressure inside the package. In this study, two step hermeticity test was applied. In the first step, bonded wafers was inserted in petri, with full of acetone. If bonded wafer was not hermetic, acetone entered into dies. Then, test was failed. However if acetone did not enter the dies, then a second method, namely as deflection method was applied. There must be a cavity inside the package in order to perform deflection test. As it was stated before, bonding was performed under vacuum environment so under normal conditions, package should be in vacuum if bonding was hermetic. The way of testing the hermeticity is to thin the Si cap wafer up to

50-100 nm remaining thickness, depending on the cavity dimensions, after the bonding. In the case of hermetic bonding, Si deflects towards to the inside of the cavity due to pressure difference between the outside and inside. Outside of the package is 1 atm while inside of the package is under vacuum. Figure 2.13 shows critical process steps for deflection test.

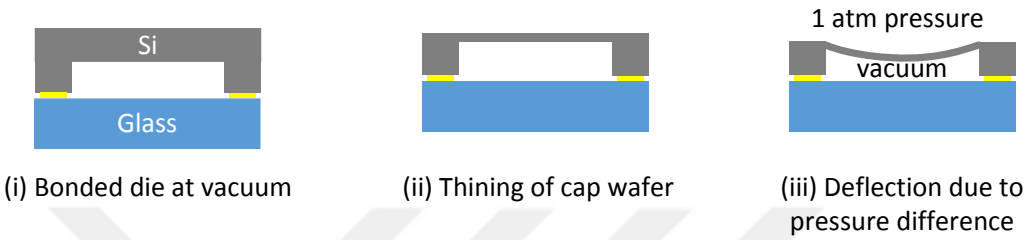

Figure 2.13: Process steps for deflection test.

CHAPTER 3

WAFER LEVEL BONDING USING Au-Sn

3.1 Introduction

MEMS are simply the integration of mechanical and electronic elements at micro scale on silicon chips. These systems have the ability for data processing, communication, actuating which makes sensing these systems smart and commercial products. Packaging of MEMS is an elusive process which makes it costly and problematic. In this study, packaging of MEMS was examined with the concern of bonding environment and process convenience. Au is widely used in clean room and it does not have native oxide. These are the main two reasons of the choice of Au for the bonding metal. Sn, on the other hand, is cheap and it has low melting temperature which are important in terms of cost and process point of view. Au and Sn are the common bonding metals used in TLP [12], [44], [45], [48]. Bonding temperature is relatively low (300°C) so it is compatible with CMOS or other type of MEMS technologies.

3.2 Experimental Procedure

In this study, experimental route comprised bonding metal thickness optimization in thermal evaporator system, adhesion layer effect on bonding metal and packaging quality, thermal and mechanical characterization, fracture analysis and finally hermeticity characterization. Fabrication consisted of mainly two different techniques, named as blank wafer and patterned wafer fabrications. Bonding metal thickness optimization, adhesion layer effect on bonding metal and thermal characterization before and after bonding were carried out in the blank wafer fabrication. Adhesion layer effect on packaging quality, mechanical characterization, fracture analysis and hermeticity characterization were conducted in the patterned wafer fabrication.

Liquid metal phase is essential for TLP and eutectic bonding. Melting point of the metal alloys is directly related to the composition. The composition of the alloy can be adjusted by the thicknesses during thermal evaporation. Therefore, bonding metal thicknesses should be known with a high precision in order to be able to perform controllable Au-Sn packaging. Figure 3.1 exhibits Au-Sn phase diagram, which was used to determine the corresponding thickness and thus corresponding composition values.

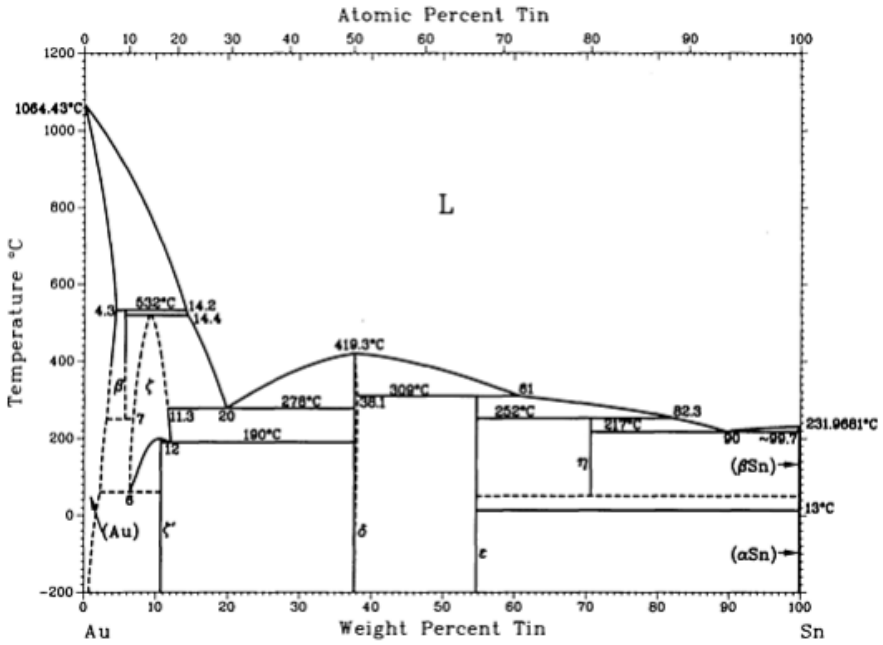

Figure 3.1: Au-Sn Phase Diagram [49].

Three main variations compositional options were studied, named as (i) eutectic bonding, (ii) TLP bonding from eutectic and (iii) TLP bonding from Sn. Figure 3.2 shows schematic illustration of three main bonding designs with different metal thicknesses. In eutectic bonding, the total Au-Sn composition corresponded to eutectic composition. In TLP bonding from eutectic and Sn, the overall composition of Au in Au-Sn corresponded to 90wt%. Only difference between TLP bonding from eutectic and TLP bonding from pure Sn was the starting metal which would be liquid during bonding. Au-Sn was at eutectic composition on the glass side in TLP from eutectic one, on the other hand, almost pure Sn was on the glass side in TLP bonding

from pure Sn. Au was used at the bottom as an adhesion layer and at the top as a protective layer against oxidation. Therefore, according to composition of the metals, while melting was expected at around 278°C in TLP bonding from eutectic design, melting is expected to occur at around 232°C in TLP bonding from Sn design. Figure 3.3 illustrates Au-Sn phase diagram with expected compositional change during bonding. Yellow line shows the compositional change of the TLP bonding from eutectic, blue line exhibits the compositional change of the TLP bonding from Sn, and red dashed line shows the final composition for both of the bonding designs.

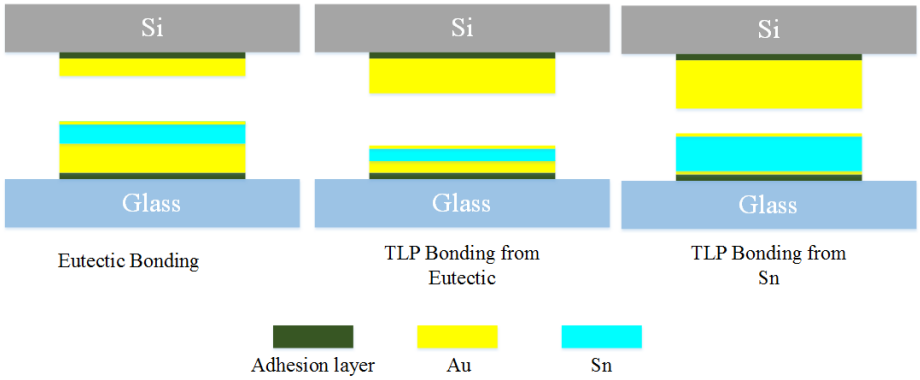

Figure 3.2: Schematic illustration of three main bonding design with various metal thicknesses.

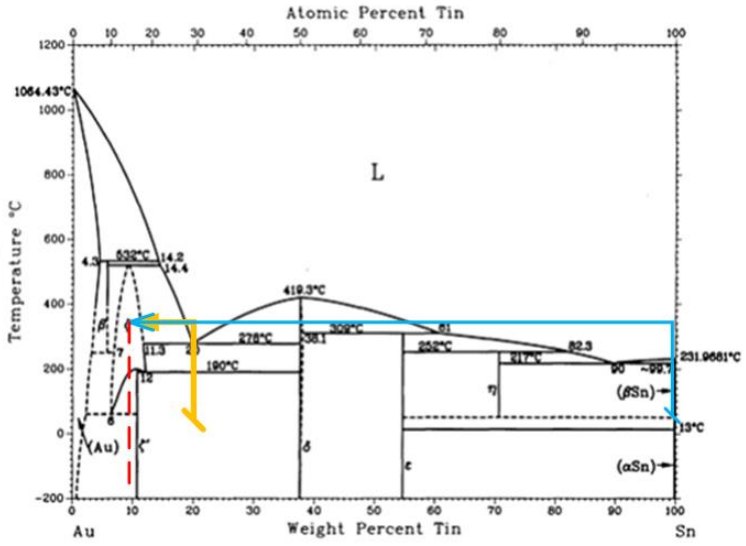

Figure 3.3: Au-Sn phase diagram with expected compositional change during bonding.

3.2.1 Blank Wafer Fabrication

Blank wafer fabrication consisted of three main parts: (i) Bonding metal thickness optimization, (ii) the effect of adhesion layer on bonding metal and (iii) thermal characterization of bonding metal.

Bonding Metal Thickness Optimization

Thickness optimization was performed for Au and Sn film deposition to obtain a fully (100%) eutectic composition. A full homogeneous eutectic is critical to allow the metals melt completely during bonding process. Single crystal Si wafer was used as a substrate blank wafer. TiW was deposited as an adhesion layer for material thickness optimization. TiW/Au 150nm/300nm metal layers were sputtered in AJA sputtering system in one chamber without breaking the vacuum and Varian thermal evaporator system was used for the deposition of Sn. The thickness ratio for Au-Sn eutectic composition is found to be 1.65 when the densities of Au and Sn are taken as 19.30 and 7.36 g/cm^3, respectively. The given densities are for the bulk materials. In this study, thin film metals were deposited with different techniques such as sputter and thermal evaporator. Depending on the metal and deposition technique, structure of the metal may be changed. For example; in sputter technology metals are deposited with flat surface while porous structure is obtained in thermal evaporator. Therefore, for the same thickness values, volume of the metal decreases, thus mass of the deposited metal diminishes. Therefore, thickness optimization should be performed to understand mass relation with deposition technique at the same thicknesses. Figure 3.4 shows schematic illustrations of Sn deposition on Si. As a starting point, Au and Sn thicknesses were chosen 300 nm and 200 nm respectively depending on their bulk densities. Then, thickness of Sn was gradually increased with 50 nm intervals. Table 3.1 shows change in Sn thickness for eutectic alloys. DSC was used like a furnace for optimization of the thicknesses. Controllable heating and cooling were performed in DSC. In addition to controllable heating and cooling, DSC also gave the type of the reaction (endothermic and exothermic). 45°C/min was used for both heating and cooling to mimic the bonder system. After DSC analysis, the 3mmx3mm TiW/Au/Sn coated Si pieces were examined under SEM/EDX for microstructural examination and compositional analysis.

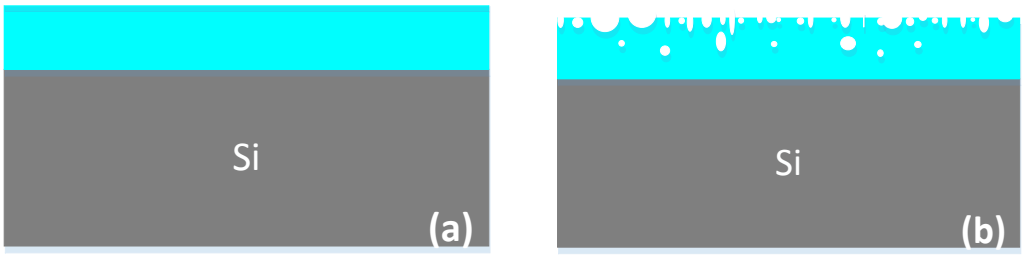

Figure 3.4: Schematic illustrations of Sn coated Si: (a) theoretical thin film deposition in sputter and (b) real thin film deposition with porous structure in thermal evaporator.

Table 3.1: Au-Sn thickness study to obtain eutectic composition.

	Au thickness (nm)	Sn thickness (nm)
Trial 1	300	200
Trial 2	300	250
Trial 3	300	300

The Effect of Adhesion Layer on Bonding Metal

Adhesion layer may be required depending on the metallization type. Particularly for the MEMS fabrication, for example; Au does not adhere to Si wafer and generally thin layer of Cr is needed to hold Au on Si. Adhesion layer plays an important role for the bonding quality. Different type of adhesion layers are frequently used [44]. In this study, Cr, TiW (90% W) and Ti were used to test their effect on bonding metal. The effect of the adhesion layer on bonding metal was observed in the blank wafer fabrication. In order to observe their effect, adhesion layer and Au were deposited on blank Si wafer in the same chamber with sputtering system. Then, Sn was deposited in thermal evaporator. Si wafers were diced and heat treated in the bonder under different conditions. Table 3.2 summarizes the material stack and their heat treatment conditions to reveal adhesion layer effect on bonding material.

Table 3.2: Material stack and their heat treatment condition to understand adhesion layer effect on bonding material.

Material Stack	Under Vacuum	Under N_2
Cr/Au/Sn/Au (50nm/250nm/300nm/50nm)	20min	20min
Cr/Au/Sn/Au (30nm/650nm/500nm/50nm)	20min	20 min
TiW/Au/Sn/Au (150nm/250nm/300nm/50nm)	20min	10min
Ti/Au/Sn/Au (20nm/20nm/460nm/100nm)	20min	-
Ti/Au/Sn/Au (50nm/300nm/350nm/50nm)	-	5min
Ti/Au/Sn/Au (25nm/50nm/600nm/100nm)	-	20min
Ti/Au/Sn/Au (25nm/500nm/600nm/100nm)	-	20min

Thermal Characterization of Bonding Metal

Thermal characterization was performed before and after bonding by using DSC, as well. The aim of the thermal characterization before bonding was to detect at what temperature melting occurs, thus, bonding must be higher than the measured temperature. On the other hand, the aim of thermal characterization after bonding was to find out re-melt temperature of the bonding which is important parameter depending on the application of device. In addition, thermal characterization before

bonding gives important information about the adhesion layer effect on bonding material when it is analyzed under SEM. Metals were deposited on Si wafer and the wafer was diced 3mmx3mm squares. Heating and cooling rate were 45°C/min. Table 3.3 shows different sets of samples that are examined using DSC to observe adhesion layer effect on melting temperature.

Table 3.3: Different sets of samples examined using DSC experiments.

<table>
<tr><th colspan="2">Various Specimens Examined in DSC</th></tr>
<tr><td>Cr/Au/Sn/Au:
30nm/650nm/500nm/50nm</td><td>Cr/Au/Sn/Au
25nm/300nm/350nm/60nm</td></tr>
<tr><td>Bonded

Cr/Au: 30nm/200nm

Cr/Au/Sn/Au:
30nm/650nm/500nm/50nm</td><td>Bonded

TiWAu: 150nm/1µm

TiW/Au/Sn/Au:
150nm/250nm/300nm/50nm</td></tr>
<tr><td>Ti/Au/Sn/Au
50nm/300nm/350nm/60nm</td><td rowspan="2">Bonded

Ti/Au/Sn/Au:
50nm/300nm/350nm/60nm

Ti/Au/Sn/Au:
50nm/300nm/350nm/60nm</td></tr>
<tr><td>TiW/Au/Sn:
150nm/300nm/300nm</td></tr>
</table>

3.2.2 Patterned Wafer Fabrication

Experimental procedure for patterned wafer fabrication starts with the fabrication of substrate and cap. Pyrex Glass wafer was used as substrate wafer and doped single crystal Si wafer was used as cap wafer. The aim of using glass and Si wafer was to make the process easier during bonding alignment. Two masks were required for the dummy bonding process. One mask was used for the metal patterning by lift-off process and the other one is used for cap cavity opening. Therefore, both masks were

dark field. Glass and Si wafer were used as device wafer and cap wafer, respectively. Lithography was performed on glass and Si wafers. Then, adhesion layer and protective Au layer were deposited using sputter techniques. Metal deposition process is completed for cap wafer. Sn and Au deposition was performed to continue fabrication of substrate wafer. Thermal evaporator was used for Sn and protective Au deposition. After Sn deposition, lift-off process was conducted. Acetone, alcohol and DI water cleaning were performed subsequently. If hermeticity testing was required, one more lithography on cap wafer was performed to open cavities. DRIE was used to open around 300μm cavity. Then, cleaning was performed by using first oxygen plasma, then PRS 1000 or SVG 14 polymer cleaners. After cleaning steps, wafers were bonded with various bonding recipes. As a result of blank wafer fabrication, number of bonding trials was decreased. Patterned wafer bonding pairs using different adhesion layers and different metal thicknesses are given in

Figure 3.. The thicknesses and adhesion layer were decided based on the blank wafer fabrication results. It should be noted that SiN was deposited as an adhesion layer for TiW adhesion to Si whenever TiW was used. While packaging processes were performed under vacuum environment, heating the wafer was tried under forming gas for some bonding trials. Heating rate was set to 45°C/min and cooling rate was the maximum available cooling rate attainable with given N_2 to the chamber for each bonding. Bonding temperature was set to 300°C based on Au-Sn phase diagram and literature[13, 48, 50, 51]. Dwell time before force application was set to 2 minutes. Bonding pressure was 3.15 MPa and applied for 20 minutes. After various packaging designs were performed, characterizations started with the optical microscope analysis. Then, acetone test and shear test were performed. Depending on the bonding quality, deflection test method was also applied. The wafer should passed the challenges of acetone test in order to perform deflection method. In addition, the dies should exhibited good mechanical properties. In acetone test, bonded wafer was inserted into acetone.

Schematic Illustration of Bonding Pair	Material Stack and their Thicknesses
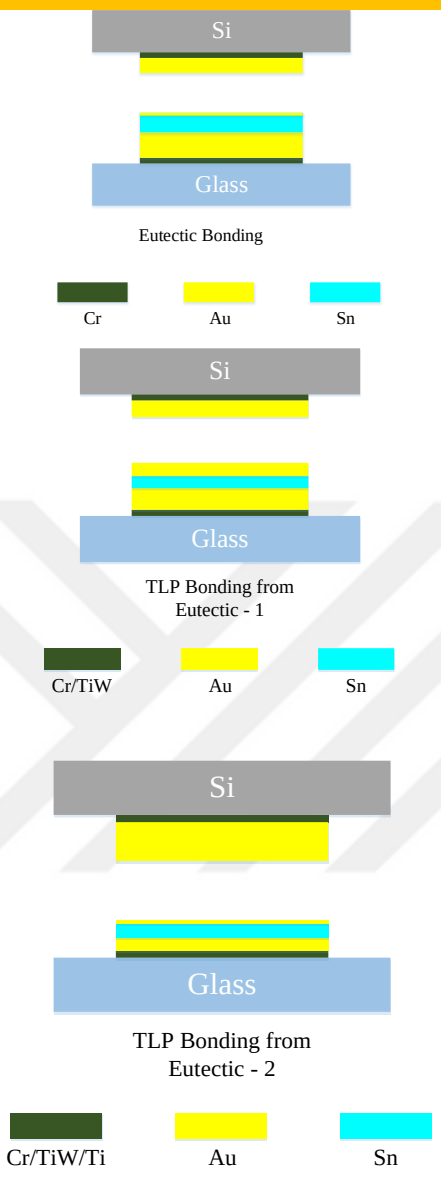	Cr/Au: 30nm/200nm Cr/Au/Sn/Au: 30nm//650nm/500nm/50nm Cr/Au: 30nm/200nm Cr/Au/Sn/Au: 30nm/600nm/300nm/200nm Cr/Au: 30nm/200nm TiW/Au/Sn/Au: 100nm/600nm/300nm/200nm TiW/Au: 150nm/1µm TiW/Au/Sn/Au: 150nm/250nm/300nm/50nm Cr/Au: 25nm/1µm TiW/Au/Sn/Au: 150nm/300nm/350nm/50nm Ti/Au:50nm/1µm Ti/Au/Sn/Au: 50nm/300nm/350nm/60nm Cr/Au:50nm/2µm Ti/Au/Sn/Au: 50nm/600nm/700nm/100nm

Figure 3.5 continued: Patterned wafer fabrication and bonding using different adhesion layers and thicknesses. 5 sort of bonding were designed namely as Eutectic Bonding, TLP Bonding from Eutectic – 1, TLP Bonding from Eutectic – 2, Eutectic Symmetric, and TLP Bonding from Sn.

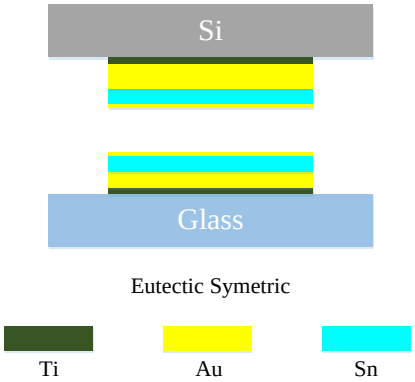

Ti/Au/Sn/Au
50nm/300nm/350nm/60nm
Ti/Au/Sn/Au
50nm/300nm/350nm/60nm

Ti/Au/Sn/Au
50nm/600nm/700nm/100nm
Ti/Au/Sn/Au
50nm/600nm/700nm/100nm

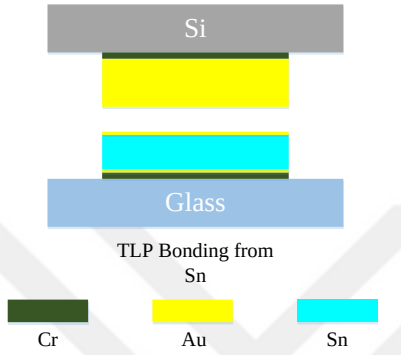

Cr/Au:30nm/2µm
Cr/Au/Sn/Au:
30nm/50nm/500nm/50nm

Figure 3.5 continued: Patterned wafer fabrication and bonding using different adhesion layers and thicknesses. 5 sort of bonding were designed namely as Eutectic Bonding, TLP Bonding from Eutectic – 1, TLP Bonding from Eutectic – 2, Eutectic Symmetric, and TLP Bonding from Sn.

As a result of openings between two wafers, acetone enters into the corridors between the dies and if the bonding is not hermetic, acetone enters into dies, as well. If bonding was hermetic to acetone, new lithography was performed for new run with cavity opening on cap wafer. Then, bonding was performed and cap wafer was thinned down to around 50µm using DRIE. Deflection on the dies were expected due to pressure difference between the outside and inside die. If the bonding was hermetic, the deflection on the wafer was permanent. The failed part was investigated by using SEM and EDS.

3.3 Results and Discussion

Thickness optimization was one of the most important parameters because it was directly related to melting characteristic of the deposited metal. As predicted, thin film characteristic of deposited metals were different than bulk metal characteristic, especially for the Sn. After metal depositions, SEM images, from cross section and top, were taken for different structures; it was found out that deposited Sn had porous structure shown in Figure 3.6, which exhibits SEM images: (a) cross sectional view of TiW/Au/Sn and (b) top view of the 300nm Sn deposited directly on Si wafer. It is clearly seen from the images that Sn had porous structure when it was deposited by thermal evaporator.

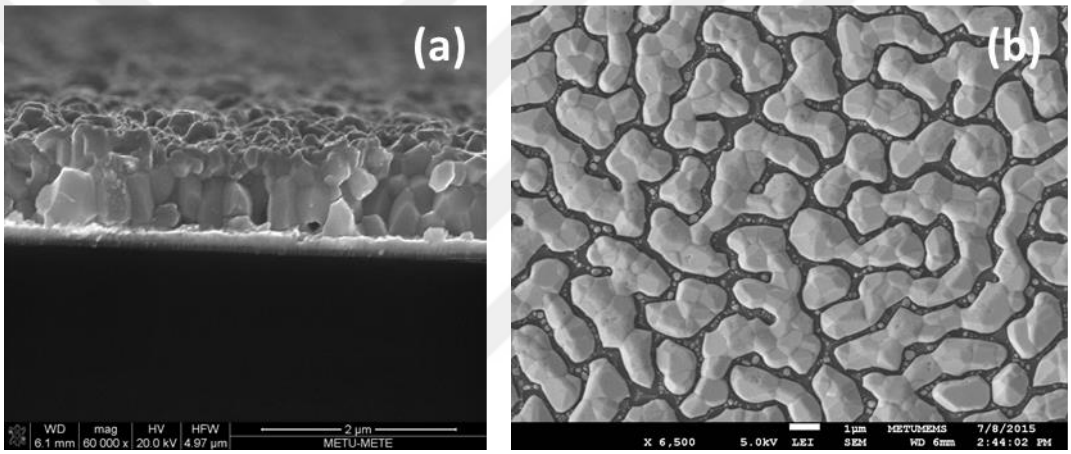

Figure 3.6: SEM images: (a) TiW/Au/Sn from cross sectional view, (b) 300nm Sn deposited directly on Si wafer from top view of the.

As a result of porous structure of Sn, probably effective volume of Sn with same thickness was decreased. Therefore, while 300nm Au and 200nm Sn creates eutectic composition in theory, it does not corresponds to theoretical eutectic composition in practice. After DSC experiments, SEM images were taken from top view for Au/Sn 300nm/200nm 300nm/250nm and 300nm/300nm thicknesses. Au/Sn 300nm/200nm showed partially eutectic microstructure with proeutectic phase. When thickness of Sn was increased 50 nm, the amount of eutectic microstructure was also increased which can be seen in Figure 3.8. Full eutectic composition was obtained with

TiW/Au/Sn 150nm/300nm/300nm sample. Figure 3.7 shows SEM image of TiW/Au/Sn 150nm/300nm/200nm.

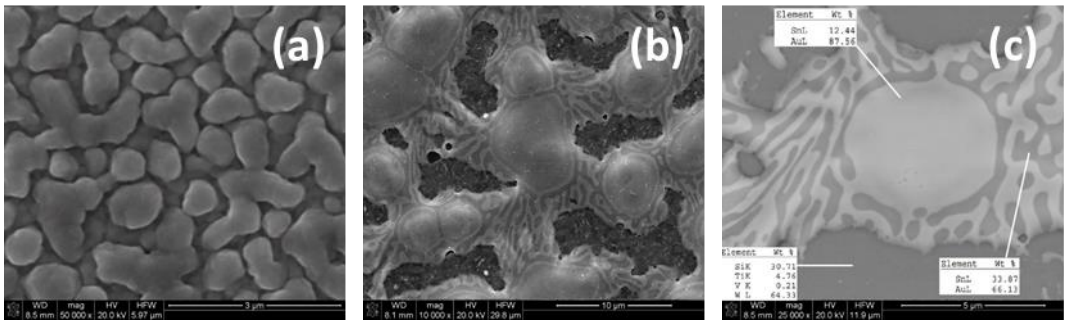

Figure 3.7: SEM image of TiW/Au/Sn 150nm/300nm/200nm: (a) as deposited, (b) after DSC experiment and (c) BSE/SEM image after DSC experiment.

Figure 3.8 and Figure 3.9 show SEM images of the TiW/Au/Sn/ 150nm/300nm/250nm and TiW/Au/Sn/ 150nm/300nm/300nm after DSC experiment, respectively. It can be concluded from the SEM images that 300nm Au and 300nm Sn corresponds to eutectic composition instead of the theoretically predicted 300nm Au and 200nm Sn values.

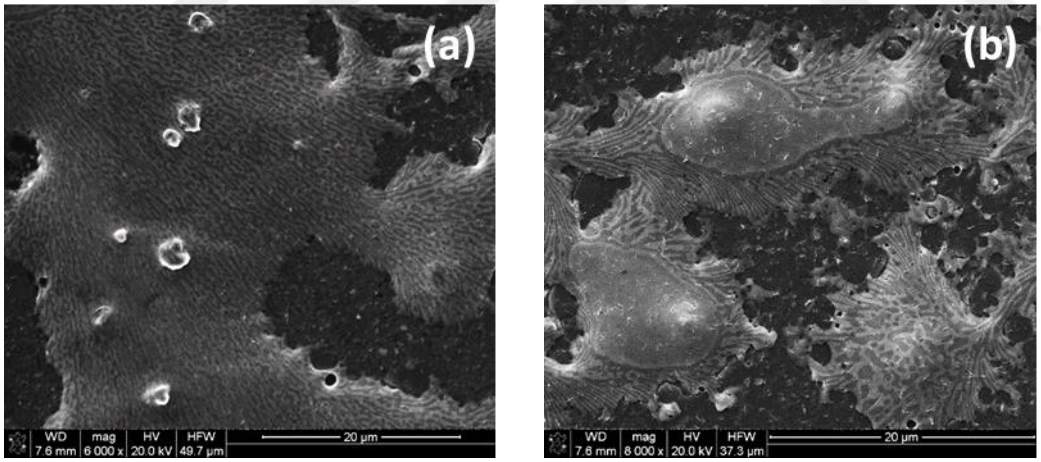

Figure 3.8 SEM images of TiW/Au/Sn 150nm/300nm/250nm after DSC experiment: (a) without proeutectic phase and (b) with proeutectic phase.

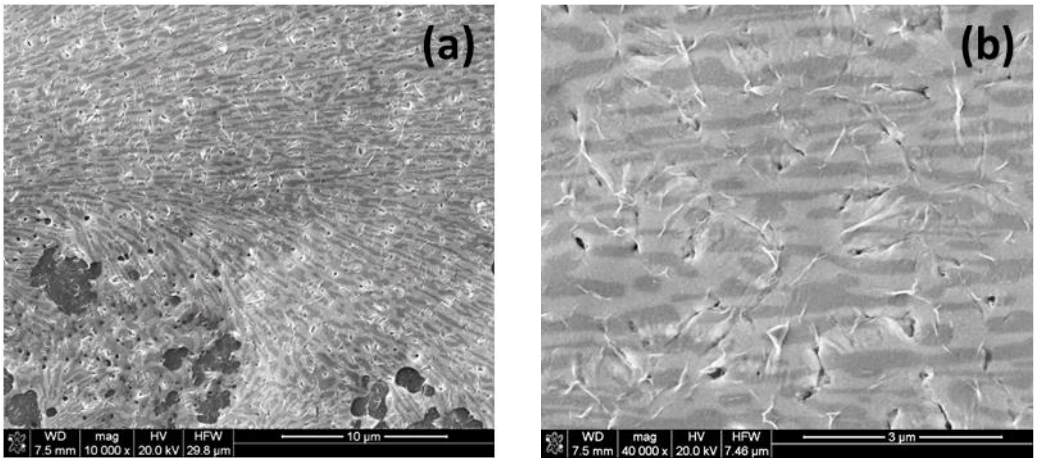

Figure 3.9: SEM images of TiW/Au/Sn 150nm/300nm/300nm after DSC experiment: (a) general view and (b) magnified view.

Depending on the process, Cr, TiW or Ti can be used as an adhesion layer. Therefore, to test their effect on deposited metal various heat treatments were applied. Figure 3.10 exhibits top SEM images of the Au/Sn/Au coated samples with Cr adhesion layer. Samples were heat treated to observe effect of adhesion layer Cr and effect of heating environment. For low thickness coatings as Figure 3.10, Cr prevents melting of Au/Sn metal probably due to diffusion of Cr into Au/Sn.

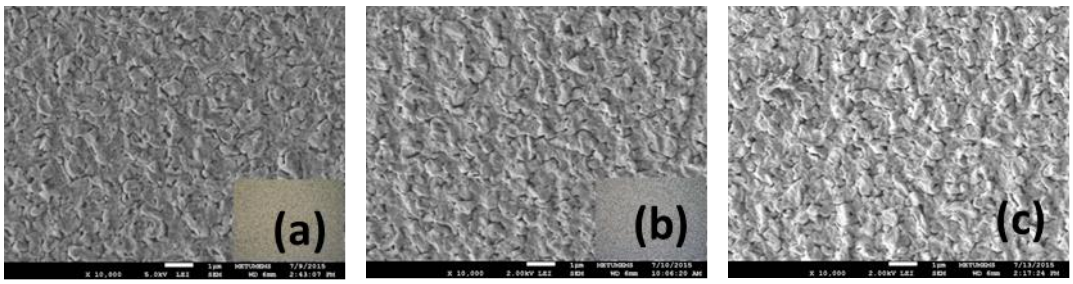

Figure 3.10: SEM images of Cr/Au/Sn/Au 50nm/250nm/300nm/50nm: (a) as deposited, (b) after heat treatment at 300°C under vacuum for 20 minutes and (c) after heat treatment at 300°C under N_2 for 20 minutes.

Cr adhesion layer effect was also tested for higher thickness values such as Au/Sn/Au 650/500/50nm. Figure 3.11 shows the SEM images of Cr/Au/Sn/Au 30nm/650nm/500nm/50nm with different annealing processes. However, there was again no change in the microstructure of the Au-Sn surface.

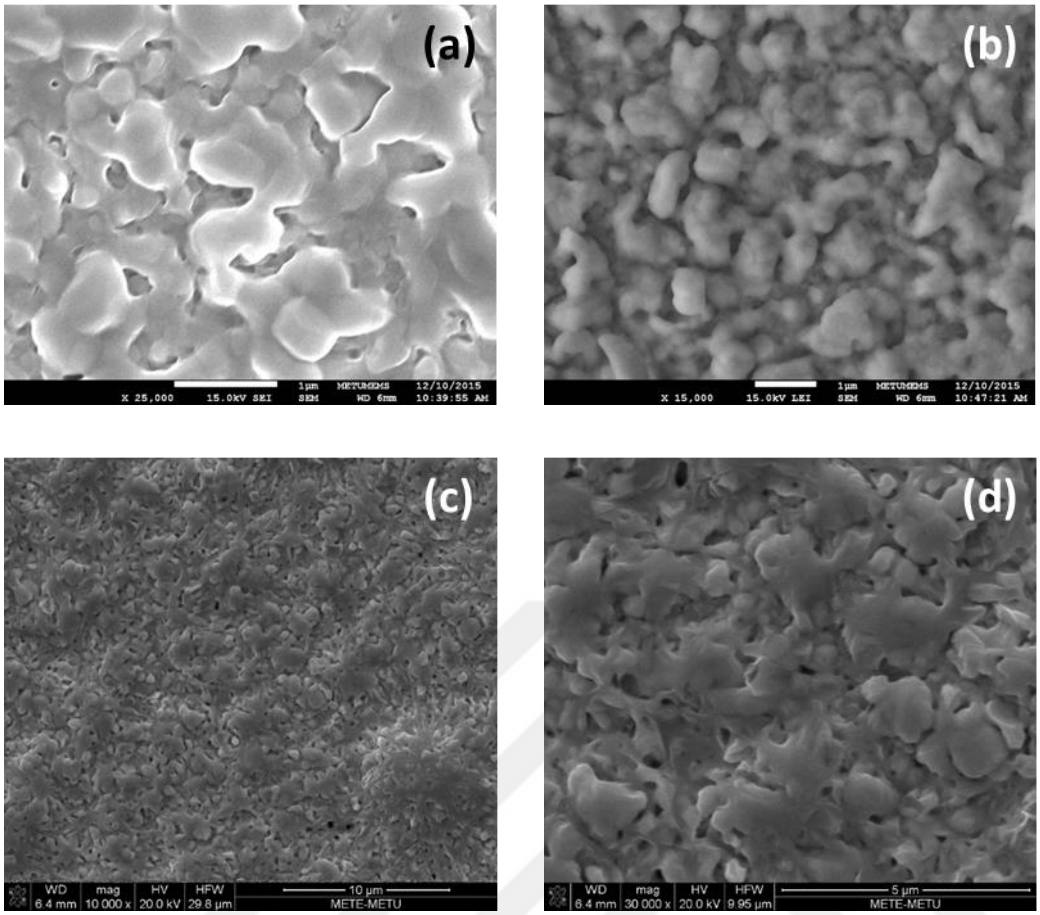

Figure 3.11: Top SEM images of the Cr/Au/Sn/Au 30nm/650nm/500nm/50nm: (a) as deposited, (b) heat treatment at 300°C under vacuum for 20 minutes, (c) and (d) heat treatment at 300°C under N_2 for 20 minutes.

After the effect of Cr was observed on thin film Au-Sn, TiW was examined as an adhesion layer. Figure 3.12 shows top SEM images of the as deposited Au/Sn/Au samples with TiW adhesion layer. Samples were heat treated to observe effect of adhesion layer (TiW) and effect of heating environment. TiW did not prevent melting of metals like Cr did; however, heating environment importance was found out. Under N_2 environment, heating provides melting of metals. Figure 3.13 shows how heating environment affected the melting characteristic of the alloy. While melting was not observed in Figure 3.13 (a), eutectic microstructure is observed easily in Figure 3.13 (b). In summary, heat treatment study of TiW tells us about importance of heating environment.

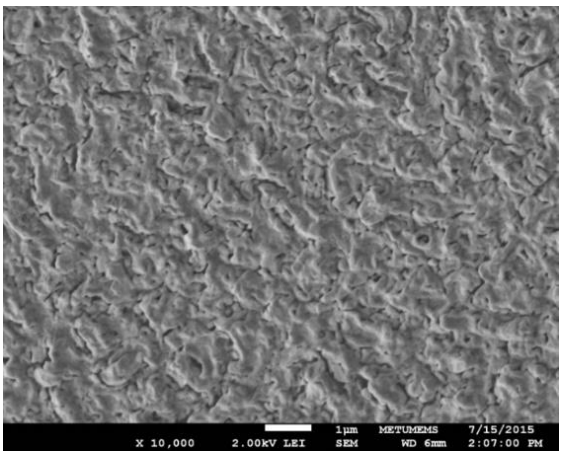

Figure 3.12: Top SEM images of the as deposited TiW/Au/Sn/Au 150nm/250nm/300nm/50nm.

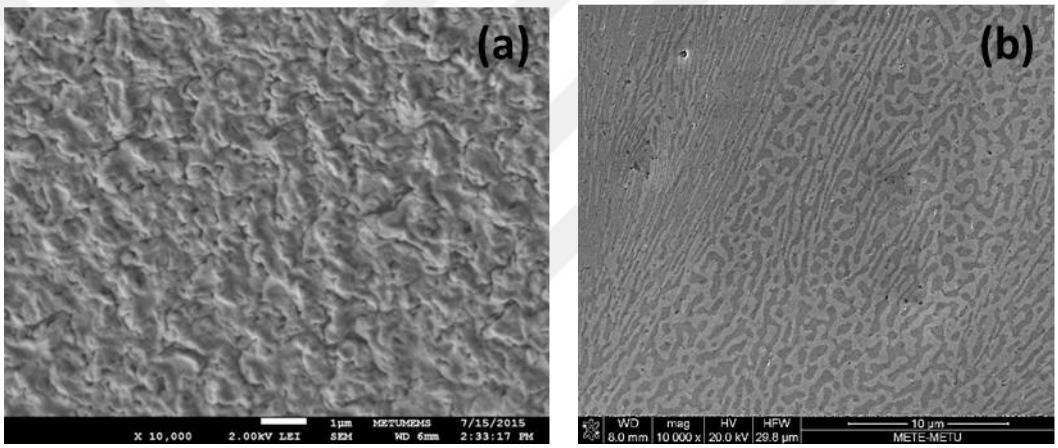

Figure 3.13: Top view SEM images of the TiW/Au/Sn/Au 150nm/250nm/300nm/50nm: (a) after heat treatment at 300°C under vacuum for 20 minutes and (b) after heat treatment at 300°C N_2 for 10 minutes.

Ti was another alternative as an adhesion layer. Figure 3.14 shows top view SEM images of the Au/Sn/Au samples with Ti adhesion layer. Samples were heat treated to observe effect of adhesion layer Ti and effect of heating environment. Some intermetallics were observed. Melting was observed under N_2 heating to 300°C for 5 minutes. Figure 3.15 shows the top view SEM image of Ti/Au/Sn/Au 20nm/20nm/460nm/100nm specimen both at as deposited and heat treated state. Sample was heated to 300°C under vacuum and it was hold at that temperature for 20 minutes.

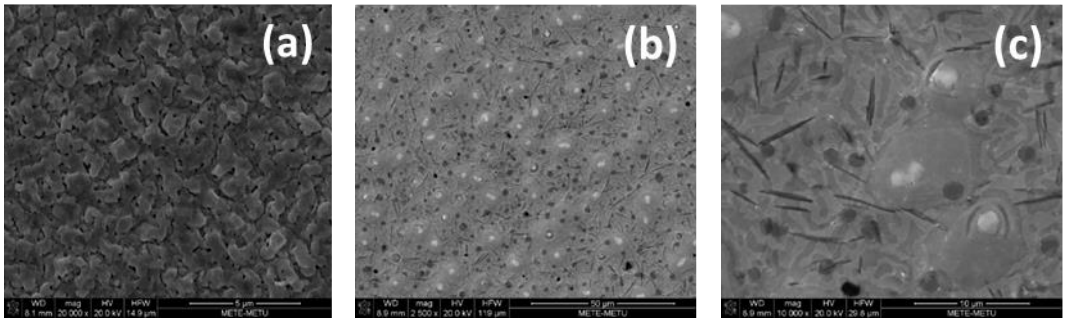

Figure 3.14: Top view SEM images of Ti/Au/Sn/Au 50nm/300nm/350nm/50nm: (a) as deposited, (b) general view after heat treatment at 300°C for 5 minutes under N_2 and (c) magnified view after heat treatment at 300°C for 5 minutes under N_2.

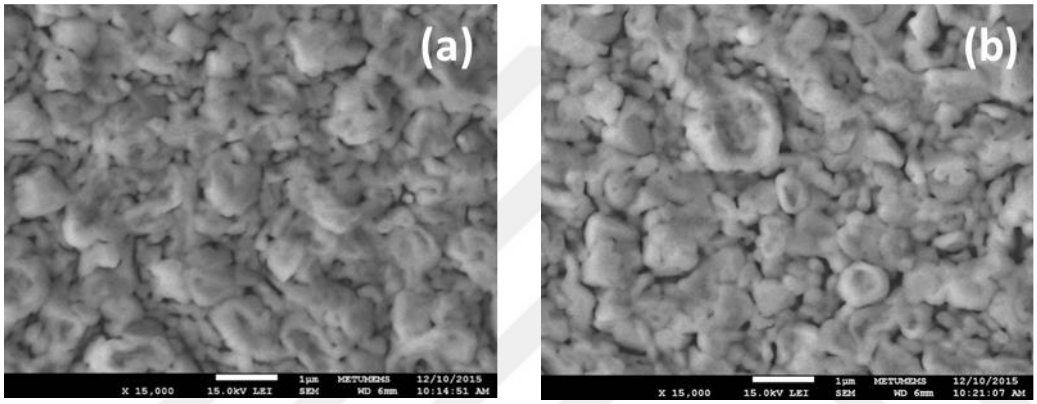

Figure 3.15: Top view SEM image of Ti/Au/Sn/Au 20nm/20nm/460nm/100nm: (a) as deposited and (b) after heat treatment at 300°C for 20 minutes under vacuum.

Almost pure Sn with Ti/Au/Sn/Au 20nm/50nm/600nm/100nm was heated under N_2 as well and melting was observed with porous structure. Figure 3.16 shows top view SEM image of Ti/Au/Sn/Au 20nm/50nm/600nm/100nm after heat treatment process at low and high magnification. Heat treatment with eutectic composition again by using Ti as an adhesion layer was also performed. Ti/Au/Sn/Au 25nm/500nm/600nm/100nm sample was heated to 300°C for 20 minutes under N_2 and melting was observed. Figure 3.17 shows top view SEM image of the Ti/Au/Sn/Au 25nm/500nm/600nm/100nm sample after heat treatment process with (a) general view and (b) magnified view. One can observe the intermetallic in Figure 3.17 (b) which was not formed when Cr or TiW were used as adhesion layer.

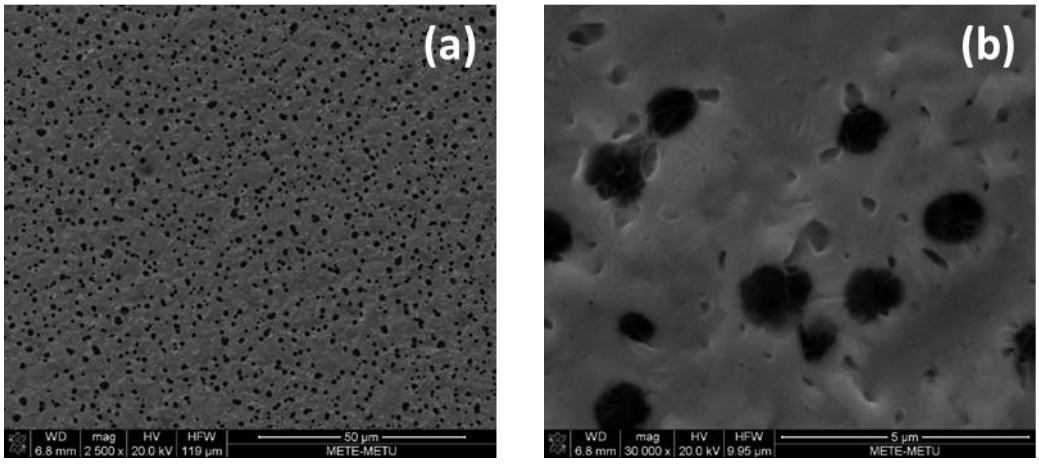

Figure 3.16: Top view SEM image of Ti/Au/Sn/Au 20nm/50nm/600nm/100nm after heat treatment at 300°C for 20 minutes under N_2: at (a) low and (b) high magnifications.

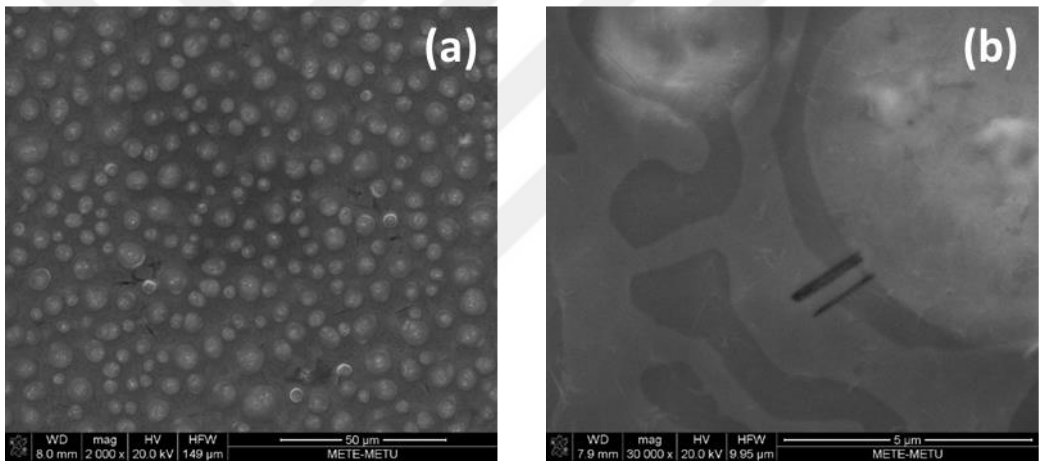

Figure 3.17: Top SEM images of the Ti/Au/Sn/Au 25nm/500nm/600nm/100nm after heat treatment at 300°C for 20 minutes under N_2: at (a) low and (b) high magnifications.

In summary of adhesion layer effect study, ternary and diffusion effect were observed due to low thicknesses of Au/Sn. While Cr prevented melting of the metals as a results of diffusion, TiW did not affect the metals due not its refractory characteristic.

DSC experiments were performed for different designs before and after bonding. The results directly gave information about at which temperature exothermic or endothermic reaction occurred. The results are given in Figure 3.18, Figure 3.19 and

Figure 3.20. The peaks towards down corresponds to endothermic reaction while the peaks on the graphs towards up means exothermic reaction take place at that temperature. Previously, Cr effect on bonding material in terms of preventing melting was checked by the DSC analysis, as well. Figure 3.18 (a) and (c) prove the Cr effect. There is no endothermic peak at the graphs shown in Figure 3.18 (a) and (c). On the other hand, endothermic peaks are clearly seen in Figure 3.18 (b) and (d) with TiW and Ti adhesion layers, respectively.

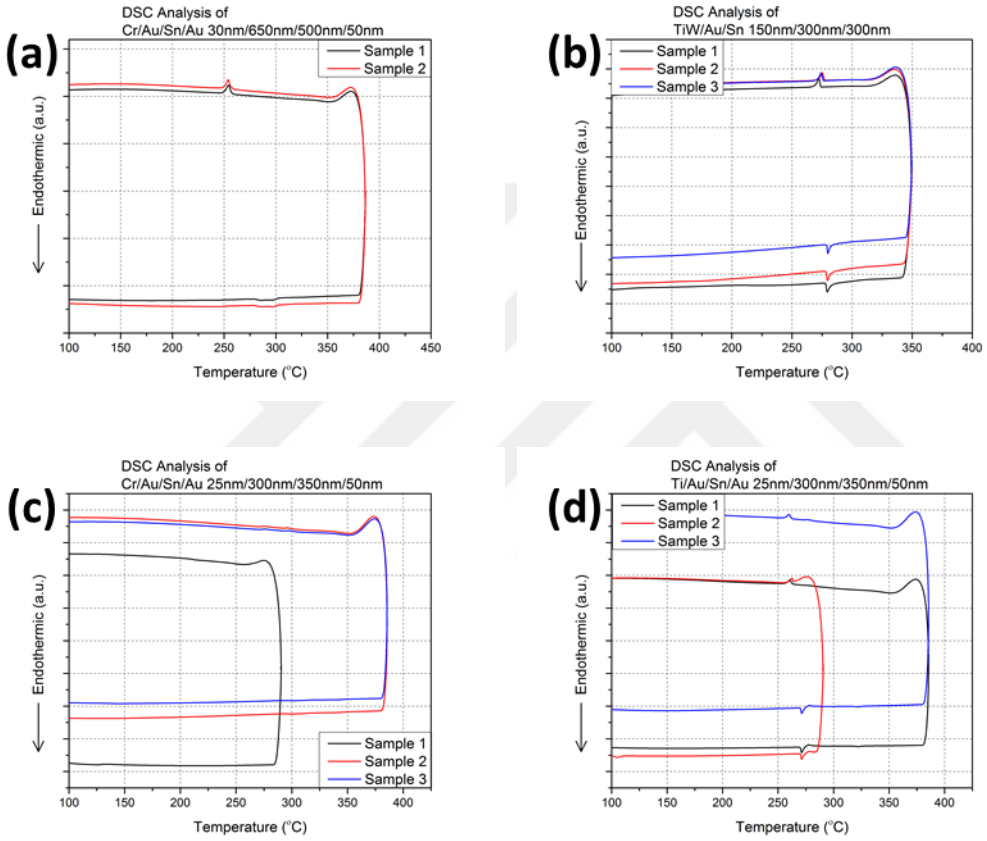

Figure 3.18: DSC analysis of single side metal deposited samples: (a) Cr/Au/Sn/Au 30nm/650nm/500nm/50nm, (b) TiW/Au/Sn 150nm/300nm/300nm, (c) Cr/Au/Sn/Au 25nm/300nm/350nm/50nm and (d) Ti/Au/Sn/Au 25nm/300nm/350nm/50nm.

DSC analysis was performed for bonded samples to detect re-melt temperature of the bonding. Two different bonding were performed as full wafer using Cr or Ti adhesion layers. Both bonding structure had eutectic composition, thus endothermic reaction

were observed at eutectic temperature at around 278°C, while heating the samples. Figure 3.19 shows DSC analysis of eutectic bonded samples: (a) with Cr adhesion layer and (b) with Ti adhesion layer.

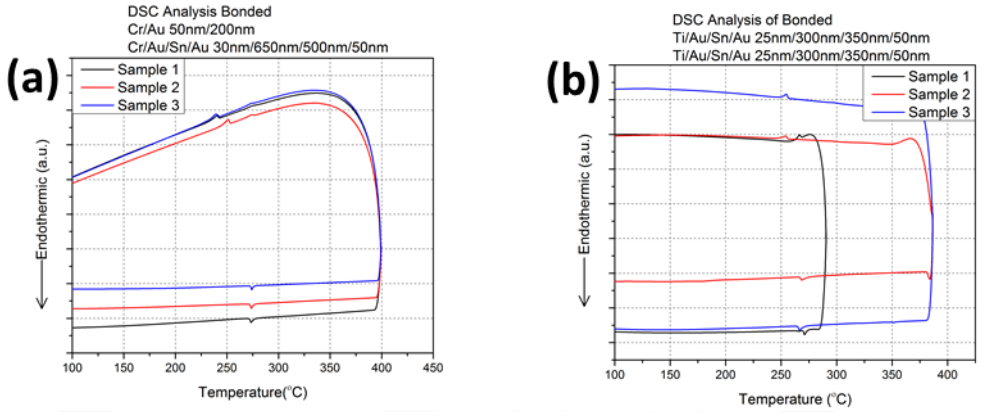

Figure 3.19: DSC analysis of the bonded sample: (a) Cr/Au 50nm/200nm – Cr/Au/Sn/Au 30nm/650nm/500nm/50nm and (b) Ti/Au/Sn/Au 25nm/300nm/350nm/50nm – Ti/Au/Sn/Au 25nm/300nm/350nm/50nm.

One more DSC analysis was performed for TLP bonding using TiW adhesion layer. DSC analysis proved that there was no endothermic reaction while heating the specimen to 500°C in DSC. Figure 3.20 shows DSC analysis of the bonded sample with TLP method showing high re-melt temperature when using TiW as the adhesion layer.

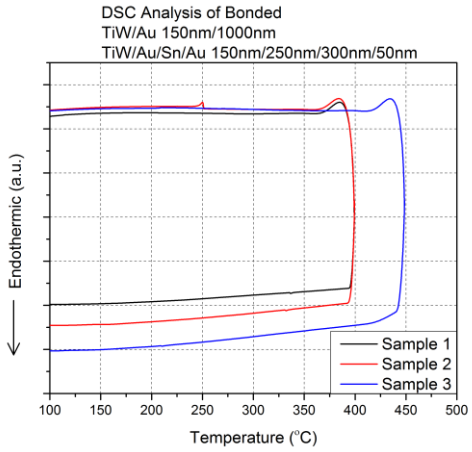

Figure 3.20: DSC analysis of the bonded sample showing high re-melt temperature TiW/Au 150nm/1000nm – TiW/Au/Sn/Au 150nm/250nm/300nm/50nm.

According to DSC analysis, one can say that melting was observed between 270°C and 280°C, which were close to theoretical eutectic temperature. Thus, the bonding temperature was chosen as 300°C for Au-Sn bonding. After analyzing metals on the blank wafer fabrication process, patterned wafer fabrication was started.

First bonding trial was the Au-Sn Eutectic Bonding at 300°C. The design consists of Cr/Au 30nm/200nm on the substrate wafer and Cr/Au/Sn/Au 30nm//650nm/500nm/50nm on the cap wafer. Figure 3.21 shows pictures representing (a) the photo of the eutectic bonding after dicing and (b) the optical microscope image with little amount of squeeze out. One can say that fully melting was obtained, according to squeeze out metals, observed in optical microscope analysis. After dicing process, shear test was applied with universal tensile test machine. Figure 3.22 shows the photo of the dies after shear test, applied with the help of Cu plate. Table 3.4 exhibits the shear test results of Au-Sn Eutectic Bonding. Shear test was applied with the help of Cu plates.

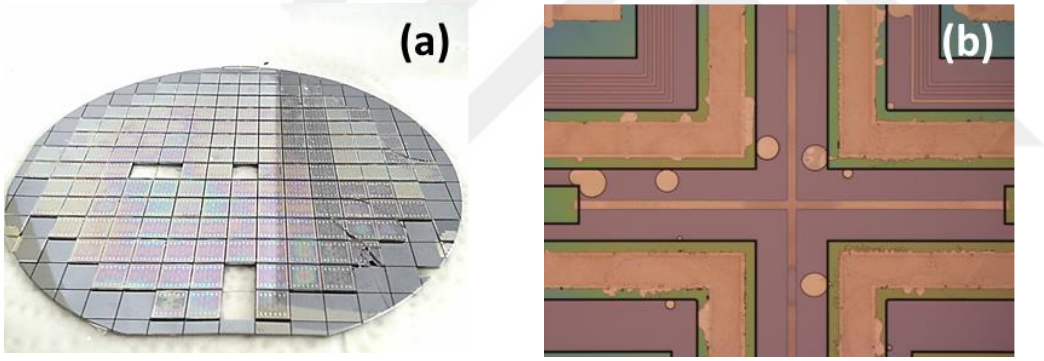

Figure 3.21: Pictures: (a) the photo of the eutectic bonding after dicing and (b) the optical microscope image with little amount of squeeze out.

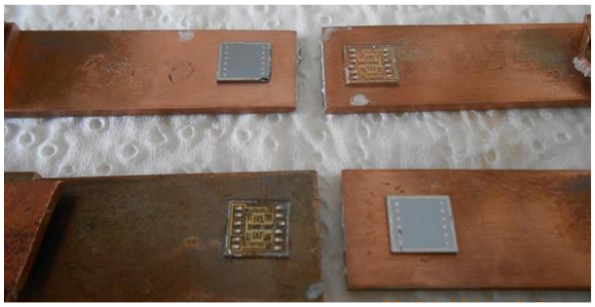

Figure 3.22: The photo of the dies after the shear test.

Table 3.4 The shear test results of Eutectic Bonding. Shear test applied with the help of Cu plates.

Die #	1	2	3	4	5	6	7	8	9	10
Strength (MPa)	20.8	29.0	34.6	19.2	11.6	13.5	24.9	31.6	36.4	29.1
Average Strength:25.1 MPa					Standard Deviation:8.6 MPa					

Bonding layer structure was appropriate for accelerometer device, so Eutectic Bonding applied to device directly. Figure 3.23 exhibits SEM image of a packaged chip. EDS analysis (bottom right) shows that the bonding metal composition is eutectic composition.

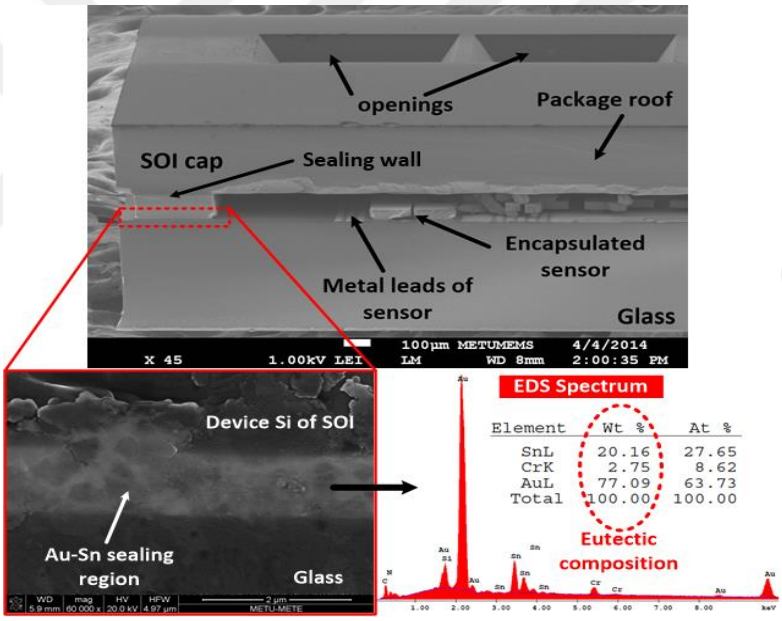

Figure 3.23: SEM image of a packaged chip. EDS analysis (bottom right) shows that the bonding metal composition is eutectic composition [52].

MEMS resonator was tested at different pressure levels in a controlled pressure environment after the wafer-level packaging process. The cavity pressure was measured as 250 mTorr which can be further decreased by applying getter activation [52]. The only problem in this packaging was the yield. Only 30% of dies on the wafer was hermetic.

In this packaging process, Ti was used as a getter. Getter could not be activated at 300°C, therefore, for the activation of the getter, TLP bonding was designed. In TLP Bonding from Eutectic-1study Cr and TiW were used separately. After TLP Bonding from Eutectic-1 using Cr as an adhesion layer, shear test was applied and failure analysis was performed. Two main broken surfaces were observed during failure analysis. First one was between the bonding metals and second one was between the bonding metal and Si wafer. This situation proved that Cr was not enough strong or Cr was lost during bonding due to diffusion. Figure 3.24 shows at low and high magnifications SEM image of the fracture surface on Si side of the packaged die.

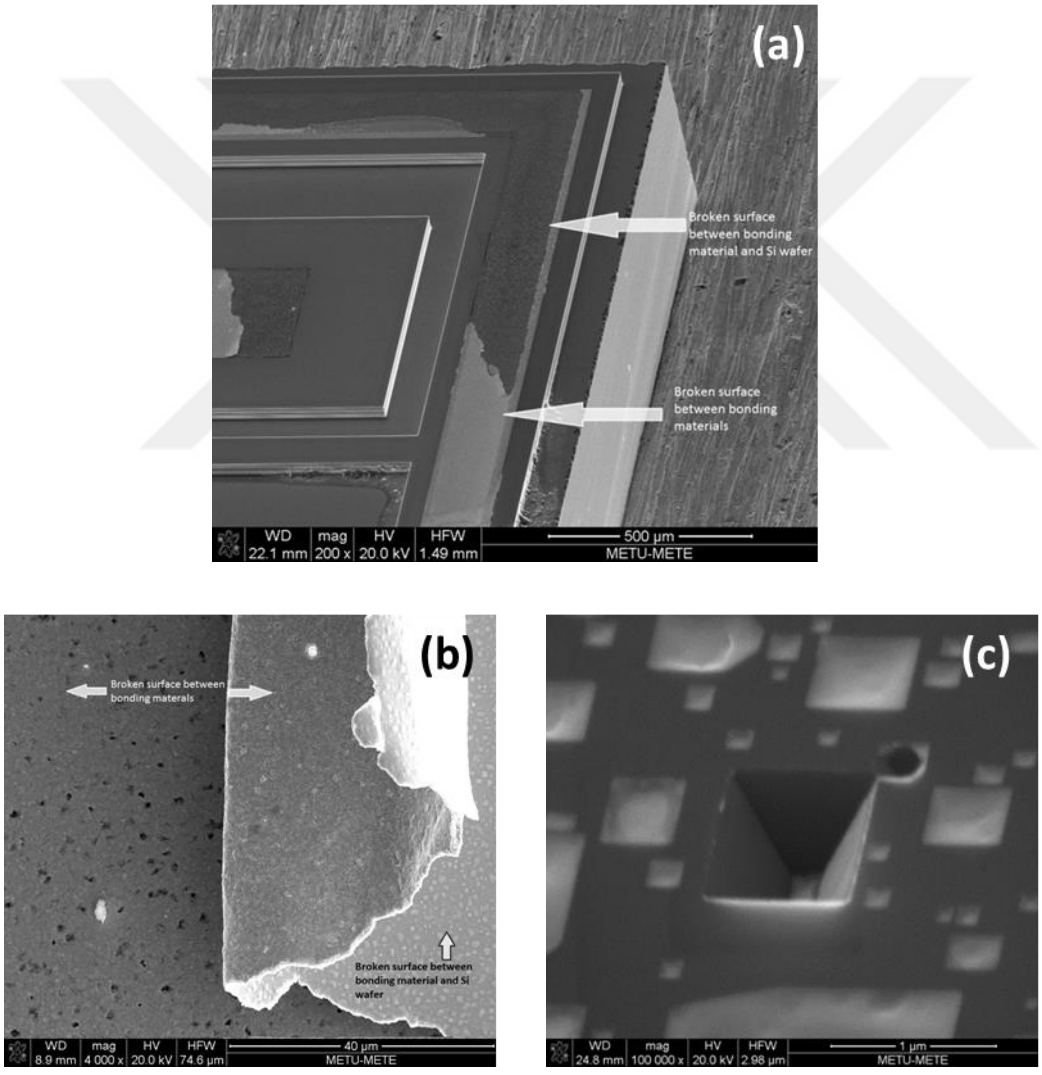

Figure 3.24: SEM image of fracture surface of the packaged chip after shear test applied: (a) Si side, (b) glass side and (c) magnified view of Si side [53].

According to these analysis, it can be concluded that almost all materials stickled to the glass side. Loss of adhesion layer property might decrease the yield of successful bonding. Same bonding structure was also applied with TiW adhesion layer. The specimen was prepared using cutter directly, thus bonding region was seen flat. This SEM image, seen in Figure 3.25, let the bonding promising. Figure 3.25 shows cross sectional SEM image of TLP Bonding from Eutectic-1 structure with TiW adhesion layer.

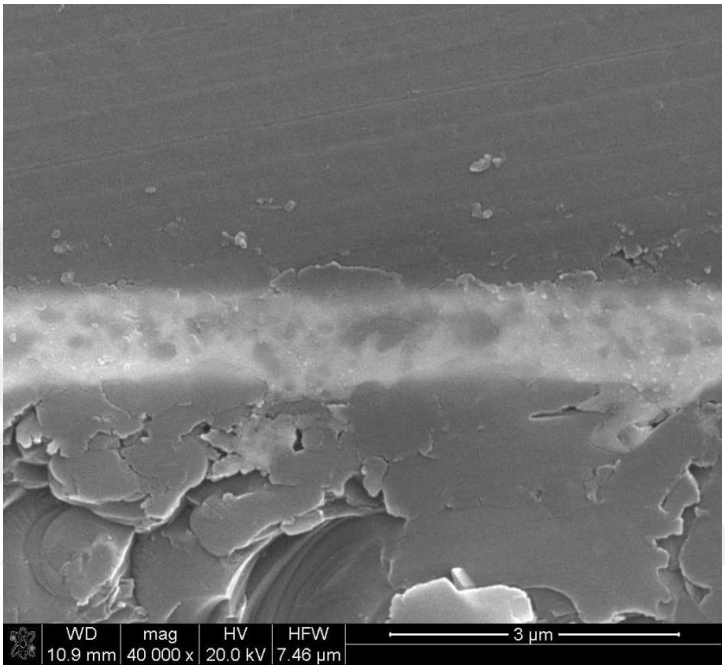

Figure 3.25: Cross sectional SEM image of TLP Bonding from Eutectic-1 structure with TiW adhesion layer.

Cross sectional SEM image was found reasonable to initiate the shear test for TLP Bonding from Eutectic-1 structure with TiW adhesion layer. Universal shear test machine was used for this bonding. Figure 3.26 shows the wafer map showing shear test results of the TLP Bonding Eutectic-1 structure with TiW adhesion layer. 37 samples were tested. Average shear strength and standard deviation were found as 18.4 MPa and 9.6 MPa, respectively. After observing promising shear test results, thinning of the cap wafer was applied to observe hermeticity of the bonding. Figure 3.27 shows the photo of the bonded and thinned wafer. Deflection was observed after

thinning Si cap wafer to 50µm thickness. Bonding was TLP Bonding Eutectic-1 structure with TiW adhesion layer.

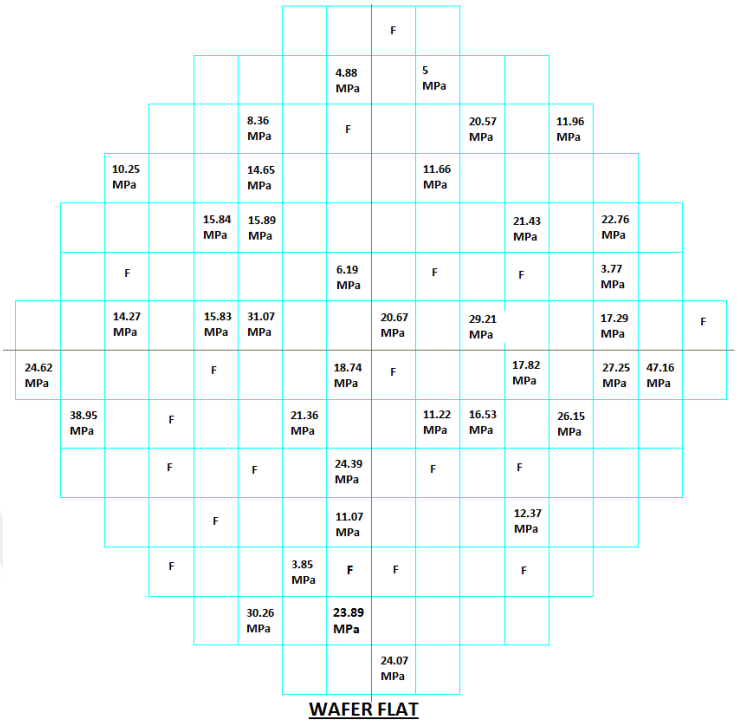

Figure 3.26: The wafer map showing shear test results of the TLP Bonding Eutectic-1 structure with TiW adhesion layer. F means fail during insertion of die into the system.

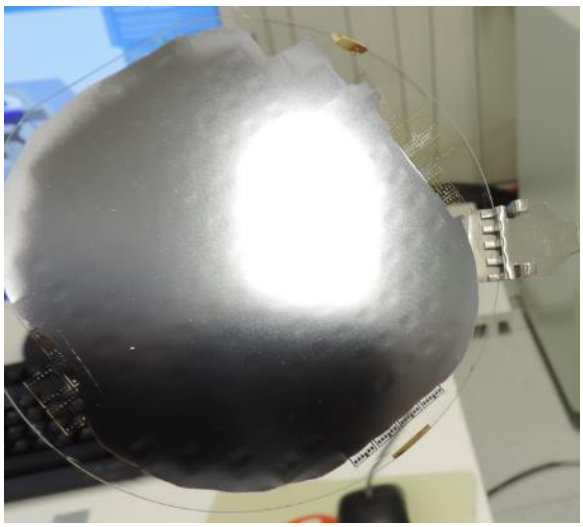

Figure 3.27: Photo of the bonded and thinned wafer. Deflection is observed after thinning Si cap wafer to 50µm thickness.

Deflection proved that pressure of the outside, which is 1 atm, was higher than inside pressure of the dies. Unfortunately, after 20 minutes, deflection was lost. It meant that there were some leakage of gas. Pressure of inside and outside of the dies were balanced, thus deflection was disappeared. It was clear that there was problem related with hermeticity even if shear test results were good. After observing problem with hermeticity, it was thought that amount of liquid during bonding and wetting may be inadequate so void may remain after bonding. Thus, TLP Bonding from Eutectic-2 design was applied with different metal thicknesses and different adhesion layers.

First results of the TLP Bonding from Eutectic-2 was obtained with TiW adhesion layer. Figure 3.28 shows cross sectional SEM image of the TLP Bonding from Eutectic-2 with TiW adhesion layer. Heating and bonding were performed under vacuum. Sample preparation was not performed directly using dicer. Dicer and razor blade were used respectively for sample preparation. Linear crack was observed. Actually, this line positioned itself on the where wafers touch each other. This was proved by measuring the metal thicknesses on the TiW. One side was around 550 µm and the other side was around 1.1 µm. These thicknesses proved that there was almost no interaction between the cap and the substrate wafer.

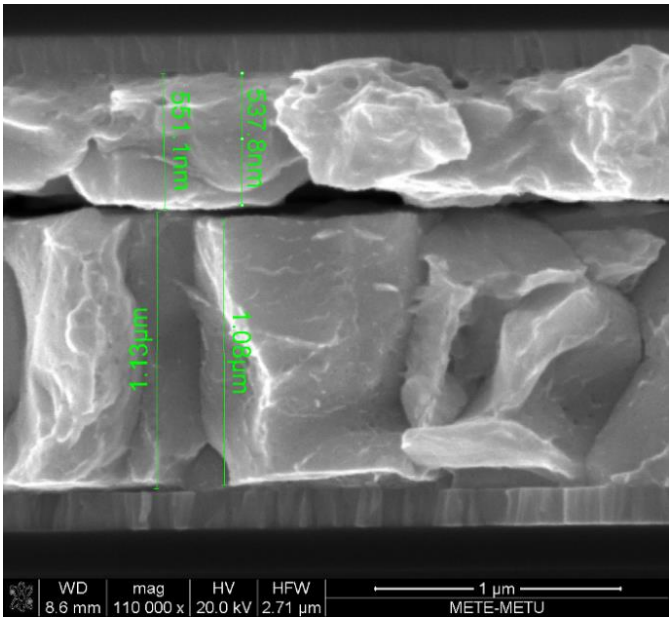

Figure 3.28: Cross sectional SEM image of the TLP Bonding from Eutectic-2 with TiW adhesion layer.

It should be noted that wafers bonded together even if there was no complete liquid formation. Some regions were bonded with thermocompression and some by liquid formation. TEM analysis was performed in order to find out the interaction in detailed manner. Figure 3.29 shows the bright field TEM image of the TLP Bonding from Eutectic-2 with TiW adhesion layer sample the numbers shows the positioning where EDS analysis was performed. Table 3.5 exhibits the corresponding EDS results. Cracks were formed unintentionally during etching in FIB.

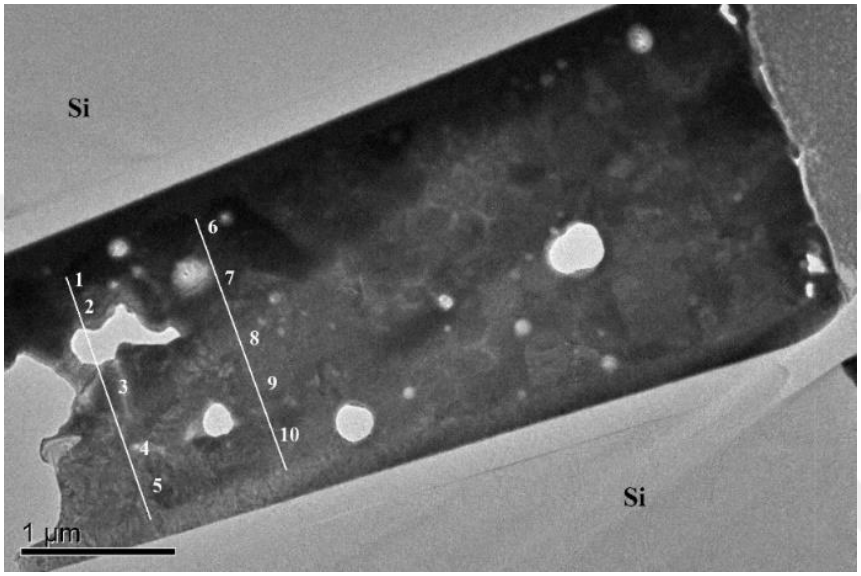

Figure 3.29: The bright field TEM image of the TLP Bonding from Eutectic-2 with TiW adhesion layer.

Table 3.5: The EDS results of TEM sample shown in Figure 3.29.

Points	w%Au	w%Sn	Points	w%Au	w%Sn
1	95.6	4.4.	6	95.6	4.4
2	100.0	0.0	7	98.6	1.4
3	96.4	3.6	8	94.5	5.5
4	99.4	0.6	9	99.0	1.0
5	92.3	7.7	10	99.2	0.8

In blank wafer fabrication, TLP Bonding from Eutectic-2 with TiW adhesion layer exhibits no melting up to 500°C. EDS analysis in TEM shown in Table 3.5 shows that the overall composition was almost pure Au which explains the high melting point.

As the other design, Cr/Au 25nm/1µm on glass and TiW/Au/Sn/Au 150nm/300nm/350nm/50nm on Si wafer was coated and bonded. Heating was performed under N_2 up to 300°C. Cr was inserted to glass side to be able to perform piranha cleaning for better bonding. After bonding, squeeze out was observed, which was good evidence for high quality bonding, as liquefaction was clearly detected. Figure 3.30 shows the optical microscope image from glass of the Au-Sn TLP bonding from Eutectic-2 using Cr on glass side and TiW on Si side.

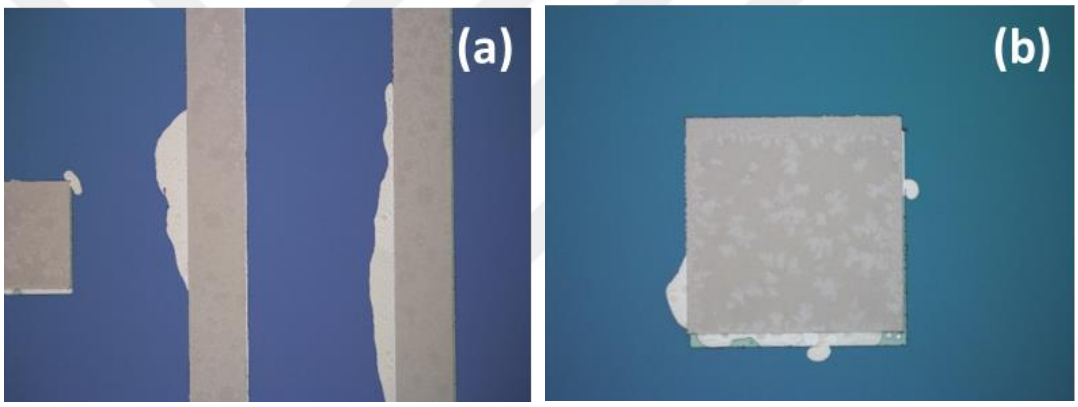

Figure 3.30: The optical microscope image from glass of the Au-Sn TLP bonding from Eutectic-2 300°C under N_2 atmosphere for 2 minutes: at (a) bonding line and (b)via region.

Figure 3.31 shows the photo of the bonded wafer TLP Bonding from Eutectic-2 with Cr on glass side. Acetone entered into some dies but still most of them survive. After dicing, shear test was applied and fracture analysis was performed. In this test, Dage 4000 Bondtester was used. Table 3.6 exhibits shear test result of the TLP Bonding from Eutectic-2 with Cr on glass side and TiW on Si side. Shear forces were relatively low.

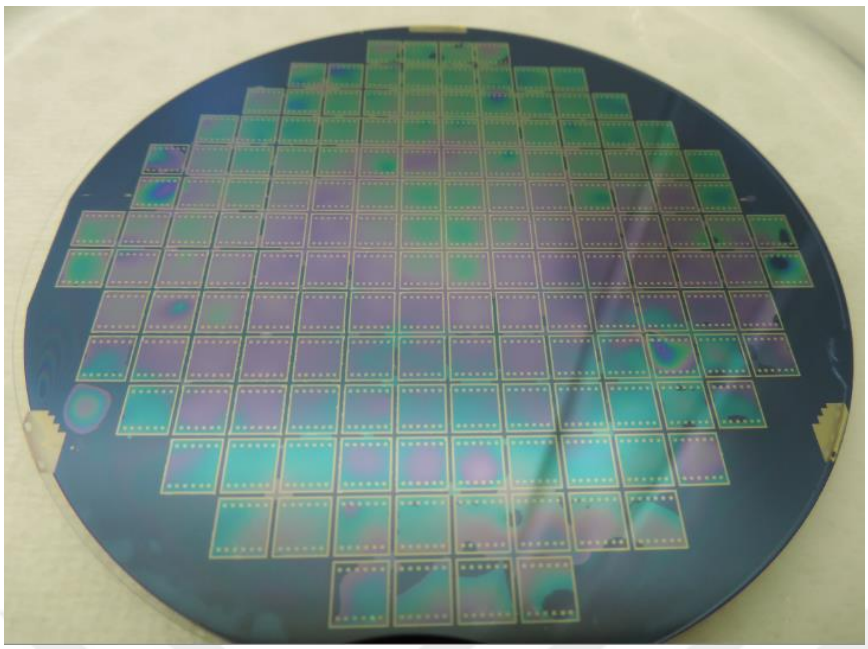

Figure 3.31: Photo of the bonded wafer TLP Bonding from Eutectic-2 with Cr on glass side and TiW on Si side.

Table 3.6: Shear test result of the TLP Bonding from Eutectic-2 with Cr on glass side and TiW on Si side.

Die #	1	2	3	4	5	6	7	8	9	10
Shear Strength (MPa)	5.8	4.7	5.9	7.1	6.3	7.4	13.4	7.7	7.0	9.9
Average Withstanding Force: 7.5 MPa					Standard Deviation: 2.5 MPa					

There was problem due to the low shear strength observed in TLP bonding from Eutectic-2 with Cr on glass side and TiW on Si side. SEM/EDS analysis was conducted to understand possible reasons of the low quality bonding. Figure 3.32 shows SEM image: (a) of Si and (b) of glass with EDS analysis. All of the bonding materials stayed on the glass side which means that there was an adhesion problem between the liquid Au-Sn and TiW.

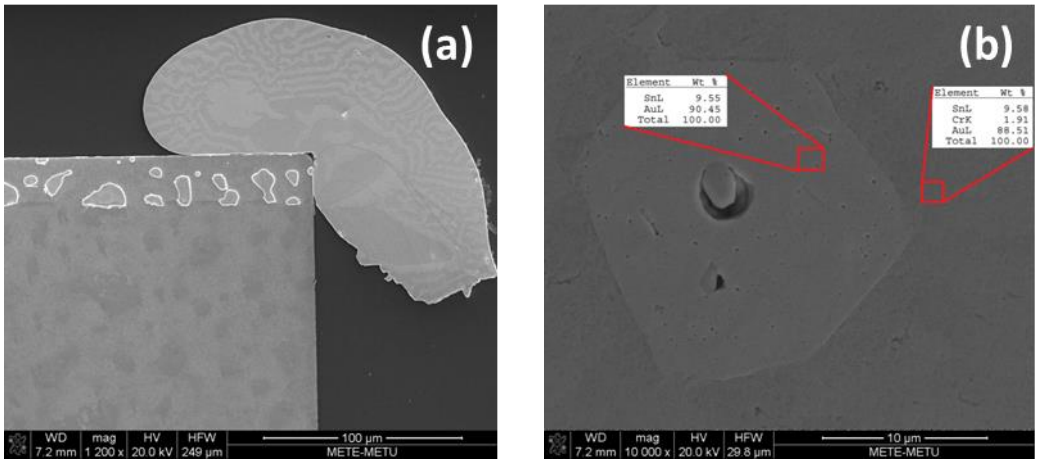

Figure 3.32: SEM image of the fracture surface: (a) Si side and (b) glass side.

One more additional experiment was performed to understand adhesion property of liquid Au-Sn to TiW. Both sides were deposited Au-Sn eutectic composition and bonding was performed, subsequently. Afterwards, bonded wafers were separated by tweezer. Figure 3.33 shows the SEM images of the fracture surfaces of the Au-Sn eutectic bonding at 300°C using same material structure TiW/Au/Sn/Au 150nm/300nm/350nm/50nm on both sides to test adhesion property of liquid Au-Sn to TiW. Some regions were observed as TiW and metal regions exhibits no adhesion to TiW which can be seen in Figure 3.33 (b).

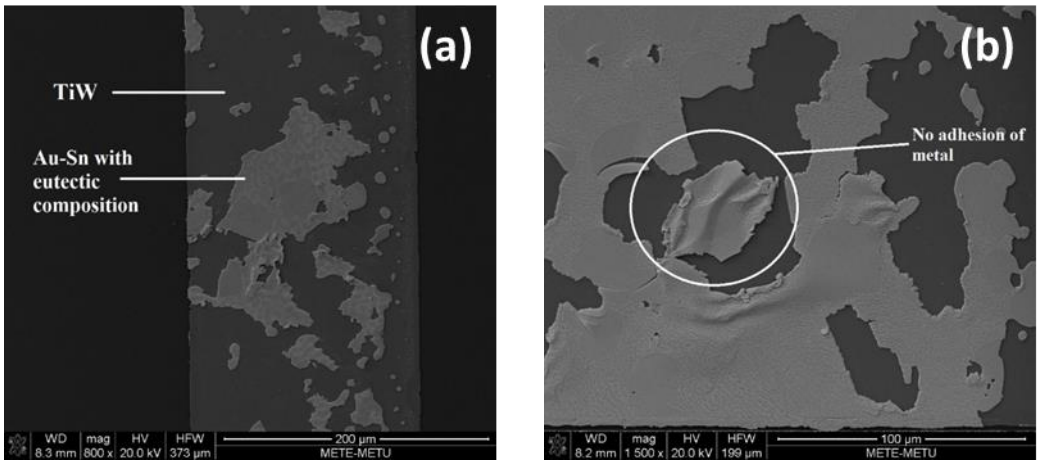

Figure 3.33: The SEM images of the fracture surfaces of the Au-Sn eutectic bonding of the Si side at: (a) low and (b) high magnifications.

TLP Bonding from Eutectic-2 with Ti was performed. In this case, the purpose was to keep adhesion of Au-Sn to Ti and not to lose Ti in Si or Au-Sn. Ti/Au 50nm/1µm, on the cap side, and Ti/Au/Sn/Au on the 50nm/300nm/350nm/50nm, on the substrate, was bonded under N_2 heating. Bonding temperature was set to 300°C. Figure 3.34 shows pictures of: (a) optical microscope image from top view of die and (b) photo of the wafer in acetone. There was no squeeze out, as it can be seen in (a), and acetone enters into dies, which can be observed in the corresponding photo of the wafer in (b). Acetone entrance proved that bonding was not hermetic. Even if it was not hermetic, shear test was applied to perform failure analysis. 4 of the specimens out of 5 have relative low strength. Only one of them showed relatively high shear strength around 16 MPa. From the fracture analysis, one can say that, some regions do not interact with the metal on the substrate and probably some holes were formed. These holes prevented the hermeticity. This could be related with the amount of bonding material and wetting ability of the metal on Ti. Therefore higher thicknesses may solve the problem.

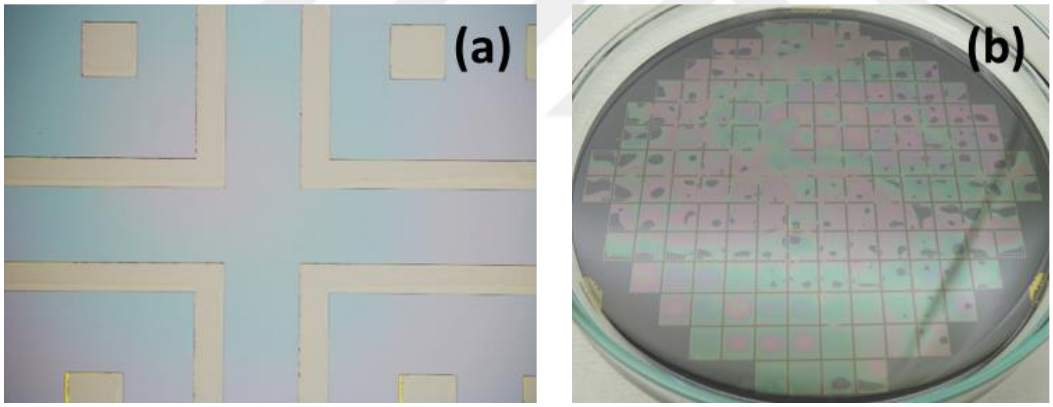

Figure 3.34: Ti/Au 50nm/1µm on the cap side and Ti/Au/Sn/Au 50nm/300nm/350nm/50nm on the substrate side bonding: (a) Optical microscope image from top view of die and (b) photo of the wafer in acetone.

Figure 3.35 exhibits top view SEM image of fracture surface on the cap side of Au-Sn TLP bonding with Ti/Au 50nm/1µm on the cap side, and Ti/Au/Sn/Au on the 50nm/300nm/350nm/60nm on the substrate side.

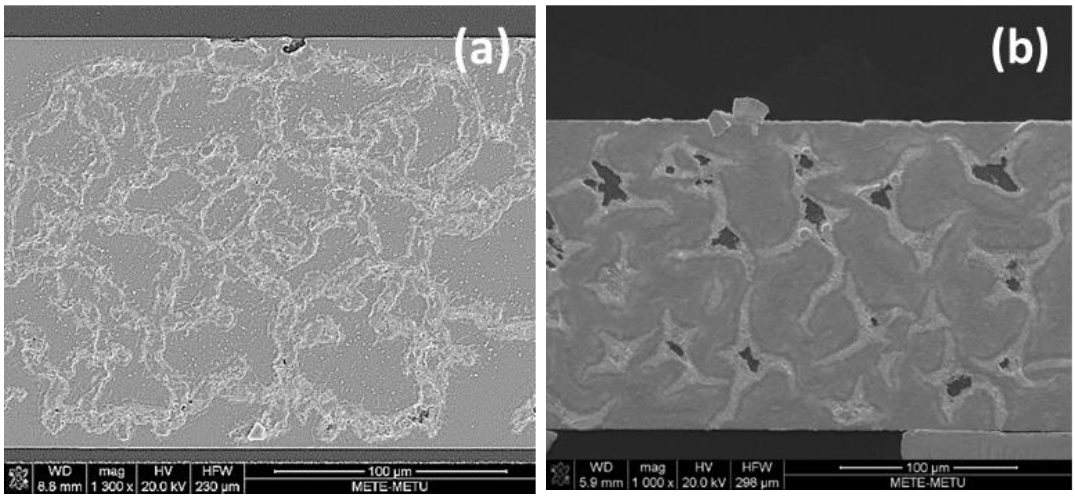

Figure 3.35: Top view SEM image of fracture surface: (a) glass side and (b) Si side. on the cap side of Au-Sn TLP bonding with Ti/Au 50nm/1µm on the cap side, and Ti/Au/Sn/Au on the 50nm/300nm/350nm/60nm on the substrate side.

Cr was inserted on the pure Au side for piranha (1:7) cleaning process because Ti does not withstand piranha solution. It was thought that piranha cleaning, before the bonding, would increase the bonding quality. Bonding pair was Cr/Au 30nm/2µm on the Si side and Ti/Au/Sn/Au 25nm/600nm/700nm/100nm on the glass side. Heating was performed under forming gas up to 300°C. Chamber was pumped and 2000 N force was applied for 20 minutes. Even if bonding quality was high, these dies were again failed in acetone test. SEM analysis was performed from the fracture surface of the cap and the glass wafer. It can be found out even if Cr lost adhesion layer property. Figure 3.36 illustrates top view SEM image of the fracture surface of the Si side. TLP Bonding from Eutectic-2 design was not hermetic although some designs showed really high shear strengths. Table 3.7 shows the shear test results of the Au-Sn TLP Bonding from Eutectic-2 using Cr/Au 30nm/2µm on the Si side and Ti/Au/Sn/Au 25nm/600nm/700nm/100nm on the glass side.

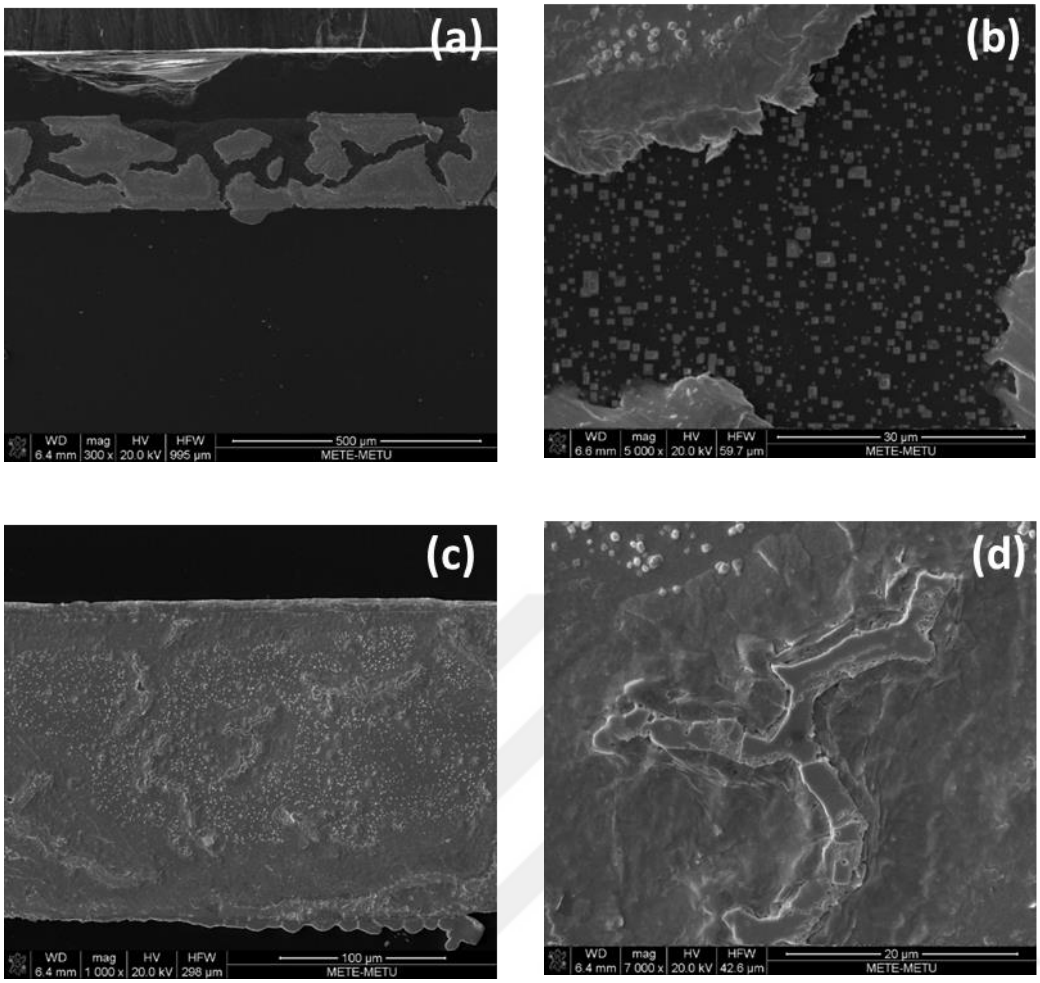

Figure 3.36: Top view SEM image of the fracture surface of the Si side of the TLP Bonding from Eutectic-2: (a) general view of Si side, (b) magnified view of Si side, (c) general view of glass side and (d) magnified view of glass side.

Table 3.7: The shear test results of the Au-Sn TLP Bonding from Eutectic-2 using Cr and TiW as an adhesion layer.

Die #	1	2	3	4	5	6	7	8	9	10
Strength (MPa)	41.3	39.9	23.6	11.5	34.3	13.4	37.7	32.2	25.0	23.5
Average Strength: 28.2 MPa					Standard Deviation:10.5 MPa					

In Eutectic Symmetric Bonding, Ti was used as an adhesion layer. In first bonding trial Ti/Au/Sn/Au 50nm/300nm/350nm/60nm symmetric structure was used on cap

and on substrate. Figure 3.37 exhibits the Au-Sn eutectic bonding with material stack as Ti/Au/Sn/Au symmetrically: (a) the photo of Au-Sn eutectic bonding, (b) the optical microscope image of the bonding line from glass side before, (c) after Au-Sn eutectic bonding. Interaction of Ti is clearly seen.

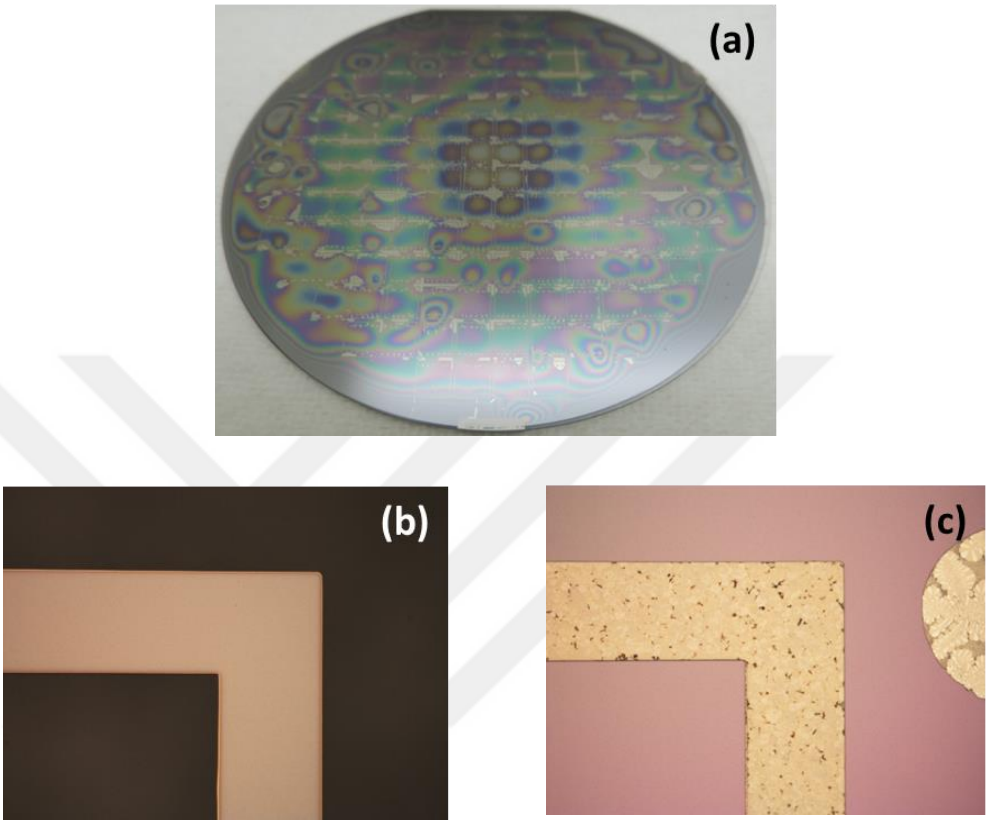

Figure 3.37: The Au-Sn eutectic bonding with material stack symmetrically: (a) the photo of Au-Sn eutectic bonded wafers, (b) the optical microscope image before the bonding and (c) the optical microscope image eutectic bonding.

As a result of bonding, a lot of squeeze out region was obtained in optical microscope analysis. Ti interaction with Au-Sn alloy can be clearly observed in Figure 3.37 (b) and (c). Generally, squeeze out bonding shows high shear strength; however, in this case the wafers were separated from each other during dicing step. SEM analysis was performed subsequently. Figure 3.38 shows SEM image of the fracture surface of Eutectic Symmetric Bonding with Ti/Au/Sn/Au 50nm/300nm/350nm material stack: (a) Si side, (b) glass side.

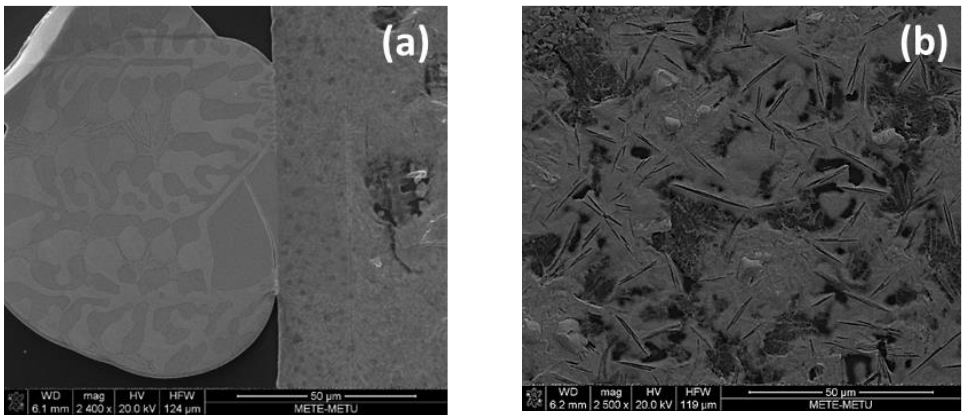

Figure 3.38: SEM image of the fracture surface of Eutectic Symmetric Bonding with Ti/Au/Sn/Au 50nm/300nm/350nm material stack: (a) Si side and (b) glass side.

From the SEM image seen in Figure 3.38, it can be said that melting was occurred. However why bonding was not good is unsolved question. It was thought that the amount of metal was low, so it could not able to bond two wafer.

Eutectic Symmetric Bonding with Ti/Au/Sn/Au 50nm/600nm/700nm/100nm was tried. Figure 3.39 exhibits optical microscope images of the wafer from the glass side after Eutectic Symmetric Bonding with Ti/Au/Sn/Au 50nm/600nm/700nm/100nm. After dicing was performed, Au-Sn Eutectic Symmetric Bonding could not survive.

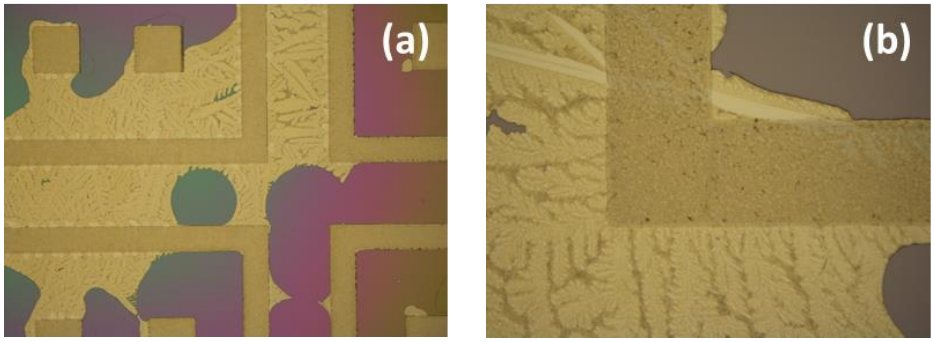

Figure 3.39: Optical microscope images of the wafer from the glass side after Eutectic Symmetric Bonding with Ti at: (a) low and (b) high magnification.

Last try was the TLP Bonding from Sn using Cr/Au 30nm/2µm and Cr/Au/Sn/Au 30nm/50nm/500nm/50nm. In this bonding, almost pure Sn exists. Cr was used because there was almost pure Sn with high amount. Even if, there was high amount

of Sn, only small amount of squeeze out was observed at the center of the wafer. Figure 3.40 shows the optical microscope image of Si to glass patterned bonding: Cr/Au 30nm/2µm – Cr/Au/Sn/Au 30nm/50nm/500nm/50nm. Bonding recipe was heating the wafer to 300°C under forming gas and holding it at that temperature for 2 minutes, then pumping and applying force for 20 minutes.

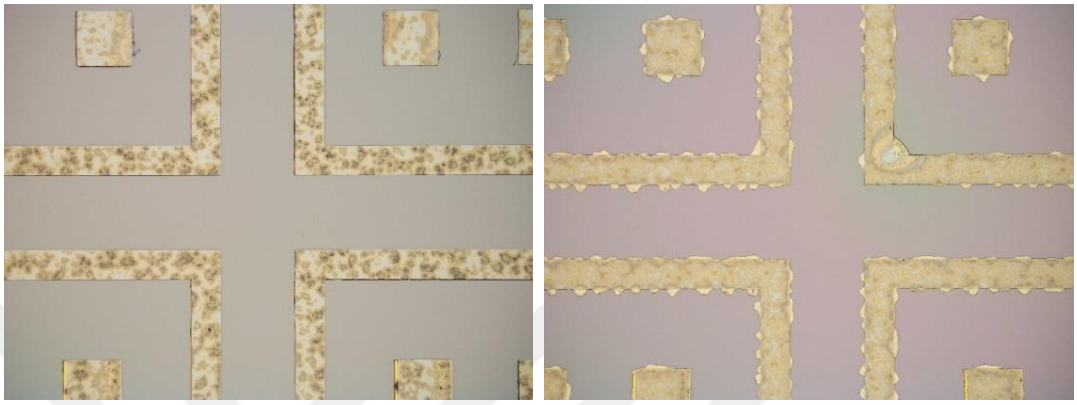

Figure 3.40 The optical microscope image of the: Cr/Au 30nm/2µm – Cr/Au/Sn/Au 30nm/50nm/500nm/50nm.

After analyzing the bonding region under optical microscope, bonded wafer was left in acetone to see its hermeticity property. Figure 3.41 exhibits the photo of the bonded wafer in acetone. Acetone entered almost all dies on the wafer, which showed that the bonding was not hermetic. Table 3.8 shows the shear test results of the TLP Bonding from pure Sn in acetone. Bonding recipe was heating the wafer to 300°C under forming gas and holding it at that temperature for 2 minutes then pumping and applying force for 20 minutes.

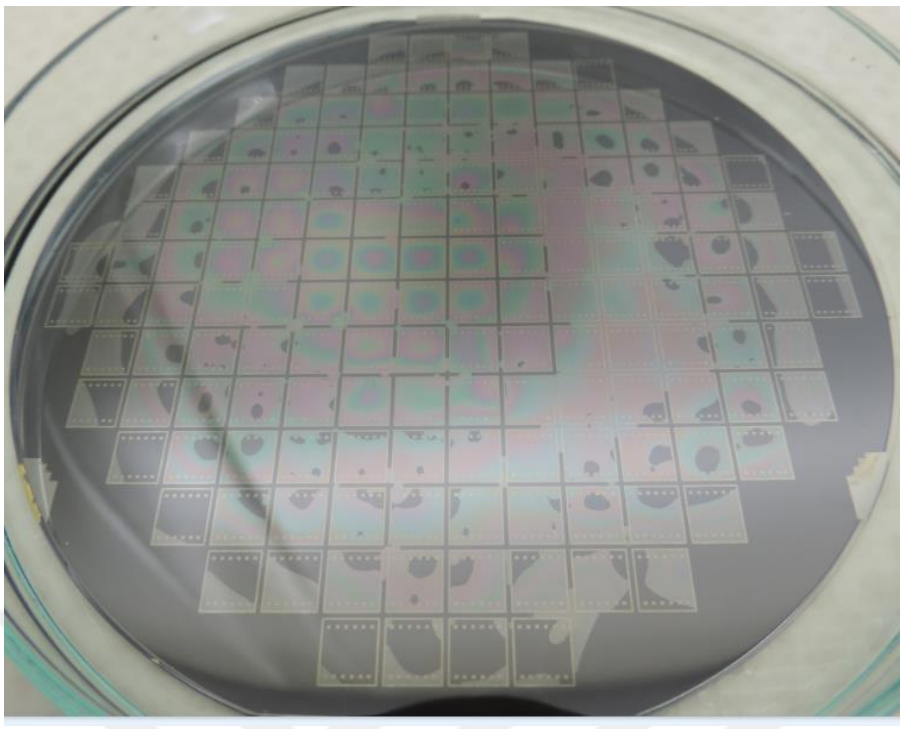

Figure 3.41. The photo of the bonded wafer TLP bonding from pure Sn in acetone.

Table 3.8: The shear test results of the Cr/Au 30nm/2µm – Cr/Au/Sn/Au 30nm/50nm/500nm/50nm.

Die #	1	2	3	4	5	6	7	8	9	10
Strength (MPa)	9.3	17.7	17.3	42.0	43.2	15.7	15.8	42.0	40.6	18.2
Average Strength: 26.2 MPa					Standard Deviation: 13.8 MPa					

After shear test, fracture analysis was performed by using SEM and EDS. Figure 3.42 exhibits the fracture surface of Si side. Figure 3.42 shows SEM image of the fracture surface with low magnification (a) and high magnification (b) and (c). Agglomeration was occurred depending on low amount of interaction. EDS results in Figure 3.42 (c) verified the low interaction.

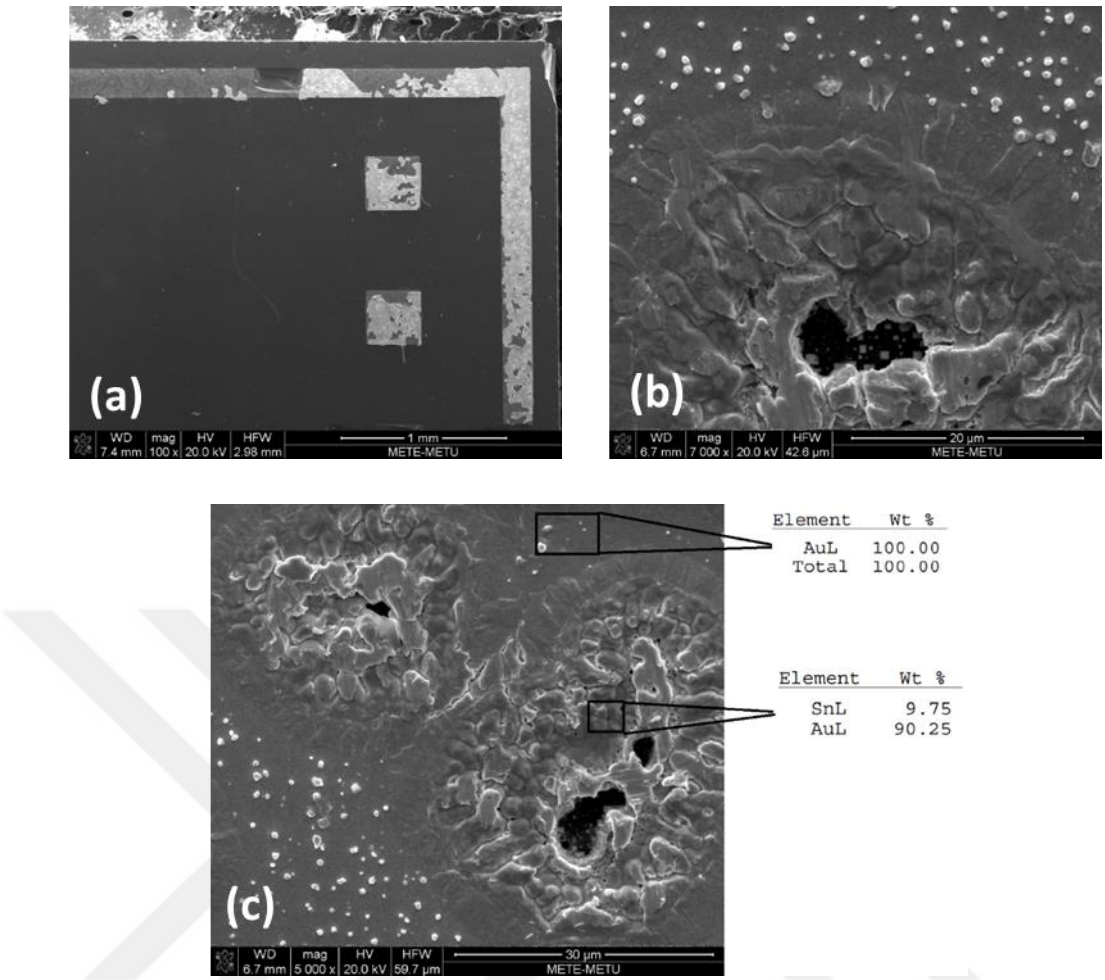

Figure 3.42: The fracture surface of Si side of the Cr/Au 30nm/2µm – Cr/Au/Sn/Au 30nm/50nm/500nm/50nm: (a) general view, (b) magnified view and (c) magnified view with EDS data.

From Au-Sn studies, it should be concluded that Cr and Ti interacted with Au and Sn or Si wafer during bonding. Cr diffusion can be problematic in two ways. First of all, for low thickness Au-Sn coating, Cr prevented melting of metal. This was proved by experimental studies. Secondly, Cr diffusion into Au and Sn resulted in loss of adhesion of metal to wafer. Therefore, only Cr as an adhesion layer is not suggested for Au-Sn bonding. Ti got also interact with Au and Sn. As a results of interaction some intermetallics were formed as observed in SEM. For eutectic bonding and TLP bonding, Ti was used. Although Ti gave high shear strength values, bonding was not hermetic. The reason was wetting ability of Au and Sn on Ti. In fracture analysis, unreacted regions were observed. Besides Cr and Ti, TiW was used as an adhesion

layer for different designs. W (a refractory metal) was used as a barrier layer for different studies. It was thought that W with Ti gives both adhesion and barrier function. In bulk bonding process and DSC study, TiW showed good property from the wetting and melting point of view. However, if all metal was melted on the TiW, metal would lose its adhesion property to TiW. During deposition of Au on TiW using sputter system, there is no problem related with adhesion. Unfortunately, it was observed that molten metal did not adhere to TiW. This was probably related with the refractory property of W. Therefore, adhesion layer which interacts with Au should be chosen. It should be noted that this interaction must be slow compared to Cr or Ti. Ni may be the best candidate for this purpose. It has both adhesion layer and barrier layer property. In addition to adhesion layer importance, heating environment was also critical for bonding quality, because it is observed that heating environment affects the melting property of metals. In vacuum environment melting of metal becomes difficult. Heating under forming gas or N_2 is important. The reason might be related with the non-heating of wafer due to vacuum environment.

Another issue was wetting of metal. Agglomeration was observed which may had several reasons. Firstly, it was definitely related with adhesion layer. Secondly, after heating the sample under N_2, waiting at bonding temperature and pumping time may become important parameter. In this study, holding time was chosen as 2 minutes at 300°C but melting occurs 280°C and liquid metal might agglomerate until the other wafer comes on to the wafer. This should be analyzed further.

Cleaning process was another important parameter. Residual photo resist or organics prevent good bonding; therefore, as much as possible wafers should be cleaned by piranha or acetone, alcohol, DI water. As a final word, low thickness values, which are under 1.5μm, did not result in hermetic bonding. Thickness phenomena was related with the nature of Sn and Au probably. This system was generally studied with electroplating method in literature. Higher thicknesses in Au-Sn and using good barrier layer with adhesion layer such as Ni and Ti would provide both hermetic and high strength bonding.

3.4 Conclusion

In this study Au-Sn metals were used as a bonding material. The ultimate aim was to obtain high shear strength and hermetic encapsulation. Many different designs with different material structures were studied. Total Au-Sn thickness was chosen as lower than 2μm. Metals were deposited with PVD method. Before the bonding trials, materials were characterized. Cr, Ti and TiW were used separately for different designs. Each of them has different characteristic and they effect the bonding quality. Hermetic bonding was obtained at 300°C with low yield around 30% using Cr. Using Ti and TiW, high shear strength values are obtained however they are not hermetic. The reason was related to the adhesion layer effect. Increase in the material thickness and usage of better barrier layer would provide better solutions to wafer level packaging of MEMS. A summary of Au-Sn bonding trials performed for this thesis study is given in Table 3.9.

Table 3.9: Summary of Au-Sn bonding trials.

Bonding Type	**Ave. Shear Strength (MPa)**	**Hermeticity**	**Adhesion Layer**
Eutectic Bonding	25.1	30%	Cr
TLP Bonding from Eutectic-1	18.1	None	TiW
TLP Bonding from Eutectic-2	37.4	None	TiW/Cr
Eutectic Symmetric	None	None	Ti
TLP Bonding from Pure Sn	26.2	None	Cr

CHAPTER 4

WAFER LEVEL HERMETIC ENCAPSULATION USING Au-In

4.1 Introduction

Hermetic encapsulation is a crucial issue, because device should be separated physically from the environment to work in reliability. Metals are frequently used to obtain hermetic bonding since their permeability is low and they can wet the substrate better than others. There are many kind of metallic bonding, and among the other metallic systems, Au-In is promising metallic system [42, 43, 54, 55]. Au-In bonding is not only used for the wafer level MEMS packaging but also it can be used as bump bonding. Their intermetallics possess relatively high shear strength. Furthermore, Au-In is a good candidate for TLP bonding as can be find out from the phase diagram in Figure 4.3. Around 50% In (wt) in Au shows high melting temperature compared to melting point of pure In. In melts at 156°C and it interacts with Au rapidly. These properties are advantages for the TLP bonding. Bonding temperature can be decreased to 200°C for Au-In system; however, getter activation is not completed at 200°C, so high pressure values can be observed. Therefore, additional heating is required to activate the getter. For example; heating the wafer 400°C and holding at that temperature for 5 minutes is enough. The activation temperature and time depend on getter material. In this study, getter material is Ti. Thus, 400°C high re-melt temperature is required. Bonding is a long term process which may extend to 20-30 minutes. This bonding time at 400°C would damage the device, but 5 minutes or lower than 5 minutes at 400°C does not damage the device. In that sense, Au-In with Ti getter represents a good choice for wafer level packaging at relatively shorter bonding durations.

4.2 Experimental Procedure

The experimental procedure to design and to produce the Au-In was quite similar with Au-Sn system and it was summarized by the following diagram shown in Figure 4.1.

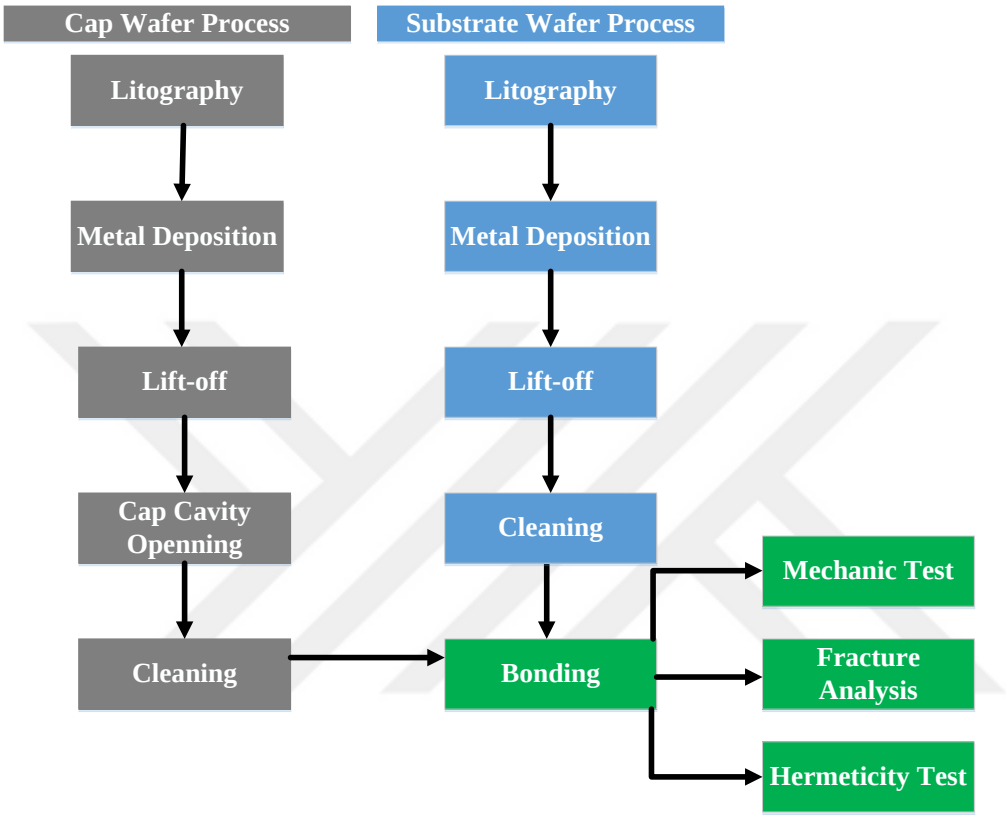

Figure 4.1: Main experimental procedure for Au-In bonding.

Si wafer was prepared as a cap, and a glass wafer was prepared as a substrate wafer. Dark field masks were used. Ti, Ni, and Au were coated using AJA sputter system. In was deposited using Varian e-beam evaporator. Ti was used as an adhesion layer and Ni was used as a barrier layer in this study. In was only deposited on glass side. The aim of deposition of In on the glass side was not to decrease degree of freedom in terms of process compatibility. Bonding was performed at 200°C. Heating rate was 45°C/min and cooling rate was the maximum cooling rate with given N_2 into the chamber. Bonding pressure was 3.15 MPa. Heating was performed under forming gas (5%H_2, 95%N_2) up to 200°C, subsequently pumping was conducted. When

pressure of the chamber become 10^{-3} atm, bonding starts with applying pressure on the wafers. Bonding time was 15 minutes for this design. Figure 4.2 exhibits schematic illustrations of two bonding design with and without Ni. Ti/Ni/Au/In 50nm/200nm/500nm/30000nm and Ti/Ni/Au 50nm/200nm/1000nm.

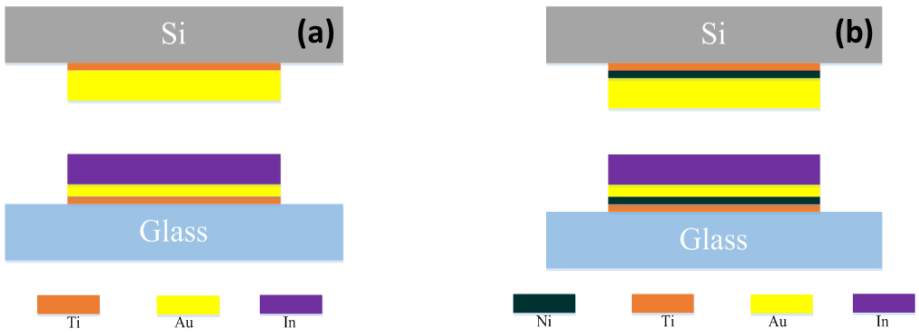

Figure 4.2: Schematic illustrations of two bonding design: (a) with Ti/Au/In 50nm/500nm/30000nm and Ti/Au 50nm/1000nm and (b) with Ti/Ni/Au/In 50nm/200nm/500nm/30000nm and Ti/Ni/Au 50nm/200nm/1000nm

Thicknesses of Au and In were adjusted according to 50wt% Au, because compositions between AuIn and $AuIn_2$ intermetallics show high re-melt temperature at around 495°C. This high re-melt temperature is enough for getter activation. Figure 4.3 shows Au-In phase diagram.

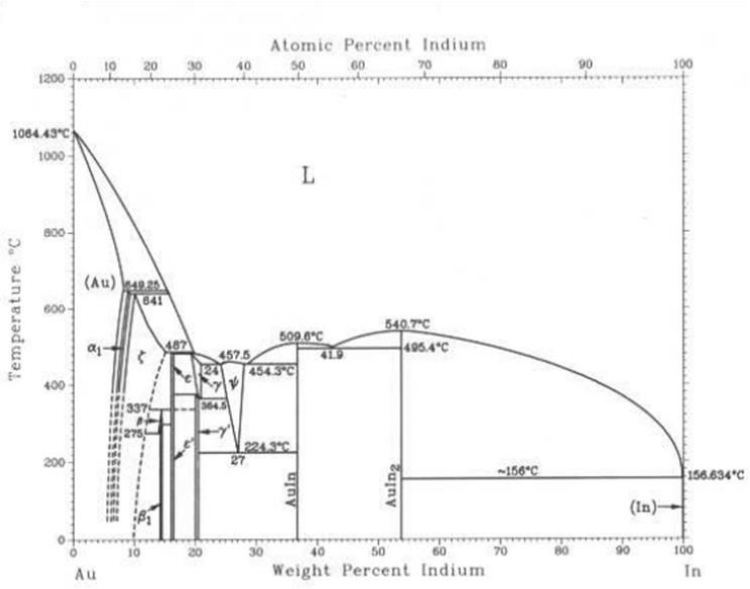

Figure 4.3: Au-In phase diagram [56].

4.3 Results and Discussion

The first analysis was to test Ti adhesion layer efficiency. After wafers were prepared as explained in the experimental part, bonding was performed at 200°C for 15 minutes. Figure 4.4 shows the optical microscope image of Au-In TLP bonding, taken place at 200°C. There was squeeze out in some regions. Ti was used as an adhesion layer.

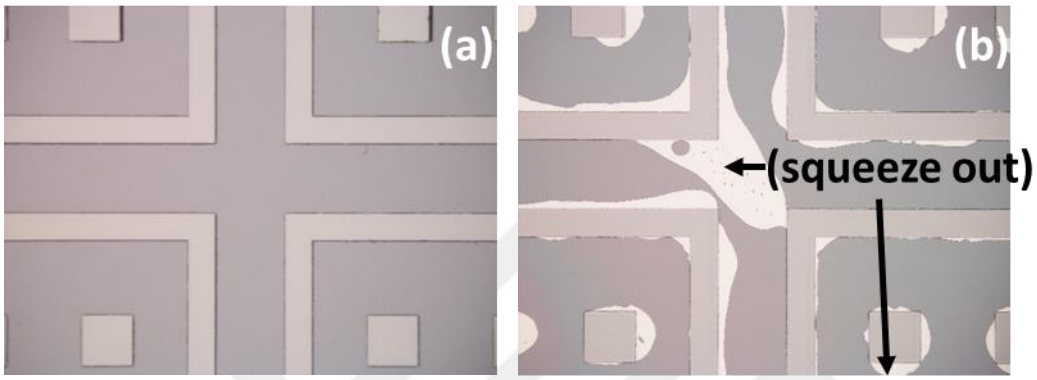

Figure 4.4: Optical microscope image of Au-In TLP bonding at 200°C: (a) without squeeze out region and (b) with squeeze out region shown by arrows.

Shear test was applied to Au-In TLP bonded wafer to reveal the effects of Ni barrier layer. Dage 4000 Bondtester was used for shear tests. Table 4.1 shows shear test results of Au-In TLP bonding without using Ni as a barrier layer.

Table 4.1: Shear test results of Au-In TLP bonding without using Ni as a barrier layer.

Die#	1	2	3	4	5	6	7	8	9	10
Shear Strength (MPa)	26.0	18.9	28.2	14.8	25.9	21.5	46.3	62.3	25.8	43.6
Average Strength: 31.3 MPa					Standard Devaiation:14.7 MPa					

Shear test results seem very successful. SEM analysis was performed for failure analysis. Fracture surface shows high interaction as can be seen from the Figure 4.5.

Unfortunately, the dies of Au-In TLP bonded without using Ni barrier layer was failed in acetone test. The dies accepted acetone inside.

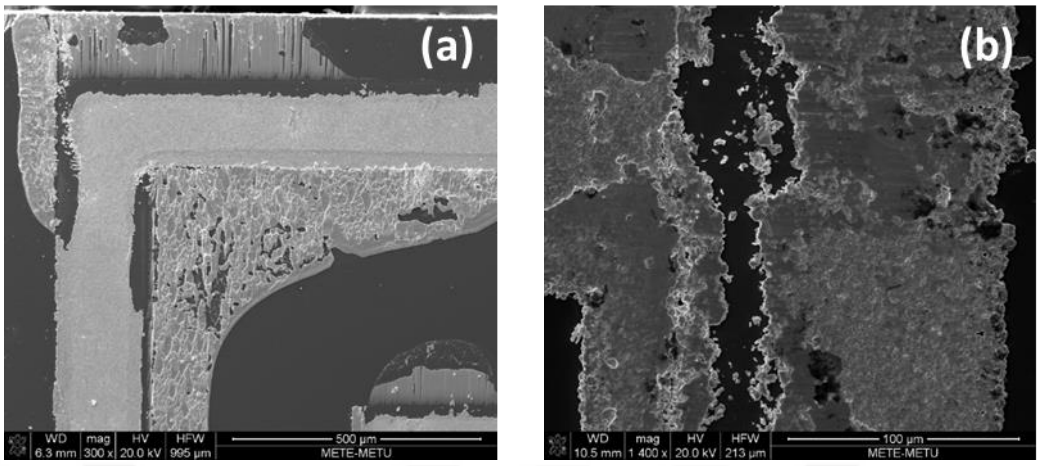

Figure 4.5: Top view SEM images of the failed surfaces of Au-In TLP bonding without Ni usage: (a) glass side and (b) Si side.

Since Au-In TLP bonding without Ni was failed in acetone test, thinning process was not applied to this bonding. Same bonding design was tested with adding Ni as a barrier layer. Figure 4.6 shows the optical microscope image of the Au-In bonding, heated under forming gas up to 150°C. Bonding was performed at 200°C under vacuum. Squeeze out was observed.

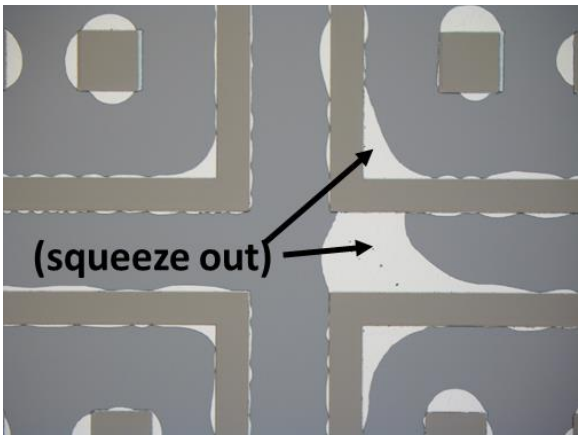

Figure 4.6: The optical microscope image of the Au-In bonding heated under forming gas up to 150°C.

After squeeze out was observed, the bonded wafer was tested under acetone. The wafer was passed the acetone test under this condition. Figure 4.7 shows the photo of the Au-In bonding in acetone. Acetone did not enter inside of the dies.

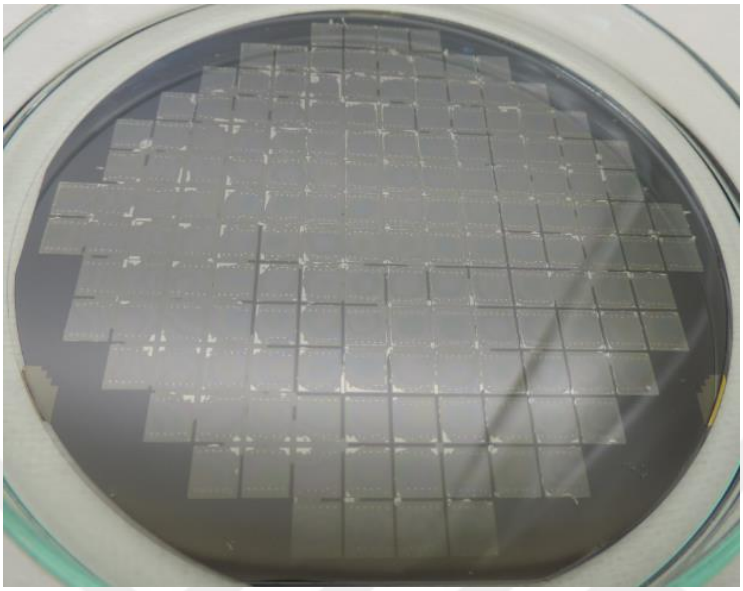

Figure 4.7: The photo of the Au-In bonding during acetone test.

Table 4.2 shows the shear strength values of the Au-In bonding under forming gas heating with using Ni barrier layer.

Table 4.2: The shear strength values of the Au-In bonding using Ni barrier layer.

Die#	1	2	3	4	5	6	7	8	9	10
Shear Strength (MPa)	29.6	27.4	37.6	23.6	71.7	40.1	42.9	59.7	34.3	76.6
Average Strength: 44.1 MPa					Standard Deviation: 18.9 MPa					

The observation of both high shear strength and hermeticity to acetone motivated us for the thinning process to test hermeticity to atmosphere. For thinning process, firstly, cap cavity was opened. Figure 4.8 shows the optical profilometer image of the die after cap cavity opening. 300µm cavity was obtained. After cavity opening, Au-In TLP bonding with Ti adhesion layer and Ni barrier layer was performed. After

bonding cap wafer was thinned down to almost zero thickness. Deflection was observed on the wafer. The deflection was permanent so it was concluded that the bonding was hermetic to atmosphere conditions. Figure 4.9 shows the photos of the deflected Si wafer after Au-In bonding.

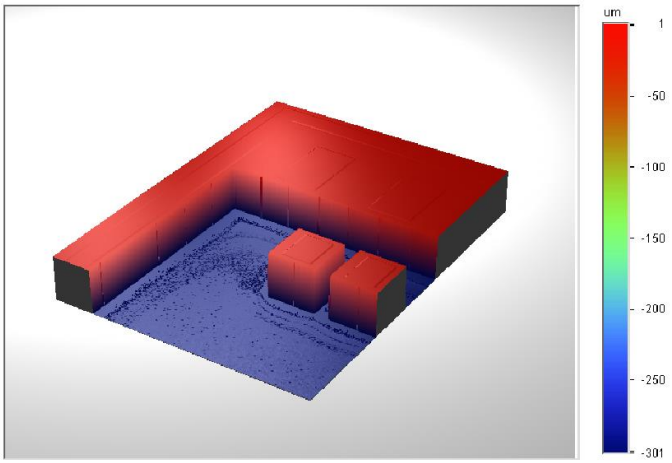

Figure 4.8: The optical profilometer image of the die after cap cavity opening.

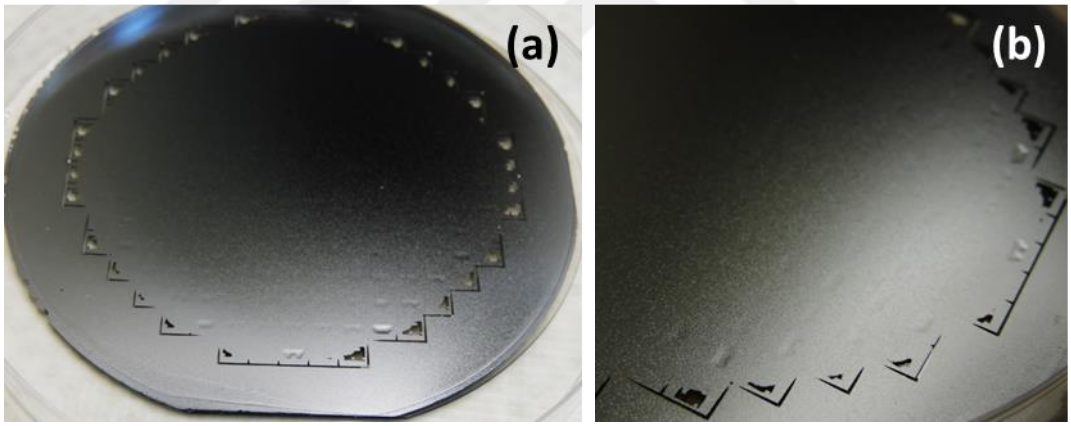

Figure 4.9: The photos of the deflected Si wafer at: (a) low and (b) high magnifications.

The wafer was heated to 400°C and was hold at that temperature for 10 minutes to test the high re-melt temperature. After this test, if the bonds were strong enough, dies would not change their strength characteristics, and they would preserve the hermeticity. Figure 4.10 shows wafer after heat treatment at 400°C for 10 minutes. The deflection seems to be preserved so it was concluded that bonding is still

hermetic. In order to check the change in shear strength of the heat treatment, 3 dies were annealed at 400°C for 10 minutes and shear test was applied. Figure 4.11 shows photo of the 3 dies which were bonded Au-In TLP bonding at 200°C. From the photos, one can say that there is almost no change in the amount of squeeze out.

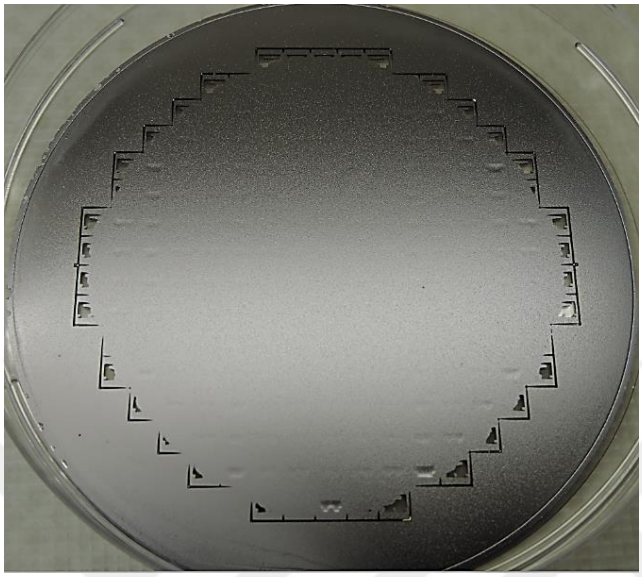

Figure 4.10: The deflected wafer after heat treatment at 400°C for 10 minutes.

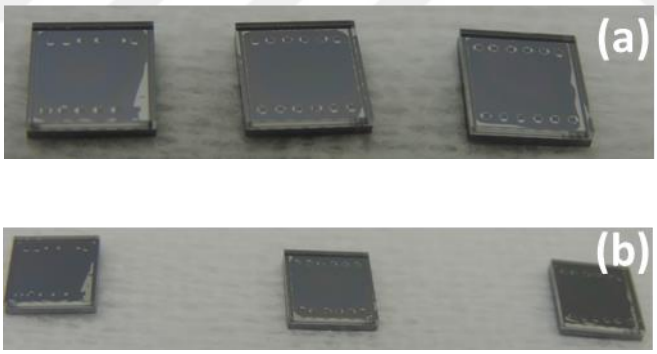

Figure 4.11: Photo of the 3 dies which are bonded Au-In TLP bonding at 200°C: (a) before the annealing at 400°C for 10 minutes and (b) after the annealing at 400°C for 10 minutes.

Shear strength values of the heat treated dies, shown in Figure 4.11, were given in Table 4.3. It can be said that shear strength was still high and getter can be activated after bonding was performed.

Table 4.3 Shear strength values of the heat treated dies shown in Figure 4.11.

Die#	1	2	3
Shear strength (MPa)	50.3	68.5	86.7
Average Strength: 68.5 MPa		Standard Deviation: 18.2 MPa	

The getter can be activated after bonding was finished; however, there was a question that when the wafer is directly heated to 400°C without removing the pressure, whether or not getter activation is completed. One final test was applied to Au-In TLP bonding to reveal its performance under pressure and heating. After bonding at 200°C for 15 minutes, 3.15 MPa of pressure was continued up to 400°C. This time acetone test exhibited that hermeticity was lost. Figure 4.12 shows photo of the Au-In TLP bonding with the pressure on the wafer heated to 400°C and hold at that temperature for 10 minutes. The dies accepted acetone inside.

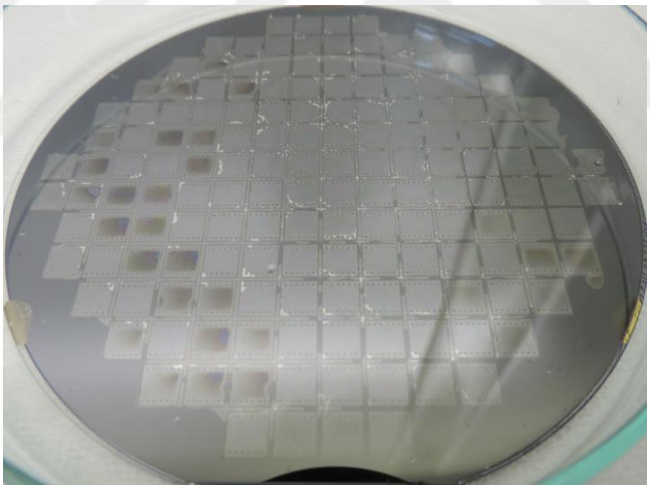

Figure 4.12: Photo of the Au-In TLP bonding with the applied pressure on the wafer heated to 400°C and hold at that temperature for 10 minutes.

The wafers were separated from each other for failure analysis under SEM. Figure 4.13 shows the SEM images of the glass side of the Au-In bonding after separation. After EDS analysis, it was observed that there was no material on the bonding ring.

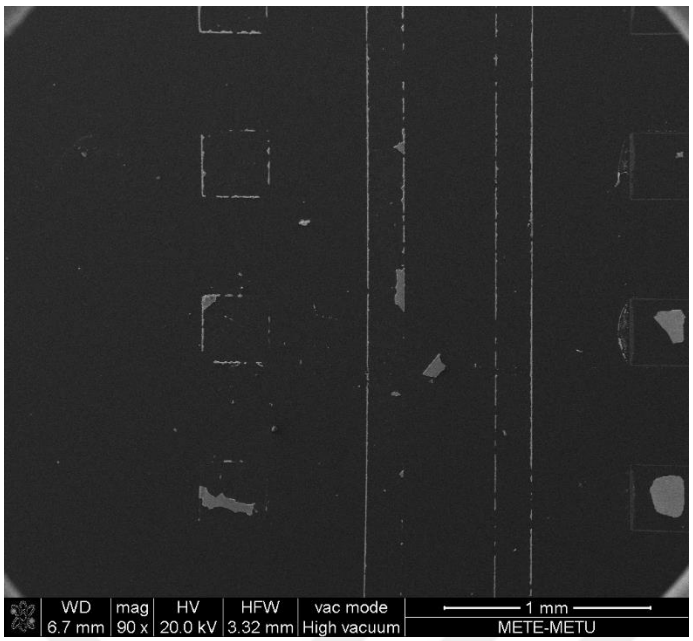

Figure 4.13: The SEM image of the glass side of the Au-In bonding after separation.

According to EDS analysis, it can be said that some adhesion problem related with Ti and glass was observed after heating the wafer to 400°C without removing pressure and breaking the vacuum. The reason was directly related with diffusion of Ti into Au-In alloy. Ti was not on the glass after heat treatment, on the other hand it was on the glass at the beginning. Applied pressure and heating from 200°C to 400°C speeded up the diffusion rate of Ti into Au-In alloy compared to heat treatment without pressure and heating from room temperature to 400°C for same time interval. Therefore, getter activation should be performed after cooling the wafer and removing the pressure from the wafer.

4.4 Conclusion

In this study, Au-In TLP hermetic bonding was performed. Compositions were adjusted to be between AuIn and $AuIn_2$ intermetallics' compositions to obtain high re-melt temperatures. TLP bondings were performed with and without Ni to test the effect of barrier layer. The bondings without Ni barrier layer was failed during acetone test, on the other hand, the one with barrier layer survived during both acetone and deflection tests. Therefore, it can be concluded that barrier layer plays

important role in hermeticity. In addition to reasonable hermetic properties, Au-In TLP bonding showed good mechanical strength against shear forces.

CHAPTER 5

CONCLUSION AND FUTURE WORK

This thesis study presents experimental efforts to develop wafer level bonding material for hermetic encapsulation of MEMS devices. In order to test bonding, special dummy masks were designed and produced to mimic real MEMS devices' fabrication and packaging. The primary aim of this study is to find effective wafer level packaging for specific MEMS devices. The desired properties from the packaging are relatively low bonding temperature, hermetic encapsulation, high shear strength and being able to compensate the topology of the wafer. Metallic bonding is the best candidate for these desired targets. Among the metals, Au-Sn and Au-In material systems were selected to be tested for bonding experiments, because of being low temperature bonding and noble Au metal. Besides, Au is well known clean room metal that can be handled.

Interaction of Au and Sn was examined in detail. Porous structure of Sn was observed and thickness optimization was performed. The adhesion layer effect on bonding metal was examined by performing heat treatment and SEM analysis by using Cr, Ti and TiW. Each one showed different characteristic. Cr was lost due to excess diffusion and prevented melting of Au-Sn metal at relatively low thicknesses around 500nm. TiW was lost its adhesion property on liquid Au-Sn. It holds the Au in solid state but after melting the Au-Sn alloy, molten material did not adhere to TiW. As a final candidate Ti exhibited some intermetallics after annealing. Different type of adhesion layer affected the bonding as well. For example; hermetic encapsulation was observed with low yield with Cr adhesion layer. Hermetic encapsulation was not obtained due to loss in adhesion with TiW adhesion layer. When Ti was used as an adhesion layer, wetting problem was observed even if good mechanical properties could be obtained.

Au-In bonding showed better mechanical properties as compared to Au-Sn bonding. Ti was used as an adhesion layer for Au-In bonding. In addition, Ni was included as a barrier layer after observing adhesion layer problems in Au-Sn bonding. Without Ni barrier layer Au-In bonding exhibits good mechanical properties; however, it failed in acetone test showing that bonding is not hermetic. When Ni was coated on Ti, package showed both good mechanical and hermetic properties. Shear test and deflection test methods proved these results. Bonded wafer was heated to 400°C for 10 minutes and deflection was still existed.

In this work, a successful Au-In bonding at 200°C was achieved with a hermeticity at room temperature and at 400°C for 10 minutes, as well. Hermetic bonding was obtained in Au-Sn at 300°C with low yield. These were succeed with lower than 2µm thicknesses for Au-Sn and lower than 4µm thicknesses for Au-In bonding. Metal deposition technics were sputter, e-beam evaporator and thermal evaporator systems, which are reliable, reproducible and precise technics. The following research topics can be considered as a future recommendations:

1. Barrier layer can be inserted on the adhesion layer for Au-Sn studies. Ni can be a good choice as it was revealed in Au-In work. In addition, adhesion layer and barrier layer thicknesses can be increased.
2. Thickness of the Au-Sn can be increased. The reason is to leave solid metal within contacted to substrate because it was observed that melting of all metal degrade the bonding. In order to increase the metal thicknesses, electroplating is the best method even if it has some disadvantages such as non-uniform coating or electric field existence.
3. Bonding parameter should be studied further. For example; in this study, heating was performed under N_2 environment and before the pressure application chamber should be pumped up. Pumping temperature and dwell time before and during bonding should be studied in a detailed manner. In this study, Au-Sn heating was performed up to 300°C and waited for 2 minutes to be sure about the complete melting of metal. Then, chamber was pumped and pressure was applied. Dwell time during bonding can be shortened to decrease

diffusion of adhesion layer, and dwell time before force applying can be decreased to increase wetting.

REFERENCES

[1] R. P. Feynman, “There ’ s Plenty of Room at the Bottom,” *J. Microeleciromechanical Syst.*, vol. 1, no. 1, pp. 60–66, 1992.

[2] L. University, "An Introduction to MEMS (Micro-electromechanical Systems)," *Lecture Notes*, January, 2002.

[3] Yole Development, “2015-2021 MEMS market forecast in US$B,” 2016. [Online]. Available: http://www.yole.fr/iso_album/illus_mems_market_yole_june2016.jpg.

[4] M. M. Torunbalci, “Wafer Level Vacuum Packaging of MEMS Sensors and Resonators,” *Master Thesis*, Midde East Technical University, 2011.

[5] J. S. Mitchell, “Low Temperature Wafer Level Vacuum Packaging Using Au-Si Eutectic Bonding and Localized Heating.,” *Ph.D. Dissertation*, The University Of Michangan, 2008.

[6] M. Moraja, “Hermetic Packaging Design of MEMS,” *Seminer Notes*, 2009.

[7] R. R. Tummala, "Fundamentals of Microsystems Packaging," Mc Graw-Hill, 2001.

[8] S. H. Choa, “Reliability Study of Hermetic Wafer Level MEMS Packaging with Through-Wafer Interconnect,” *Microsyst. Technol.*, vol. 15, no. 5, pp. 677-686, 2009.

[9] D. Q. Yu and M. L. Thew, “Newly Developed Low Cost, Reliable Wafer Level Hermetic Sealing using Cu/Sn System,” *Electron. Syst. Integr. Technol. Conf. ESTC 2010 - Proc.*, 2010.

[10] A. Garnier, X. Baillin, and F. Hodaj, “Solidification and Interfacial Interactions in Gold-Tin System during Eutectic or Thermo-Compression

Bonding for 200 mm MEMS Wafer Level Hermetic Packaging," *J. Mater. Sci. Mater. Electron.*, vol. 24, no. 12, pp. 5000–5013, 2013.

[11] H. J. Van De Wiel, A. S. B. Vardøy, G. Hayes, H. R. Fischer, A. Lapadatu, and M. M. V Taklo, "Characterization of Hermetic Wafer-Level Cu-Sn SLID Bonding," *2012 4th Electron. Syst. Technol. Conf. ESTC 2012*, 2012.

[12] S. Giudice and C. Bosshard, "Au-Sn Transient Liquid Phase Bonding for Hermetic Sealing and Getter Activation," *EMPC*, pp. 1–5, 2013.

[13] A. Garnier, E. Lagoutte, X. Baillin, C. Gillot, and N. Sillon, "Gold-Tin Bonding for 200mm Wafer Level Hermetic MEMS Packaging," *Proc. - Electron. Components Technol. Conf.*, pp. 1610–1615, 2011.

[14] R. N. Candler, W. T. Park, H. Li, G. Yama, A. Partridge, M. Lutz, and T. W. Kenny, "Single Wafer Encapsulation of MEMS Devices," *IEEE Trans. Adv. Packag.*, vol. 26, no. 3, pp. 227–232, 2003.

[15] P. Monajemi, F. Ayazi, P. J. Joseph, and P. A. Kohl, "A Low Cost Wafer-Level MEMS Packaging Technology," *Micro Electro Mech. Syst. 2005. MEMS 2005. 18th IEEE Int. Conf.*, pp. 634–637, 2005.

[16] Q. Li, H. Goosen, F. Van Keulen, J. Van Beek, and G. Zhang, "Assessment of Testing Methodologies for Thin-Film Vacuum MEMS Packages," *Microsyst. Technol.*, vol. 15, no. 1 SPEC. ISS., pp. 161–168, 2009.

[17] B. H. Stark and K. Najafi, "A Low-Temperature Thin-Film Electroplated Metal Vacuum Package," *J. Microelectromechanical Syst.*, vol. 13, no. 2, pp. 147–157, 2004.

[18] W. I. Cornelius Welch, "Vacuum and Hermetic Packaging of MEMS Using Solder by," *Ph.D. Dissertation*, The University Of Michangan, 2008.

[19] D. Pomerantz, "Anodic bonding," *US Pat. 3,397,278*, 1968.

[20] M. M. Torunbalci, S. E. Alper, and T. Akin, "Wafer Level Hermetic Sealing of MEMS Devices with Vertical Feedthroughs using Anodic Bonding,"

Sensors Actuators, A Phys., vol. 224, pp. 169–176, 2015.

[21] M. M. Torunbalci, S. E. Alper, and T. Akin, "A Method for Wafer Level Hermetic Packaging of SOI-MEMS Devices with Embedded Vertical Feedthroughs using Advanced MEMS Process," *J. Micromechanics Microengineering*, vol. 25, no. 12, p. 125030, 2015.

[22] J. S. G. J. S. Go and Y.-H. C. Y.-H. Cho, "Experimental Evaluation of Anodic Bonding Process using Taguchi Method for Maximum Interfacial Fracture Toughness," *Proc. MEMS 98. IEEE. Elev. Annu. Int. Work. Micro Electro Mech. Syst. An Investig. Micro Struct. Sensors, Actuators, Mach. Syst. (Cat. No.98CH36176*, pp. 318–321, 1998.

[23] C. Li, T. Lee, C. Chiang, and F. Lo, "Enhancement of Bonding Strength for Low Temperature Si3N4/Si3N4 Direct Wafer Bonding by Nitrogen-Plasma Activation and Hydrofluoric Pre-dip," *ECS Transaction*, vol. 64, no. 5, pp. 111–117, 2011.

[24] D. Sparks, S. Massoud-Ansari, and N. Najafi, "Reliable Vacuum Packaging Using NanoGetters™ and Glass Frit Bonding," *Proc. SPIE - Int. Soc. Opt. Eng.*, vol. 5343, pp. 70–78, 2004.

[25] C.-T. Pan, H. Yang, S.-C. Shen, M.-C. Chou, and H.-P. Chou, "A low-Temperature Wafer Bonding Technique using Patternable Materials," *J. Micromechanics Microengineering*, vol. 12, no. 5, pp. 611–615, 2002.

[26] F. Niklaus, H. Andersson, P. Enoksson, and G. Stemme, "Low Temperature Full Wafer Adhesive Bonding of Structured Wafers," *Sensors Actuators, A Phys.*, vol. 92, no. 1–3, pp. 235–241, 2001.

[27] H. Kim and K. Najafi, "Characterization of Low-Temperature Wafer Bonding using Thin-Film Parylene," *J. Microelectromechanical Syst.*, vol. 14, no. 6, pp. 1347–1355, 2005.

[28] X. Zhu, G. Liu, Y. Guo, and Y. Tian, "Study of PMMA Thermal Bonding," *Microsyst. Technol.*, vol. 13, no. 3–4, pp. 403–407, 2007.

[29] J. S. Mitchell and K. Najafi, "A Detailed Study of Yield and Reliability for Vacuum Packages Fabricated in a Wafer-Level Au-Si Eutectic Bonding Process," *15th Int. Conf. Solid-State Sensors, Actuators Microsystems*, pp. 841–844, 2009.

[30] M. Haubold, Y. C. Lin, J. Frömel, M. Wiemer, M. Esashi, and T. Geßner, "A Novel Approach for Increasing the Strength of an Au/Si Eutectic Bonded Interface on an Oxidized Silicon Surface," *Microsyst. Technol.*, vol. 18, no. 4, pp. 515–521, 2012.

[31] R. F. Wolffenbuttel and K. D. Wise, "Low-Temperature Silicon Wafer-to-Wafer Bonding using Gold at Eutectic Temperature," *Sensors Actuators A. Phys.*, vol. 43, no. 1–3, pp. 223–229, 1994.

[32] E. Jing, B. Xiong, and Y. Wang, "The Bond Strength of Au/Si Eutectic Bonding Studied by IR Microscope," *IEEE Trans. Electron. Packag. Manuf.*, vol. 33, no. 1, pp. 31–37, 2010.

[33] R. P. Elliott and F. A. Shunk, "The Au-Si (Gold-Silicon) System," *Bull. Alloy Phase Diagrams*, vol. 4, no. 4, p. 362, 1983.

[34] F. Forsberg, N. Roxhed, A. C. Fischer, B. Samel, P. Ericsson, N. Hoivik, A. Lapadatu, M. Bring, G. Kittilsland, G. Stemme, and F. Niklaus, "Very Large Scale Heterogeneous Integration (VLSHI) and Wafer-Level Vacuum Packaging for Infrared Bolometer Focal Plane Arrays," *Infrared Phys. Technol.*, vol. 60, pp. 251–259, 2013.

[35] R. Agarwal, W. Zhang, P. Limaye, and W. Ruythooren, "High Density Cu-Sn TLP Bonding for 3D Integration," *Proc. - Electron. Components Technol. Conf.*, vol. 32, no. 0, pp. 345–349, 2009.

[36] N. S. Bosco and F. W. Zok, "Strength of Joints Produced by Transient Liquid Phase Bonding in the Cu-Sn System," *Acta Mater.*, vol. 53, no. 7, pp. 2019–2027, 2005.

[37] C. Floetgen, K. Corn, M. Pawlak, H. J. van de Wiel, G. R. Hayes, and V.

Dragoi, "Cu-Sn Transient Liquid Phase Wafer Bonding: Process Parameters Influence on Bonded Interface Quality," *ECS Trans.*, vol. 50, no. 7, pp. 177–188, 2013.

[38] L. Deillon, A. Hessler-Wyser, T. Hessler, and M. Rappaz, "Solid-Liquid Interdiffusion (SLID) Bonding in the Au–In System: Experimental Study and 1D Modelling," *J. Micromechanics Microengineering*, vol. 25, no. 12, p. 125016, 2015.

[39] B. Grummel, H. A. Mustain, Z. J. Shen, and A. R. Hefner, "Comparison of Au-In Transient Liquid Phase Bonding Designs for SiC Power Semiconductor Device Packaging," *23rd Inter.l Symp. on Power Semiconductor Devices & IC's*, pp. 77–83, 2011.

[40] B. J. Grummel, Z. J. Shen, H. A. Mustain, and A. R. Hefner, "Thermo-Mechanical Characterization of Au-In Transient Liquid Phase Bonding Die-Attach," *IEEE Trans. Components, Packag. Manuf. Technol.*, vol. 3, no. 5, pp. 716–723, 2013.

[41] W. Zhang and W. Ruythooren, "Study of the Au/In Reaction for Transient Liquid-Phase Bonding and 3D Chip Stacking," *J. Electron. Mater.*, vol. 37, no. 8, pp. 1095–1101, 2008.

[42] R. Straessle, Y. Pétremand, D. Briand, M. Dadras, and N. F. de Rooij, "Low-Temperature Thin-Film Indium Bonding for Reliable Wafer-Level Hermetic MEMS Packaging," *J. Micromechanics Microengineering*, vol. 23, no. 7, 2013.

[43] W. Qian, J. Kyudong, C. Minseog, K. Woonbae, H. Sukjin, J. Byunggil, and M. Changyoul, "Low Temperature, Wafer Level Au-In Bonding for ISM Packaging," *2006 7th Int. Conf. Electron. Packag. Technol. ICEPT '06*, 2007.

[44] T. A. Tollefsen, A. Larsson, O. M. LØvvik, and K. Aasmundtveit, "Au-sn SLID Bonding - Properties and Possibilities," *Metall. Mater. Trans. B Process Metall. Mater. Process. Sci.*, vol. 43, no. 2, pp. 397–405, 2012.

[45] K. E. Aasmundtveit, K. Wang, N. Hoivik, J. M. Graff, and A. Elfving, "Au – Sn SLID Bonding : Fluxless Bonding with High Temperature Stability , to Above 350 o C," *Microelectron. Packag. Conf. 2009. EMPC 2009. Eur.*, no. C, pp. 1–6, 2009.

[46] S. W. Yoon, M. D. Glover, and K. Shiozaki, "Nickel-Tin Transient Liquid Phase Bonding Toward High-Temperature Operational Power Electronics in Electrified Vehicles," *IEEE Trans. Power Electron.*, vol. 28, no. 5, pp. 2448–2456, 2013.

[47] S. W. Yoon, K. Shiozaki, S. Yasuda, and M. D. Glover, "Highly Reliable Nickel-Tin Transient Liquid Phase Bonding Technology for High Temperature Operational Power Electronics in Electrified Vehicles," *Conf. Proc. - IEEE Appl. Power Electron. Conf. Expo. - APEC*, pp. 478–482, 2012.

[48] Z. Fang, X. Mao, J. Yang, and F. Yang, "A Wafer-Level Sn-Rich Au–Sn Intermediate Bonding Technique with High Strength," *J. Micromechanics Microengineering*, vol. 23, no. 9, p. 095008, 2013.

[49] H. Okamoto, "Au-Sn (Gold-Tin)," *J. Phase Equilibria Diffus.*, vol. 28, no. 5, p. 490, 2007.

[50] C. Manier, K. Zoschke, H. Oppermann, D. Ruffieux, S. D. Piazza, T. Suni, J. Dekker, G. Allegato, and F. Izm, "Vacuum Packaging at Wafer Level for MEMS using Gold - Tin metallurgy," *EMPC*, 2013.

[51] M. Nishiguchi, N. Goto, and H. Nishizawa, "Highly Reliable Au-Sn Eutectic Bonding with Background GaAs LSI Chips," *IEEE Trans. components, hybrids, Manuf. Technol.*, vol. 14, no. 3, pp. 523–528, 1991.

[52] M. M. Torunbalci, E. C. Demir, I. Donmez, S. E. Alper, and T. Akin, "Gold-Tin Eutectic Bonding for Hermetic Packaging of MEMS Devices with Vertical Feedthroughs," pp. 6–9, 2014.

[53] E. C. Demir, M. M. Torunbalci, I. Donmez, Y. E. Kalay, and T. Akin, "Fabrication and Characterization of Gold-Tin Eutectic Bonding for Hermetic

Packaging of MEMS Devices," *Proc. 16th Electron. Packag. Technol. Conf. EPTC 2014*, pp. 241–245, 2014.

[54] V. Chidambaram, C. Bangtao, G. C. Lip, and D. Rhee Min Woo, "Au-In Based Hermetic Sealing for MEMS Packaging for Down-Hole Application," *J. Electron. Mater.*, vol. 43, no. 7, pp. 2498–2509, 2014.

[55] B. J. Grummel, H. A. Mustain, Z. J. Shen, J. C. Elmes, and A. R. Hefner, "Reliability Characterization of Au – In Transient Liquid Phase Bonding Through Electrical Resistivity Measurement," *CPMT*, vol. 5, no. 12, pp. 1726–1733, 2015.

[56] H. Okamoto, "Au-In (Gold-Indium)," *J. Phase Equilibria*, vol. 14, no. 4, p. 532, 1993.